Title
Design of Passive Artificial Knee For Individuals with Paralysis

Author
Wu, Shang-Li

Publication Date
2017

Peer reviewed|Thesis/dissertation

Design of Passive Artificial Knee For Individuals with Paralysis

By

Shang-Li Wu

A dissertation submitted in partial satisfaction of the

requirements for the degree of

Doctor of Philosophy

in

Engineering - Mechanical Engineering

in the

Graduate Division

of the

University of California, Berkeley

Committee in charge:

Professor Homayoon Kazerooni, Chair

Professor Lisa Pruitt

Professor Ronald Fearing

Fall 2017

Design of Passive Artificial Knee for Individuals with Paralysis

By

Shang-Li Wu

Abstract

Design of Passive Artificial Knee For Individuals with Paralysis

by

Shang-Li Wu

Doctor of Philosophy in Engineering – Mechanical Engineering

University of California, Berkeley

Professor Homayoon Kazerooni, Chair

The objective of this research is to design an artificial knee (either a prosthetic knee or an orthotic knee) to exhibit the basic behavior of the human knee. Such artificial knee should exhibit three behaviors:

1. Resist the knee flexion during the stance phase to help support a portion of user's weight.
2. Encourage knee flexion during the swing flexion phase to assist in toe clearance.
3. Allow free swing extension in the swing extension phase.

An important aspect of this invention is that all of the above specifications are achieved passively without the use of any actuators, computers and sensors. This knee device has designed, fabricated, and tested to enable paraplegics to walk in an exoskeleton. This invention is a planar machinery that achieves the above specifications in a simple architecture. Such knee has shown to be a good fit for certain paraplegics who prefer more rehabilitating work out because it allows more freedom and provides adjustable support. This artificial knee is highly adaptable for its modularity, and the simple yet highly functional design has the potential to significantly decrease the manufacturing cost.

Table of Contents

1 INTRODUCTION 1

1.1 MOTIVATION 1
1.2 PRIOR ARTS 2
1.2.1 EXOSKELETONS 2
1.2.2 PASSIVE KNEE-ANKLE-FOOT ORTHOSES (KAFOS) 4
1.2.3 STANCE CONTROL ORTHOSES (SCOS) 5
1.3 DESIGN DIRECTIONS 15

2 BIOMECHANICAL ANALYSIS 17

2.1 HUMAN GAIT AND DEFINITION 17
2.1.1 BIOMECHANICAL PLANES AND ANGLES 17
2.1.2 GAIT CYCLE AND CLINICAL GAIT ANALYSIS (CGA) DATA 18
2.1.3 DESIGN FOR MEDICAL APPLICATION 19
2.2 KNEE TORQUE ANALYSIS 19
2.2.1 PREVENT KNEE FROM FLEXING 19
2.2.2 ALLOW THE KNEE TO FLEX 24
2.2.3 ASSIST IN TOE CLEARANCE 25
2.3 REMARKS 27

3 MECHANISM 29

3.1 DESIGN REQUIREMENTS 29
3.2 PROPOSED MECHANISM 32
3.2.1 MECHANISM STATES IN GAIT CYCLE 40
3.2.2 RESET RANGE AND SUPPORTIVE RANGE 42
3.2.3 POSITION OF THE CONSTRAINT 43
3.2.4 ENERGY STORAGE 45
3.2.5 ADDING EXTENSION LINK TO EXPAND RANGE OF MOTION 46
3.2.6 PREVENTING OVEREXTENSION 47
3.3 SIMULATION TORQUE PROFILE 48
3.3.1 TORQUE CALCULATION 48
3.3.2 PARAMETERS OF A TORQUE PROFILE 50
3.4 DESIGN PROCESS 53
3.4.1 THE DESIGNED PARAMETERS AND THE UNKNOWN PARAMETERS 53
3.4.2 DESIGN PROCESS IN THREE STEPS 55
3.4.3 FULL DESIGN PROCESS 58
3.5 PHYSICAL DESIGN 59
3.5.1 SPECIFICATIONS 59
3.5.2 ADJUSTABILITY 59
3.5.3 PHYSICAL DESIGN 61
3.5.4 EXPERIMENTAL TORQUE PROFILE 67

4 EVALUATIONS 70

4.1 CASE I: COMPLETELY PARALYSIS **70**
4.1.1 METHOD 70
4.1.2 RESULTS 71
4.1.3 DISCUSSION 72
4.2 CASE II: INCOMPLETE PARALYSIS **73**
4.2.1 METHOD 74
4.2.2 RESULTS 75
4.2.3 DISCUSSION 78
4.3 CONCLUSIVE REMARKS **79**

5 QUALITATIVE EVALUATIONS **80**

5.1 SPLIT STAND **80**
5.2 PARALLEL STAND **83**
5.3 STANDING UP **85**
5.4 SITTING DOWN **86**
5.5 TURNING AROUND **87**
5.6 POPPING NOISE **87**
5.7 CONCLUSION REMARKS **87**

6 CONCLUSION **89**

REFERENCES **90**

7 APPENDIX: COMPUTATIONAL MODEL **94**

7.1 PRE-SWING MODEL **94**
7.2 SWING DYNAMICS MODEL **95**

Nomenclature

l_{SHANK}	length of shank (from knee joint to ankle joint)
l_D	length of the driver link (of the four bar linkage)
l_G	length of the ground link (of the four bar linkage)
l_F	length of the follower link (of the four bar linkage)
l_{CP}	length of the coupler (of the four bar linkage)
l_{CP0}	original length of the coupler link (of the four bar linkage)
θ_{TORSO}	angle of the torso relative to the ground
θ_{HIP}	angle of the thigh relative to the torso
θ_{KNEE}	angle of the shank relative to the thigh
θ_I	angle of the shank to the ground
θ_{ENG}	engagement angle
θ_{TOG}	toggle angle
θ_{REL}	release angle
θ_{TO}	knee angle at toe off
θ_{START}	starting angle
θ_{END}	end angle
θ_{MIN}	minimum knee angle during gait
θ_{MAX}	maximum knee angle during gait
$\theta_{MAX,ST}$	maximum knee angle at early stance
$\Delta\theta_{SUP}$	supportive range
$\Delta\theta_{RESET}$	reset range
θ_{OFF}	angle between center angle of the supportive range and the center angle of the reset
θ_{CON}	angle between the ground link and the angle when the follower is constrained

θ_{ROTATE}	angle between the ground link and the angle when the follower is constrained
$\theta_{THIGH.D}$	angle between thigh and the driver link
$\theta_{SHANK,G}$	angle between shank and the ground link
T_{TORSO}	torque on the torso from constraint (control)
T_{HIP}	torque on hip
T_{KNEE}	torque on knee
T_{MECH}	torque from the mechanism
$T_{MECH,MAX}$	maximum torque from the mechanism
F_{SPRING}	force of the spring
m	body weight
g	gravitational constant [9.81 m/s^2]
$\%mg$	percentage of the body weight
μ	transmission angle of the four bar mechanism
μ_S	coefficient of static friction

Acknowledgement

First and foremost, I want to thank my research advisor, Professor Homayoon Kazerooni, for all his support along this journey. Thanks for setting up this amazing environment that encourages us to build and make a difference by our own hands, leading us along the process of thinking and writing, and demonstrates how to move forward with your strong sense of mission. I appreciate your recognition of my work and all your support during those countless midnight phone calls and weekend meetings in these years.

I also want to thank my dissertation and qualification committee, Professor Ron Fearing, Professor Lisa Pruitt, Professor Dennis Lieu, Professor Grace O'Connell and Professor Ruzena Bajcsy. Thank you all for understanding the difficulties of being a non-native speaker and all your instruction, guidance and recognition along these years.

I would like to express my appreciation toward the staffs in the machine shop: Dennis, Jesse, Scott, Jeff, and Jacob. Machine shop is one of the places that I enjoyed and learned the most at Berkeley. Thank you for patiently teaching me how to build things without killing myself, and making me a better designer.

I want to also thank all of my colleagues and friends in the lab and in the company that enable these entire miracles happened. Thank Nick Errico for coming along with me, carrying me, and patiently bring me into this culture. Thanks Wayne Tung for introducing the lab to me at the first day, sharing your tips of how to be a good boy, and bully me on the basketball court. Thanks Minerva Pillai for always being so patient and understandable as such a good mentor in the aspects of knowledge and life. Thanks Yoon Jeong for the physical help on the testing, writing, and those mental support through those difficult times. Thanks Michael Mckinley, Brad Perry and the software team for being so easy to collaborate with whenever I need. Thanks Mimi Parker for editing my English writing so thoroughly even if it was so hard to understand. Thanks Anna Sternin for the suggestions and help on the testing and writing. Thanks Jose Chavarria and Raghid Mardini for making everyday so fun and young, and share the cute memory of the makeathon. Thanks XiaoYue and Katherine for sharing life and fruits. Thanks Christina Yee for the help during the preparation of my qualifying exam, and being such a good friend of life. Thanks Yi-Wen Liao and Octavio for the old memories and always being unselfish on sharing your knowledge. I would also like to express my appreciation toward those who helped me in the project and class, in the qualifying exam and in many other forms, and those who build the giant so now I can stand on its shoulder.

Thanks all my friends for your encouragement and companion in the countless study nights: Victoria, Chin-Yi, Hsien-Chung, Angela, Chen-Yu, Jessie, Katherine, Ahbae, Aahshen, Chienhsia, Kidlands', and more. How you believe that I can do this is truly important for me.

Finally, I want to thank my families for giving me unconditional love and making me become who I am. In particular, thanks grandma for raising me up and waiting for me these years. You are the reason why I am here.

1 INTRODUCTION

1.1 MOTIVATION

According to National Spinal Cord Injury Statistical Center, in 2017 there were approximately 285,000 individuals in the United States suffering from spinal cord injury (SCI), with an estimated 17,500 new SCI cases each year. Out of this number, around 40.6% resulted in complete or incomplete paraplegia [1]. Experiencing paralysis affects patients' quality of life through loss of physical function, independency, accessibility, and emotional of well-being. This influences not only on the patients themselves, but also on their families and the caregivers.

Wheelchair is the most popular solution for individuals with paralysis to maintain their mobility. While the wheelchair and other similar mobility devices have improved over the years, standing up and walking are still extremely difficult tasks for individuals suffering from paraplegia and quadriplegia. Assisted standing addresses the secondary complications created by prolonged wheelchair use, and has the following medical benefits [2]:

- Prevention or reversal of osteoporosis and resultant hypercalciuria
- Prevention of contractures and improvement in joint range of motion
- Reduction of spasticity
- Improvement in renal function, drainage of the urinary tract, and reduction in urinary calculi
- Prevention of pressure ulcers
- Improvement in circulation, as it relates to orthostatic hypotension and other benefits of good circulation
- Improvement of bowel function

Based on these reasons, standing sessions are commonly prescribed in physical medicine and rehabilitation. Traditional standing tables require multiple people to assist paralysis to stand up. To ease this process, use of an assisted standing equipment is usually suggested in physical medicine and rehabilitation, such as lift beds or standing wheelchairs shown in Figure 1-1.

Besides the physical benefits, standing up and walking also benefit individuals from a psychological aspect. Studies show that Americans with long-term disabilities are two to three times as likely to suffer from depression than the non-disabled population [3]. This may be caused by the loss of physical function, independence, accessibility, and emotional well-being of those suffering from paraplegia and quadriplegia - all of which are great factors when evaluating an individual's quality of life [4]. The invention of mobility assistant devices plays a crucial role for disabled individuals both physically and psychologically.

(A) **(B)**

Figure 1-1: Examples of assisted standing equipment (A) Vital Go total lift bed (left) (B) SMFE standing wheelchair (right).

1.2 PRIOR ARTS

1.2.1 Exoskeletons

The invention of the powered exoskeleton wrote a new page for paraplegic mobility. Powered exoskeletons benefit paraplegics by allowing them to walk upright and overcome their disability, and giving them independence, a healthier lifestyle, and an overall increased quality of life.

Ekso, Rewalk, Indego are well known exoskeletons in today's exoskeleton industry. They all have four actuators: one on each hip and one on each knee. They allow paraplegics with sufficient upper body strength to walk with help of the crutches or walker [5]–[7]. Rex is the only exoskeleton to the author's knowledge that requires no upper body strength. However, Rex is extremely bulky (with 10 motors and weighing in at 39 kilograms) and has slow walking speed [8]; thus, although it can accommodate higher-level injuries, it is not widely accepted by the market. The Phoenix exoskeleton, developed from Professor Kazerooni's Human and Robotics Laboratory at the University of California, Berkeley, is one of the lightest medical exoskeletons in the exoskeleton industry (12 kilograms). Its non-actuated knee mechanics, which distinguishes Phoenix from other exoskeleton that are currently out in the market, trims the weight and cost down, while enhancing subjects' accessibility. An overview of the existing exoskeleton technologies is shown in Table 1-1.

Table 1-1: Overview of exoskeleton technologies [8]–[16].

Robot Name		Phoenix	Ekso	ReWalk	Indego	Rex
Company		SuitX	Ekso Bionics (Berkeley Bionics)	Argo Medical	Parker Hannifin	Rex Bionics
Picture						
Country		USA	USA	Israel	USA	New Zealand
Weight (kg)		12	20	20	12	39
Walking velocity (m/s)		0.475	0.19	0.03~0.45	0.22	0.05
Approximated Price (USD)		40,000	130,000	95,000	80,000	150,000
Powered Degree of freedom	#	2	4	4	4	10
	Location	1 at each hip	1 at each hip 1 at each knee	1 at each hip 1 at each knee	1 at each hip 1 at each knee	2 at each hip 1 at each knee 2 at each ankle
Human Machine Interface HMI		Buttons on the crutches	1.Buttons on the crutches or walker. 2. Weight shift plus the initiation of forward leg movement.	Upper body Orientation	Upper body orientation	Brain-machine-interface
Foot Fixture Method		Insole	Outsole binding	Insole	Insole	Outsole binding
FDA Approval		Seeking FDA approval	FDA approved for clinical use	FDA approved for clinical and personal use	FDA approved for clinical and personal use	Not registered with the U.S. FDA
Allowable Spinal Cord Injury Level		(Worked with) complete T6 or lower	(FDA approved) T4-L5, C7-T3 (ASIA D), and Stroke: use in rehabilitation institution	(FDA approved) T7-L5: with specially trained companion T4-T6: use in rehabilitation institution	(FDA approved) T7-L5: with specially trained companion T4-T6: use in rehabilitation institution	(Worked with) up to C4/5 level

1.2.2 Passive Knee-Ankle-Foot Orthoses (KAFOs)

Traditional knee-ankle-foot orthoses (KAFOs) support the knee by locking it in full extension throughout the gait. They are often prescribed for patients with quadriceps weakness or paralysis; they are also prescribed to those having pathological conditions such as cerebral palsy, hemiplegia, genu recurvatum, genu varum, or genu valgum.

(A) (B) (C)

Figure 1-2: (A) Becker S2005 Free motion knee joint (B) Fillauer 2755 free motion posterior offset knee joint (C) Becker polycentric free motion knee joint [17], [18]**.**

There are three types of KAFO knee joints: straight-set knee joint, posterior offset knee joint and polycentric knee joint. The straight-set knee joint (Figure 1-1(A)) has a simple hinge located approximately at the anatomic knee joint. The posterior offset knee joint (Figure 1-2(B)) has a hinge located posteriorly to the anatomic knee joint. The posterior offset knee joint increase the space that the ground reaction force (GRF) passes the anterior of the mechanical knee joint, which prevents the knee from buckling. This provides more stability during stance.

The polycentric knee joint (Figure 1-2(C)) more closely mimics the anatomical motion of the knee. However, a polycentric joint is more complex and requires more maintenance. It has not been proven to be more beneficial over the straight-set knee [19].

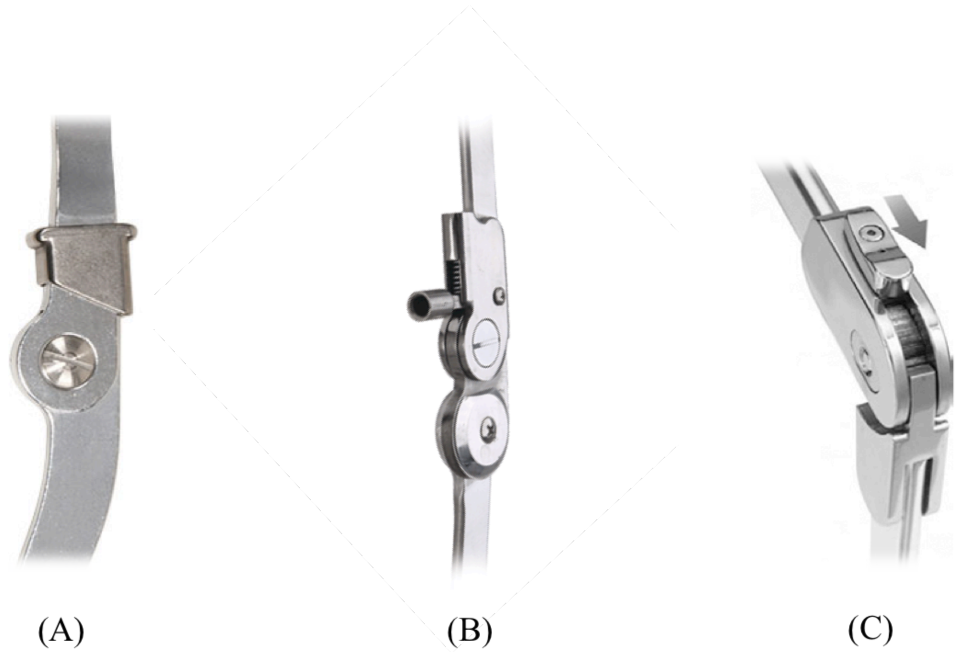

Figure 1-3: (A) Fillauer drop lock knee joint (B) Becker model 1007 adjustable extension automatic spring level knee joint (C) Becker model 1014 ratchet lock™ knee joint [17], [18]**.**

Locks are incorporated into these joints to provide knee stability. Four locking mechanisms have been identified in the literatures: drop lock, bail lock, ratchet lock and the dial lock. Drop lock (Figure 1-3(A)) and bail lock (Figure 1-3(B)) assist in locking the knee at full extension by using a sleeve or a spring-loaded bail. Dial lock is able to lock the knee at different angles to accommodate various knee contractures. Ratchet (Figure 1-3(C)) lock allows the knee to extend but lock in flexion to provide stability.

KAFOs have been in used for a long time, but their long-term use rate is low as approximate 58 to 79 percent of KAFOs are abandoned as ineffective by their wearers. More than 40 percent of KAFO wearers express dissatisfaction with their orthoses even though they continue to wear them [20]. This is because walking with a locked knee for the entire gait cycle requires specific gait compensations including hip hiking, vaulting, and circumduction.

1.2.3 Stance Control Orthoses (SCOs)

Stance control orthoses (SCOs) were originally developed to overcome the limitations of traditional KAFOs. They are designed to allow users to flex their knees during swing while still preventing knee buckling during weight bearing. The following section introduce current technologies of the SCO [19], [21].

1.2.3.1 Ottobock Free Walk/ Becker Orthopedic UTX [21], [22]

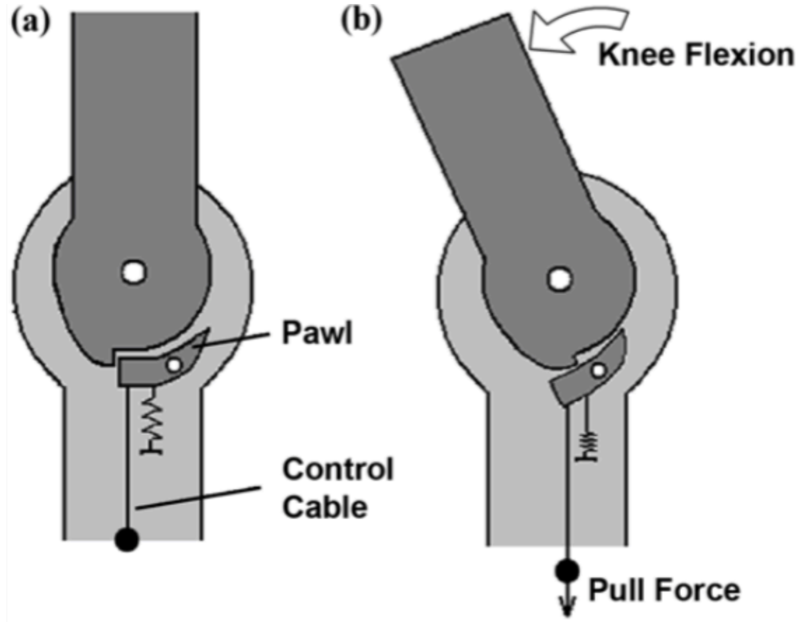

Figure 1-4: Ottobock free walk and Becker orthopedic UTX share the same pawl and ratchet design [21], [22].

Recent SCO devices achieve providing support as well as allowing free swing using many different locking or unlocking sensing system and strategies. OttoBock Free Walk and Becker Orthopedic UTX share the same pawl and ratchet design as shown in Figure 1-4. They both have a spring-loaded pawl to lock the knee when the knee is fully extended and they unlock the knee when the foot dorsiflexes to 10 degrees at the end of the stance phase. It utilizes of a pushrod connected to the ankle to sense the dorsiflexion. Simultaneous extension of the knee with 10 degrees dorsiflexion is required to eliminate flexion moments about the knee and to free the pawl from friction for disengagement.

However, since the knee requires full extension to be locked, the knee will become unsupported if the knee is flexed during limb loading. Moreover, since the disengagement mechanism requires 10 degrees dorsiflexion, the device cannot be used for patients with limited dorsiflexion range. Yet, these technologies are the lightest and most cosmetically attractive SCOs [21].

1.2.3.2 Hortan Stance Control Orthosis [21], [23]

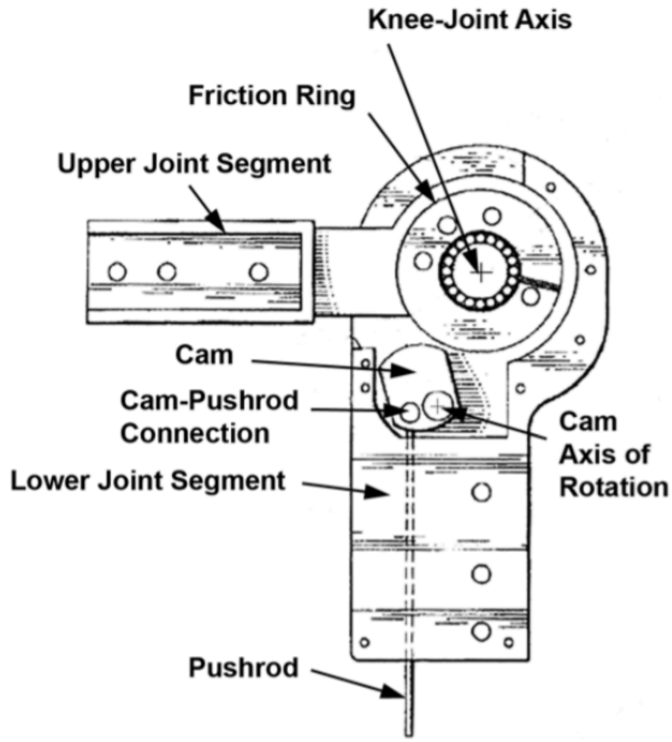

(A)

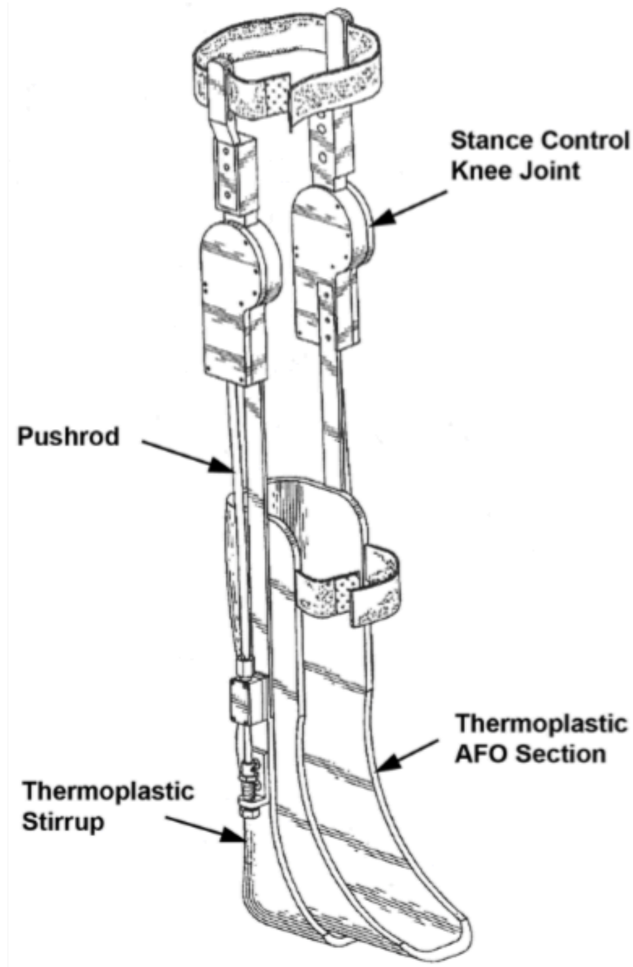

(B)

Figure 1-5: Hortan stance control orthosis [21], [23]**.**

Hortan stance control orthosis (shown in Figure 1-5) utilizes a self-locking mechanism to create a one-way clutch that can prevent knee flexion during stance at any knee angle. The sensing mechanism is a stirrup that is pushed upward upon heel contact. The mechanism prevents the knee from buckling at any angle. However, a knee extension moment is required to eliminate friction forces on the cam and disengage the joint. Also, the knee joint itself is bulky and the sensing mechanism can be problematic: objects such as clothing and socks may lodge between the foot and stirrup. The ankle-driven pushrod option cannot be used for users with ankle mobility problems.

1.2.3.3 Fillauer Swing Phase Lock [24]

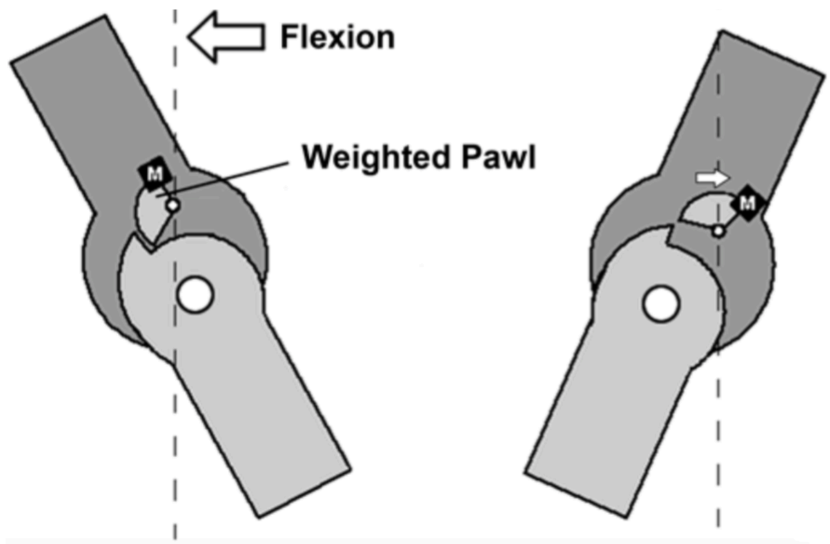

Figure 1-6: Concept of Fillauer swing phase lock [24]**.**

Fillauer swing phase lock uses a pawl latch design as shown in Figure 1-6. The pawl itself is an inverted pendulum that is able to sense the thigh angle and drop into different positions to lock and unlock the knee. While this mechanism is lightweight by design, the knee must be fully extended for the pawl to fall into this locked position. Also, an extension knee moment is required to allow the pawl to disengage.

1.2.3.4 The Becker Orthopedic 9001 E-Knee

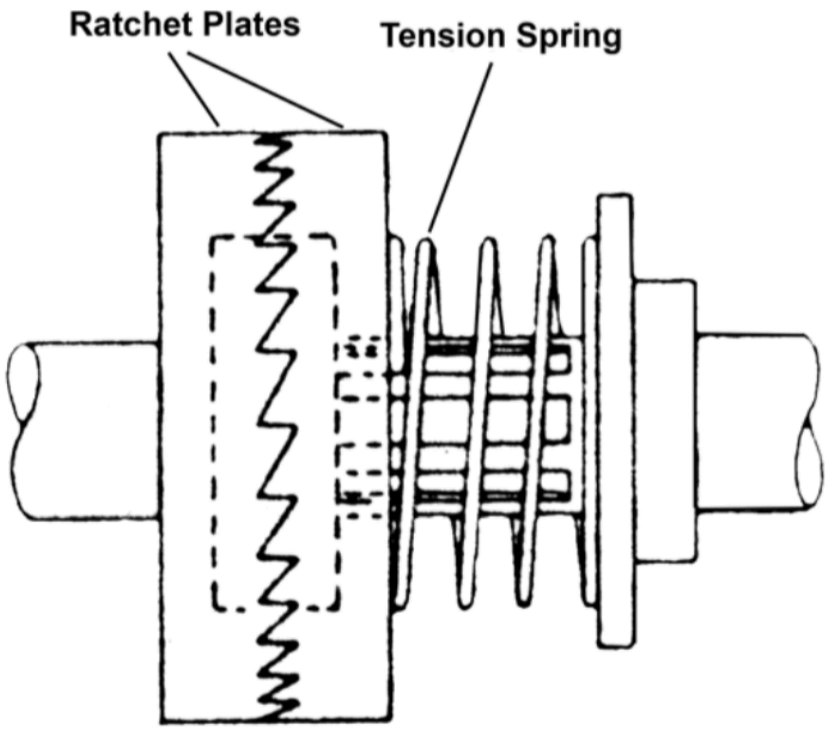

Figure 1-7: Becker Orthopedic 9001 E-Knee [25]**.**

The Becker Orthopedic 9001 E-Knee uses a magnetically activated one-way dog clutch as shown in Figure 1-7. The joint consists of two ratchet plates that are kept by a spring. One of the ratchet plates is positioned within an electromagnetic coil. When a pressure sensor below the foot detects foot contact, the electromagnetic coil is energized to bring the ratchet plates together.

However, this ratchet device suffers from two inherent disadvantages. First, it generates a clicking sound when rotated under engagement. This sound is not preferred for cosmetics reason. Second, while it provide finite locking angle, it can have up to 6 degrees of free flexion before the ratchet is locked. It is also bulky and expensive compared to other SCOs.

1.2.3.5 Dynamic Knee Brace System (DKBS) [26]

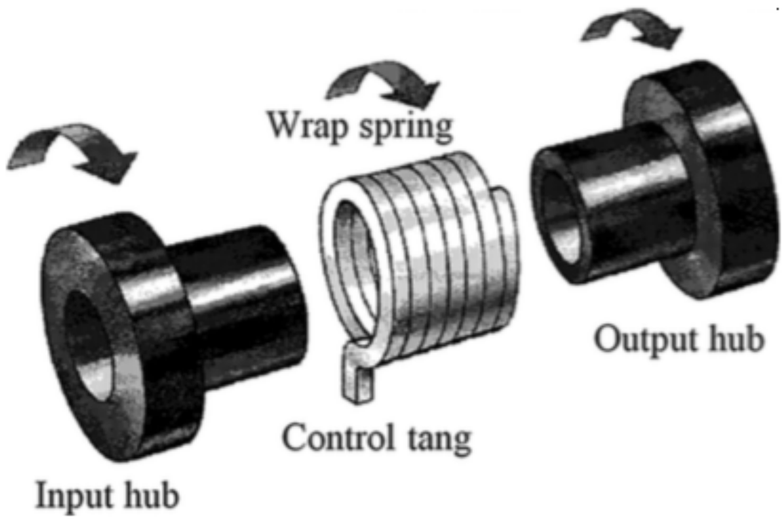

Figure 1-8: Dynamic knee brace system utilizing wrap spring to lock and unlock the knee.

Dynamic knee brace system utilizes a pressure sensor on the footplate and a microcontroller to control a solenoid that engages and disengages a wrap spring crutch in the knee joint. The wrap spring clutch design as shown in Figure 1-8 is similar to a one-way clutch that can lock in one direction or unlock and allow free motion in both directions. The advantage of the wrap spring clutch is that it can be unlocked even when the knee is loaded. This feature is found to be important for providing smooth transition between stance and swing phase, and this mechanism is the only currently available technology that has this feature to the author's knowledge [21].

The Phoenix exoskeleton's wrap spring knee utilizes similar technology after became clear that unlocking the knee while fully unloaded is unrealistic and energetically inefficient [27]. However, manufacturing difficulties lead to a higher device price because the wrap spring requires tricky machining process and tight tolerance. OttoBock's Sensor Walk utilizes this technology and is the most expensive SCO, selling at USD $8,500.

1.2.3.6 Ottawalk Belt-Clamping Knee Joint [28], [29]

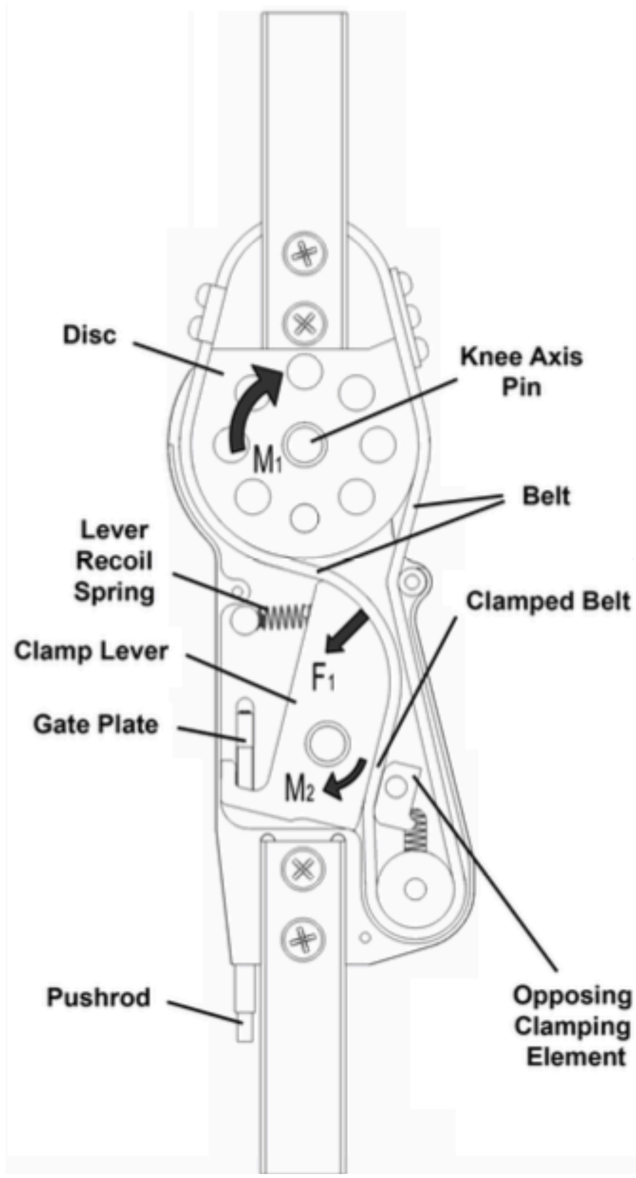

Figure 1-9: Ottowalk belt-clamping knee joint.

Ottawalk belt-clamping knee joint uses a belt clamping mechanism to provide free knee motion during swing. The design is shown in Figure 1-9. During stance, the mechanism resists knee flexion but allows extension at any knee angle. The belt clamp is triggered by a pushrod connected on the foot. Elasticity in the belt allows some knee flexion in early stance rather than an abrupt mechanical locking. This helps absorb shock at heel strike and, potentially, smooth the path of the center of mass (COM) as it occurs in normal gait [30]. The knee also has to be unloaded to disengage the clamping to switch from stance to swing.

1.2.3.7 Dual Stiffness SCO

To the author's knowledge, three groups had attempted to design a knee that simulates the stiffness of the knee in a gait cycle. They all utilize two-spring systems activated in turns during stance and swing phase.

1.2.3.7.1 Shamaei at el. [31]

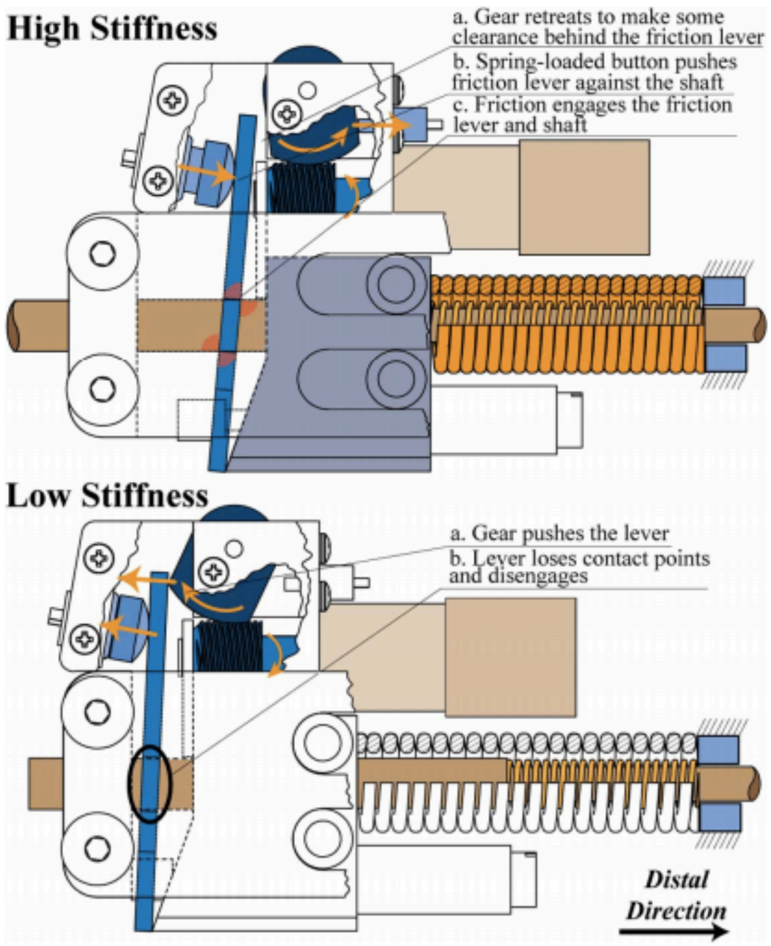

Figure 1-10: The dual-stiffness SCO developed by Shamaei at el. [31]

Shamaei at el. developed a quasi-passive compliant knee that has two springs with different stiffness. The top and front view of the design are shown in Figure 1-10. The knee uses the higher stiffness spring to create support during stance, and switches to a lower stiffness spring in swing. It utilizes a self-locking mechanism to create a one-way linear clutch by engaging a lever and a shaft. When the clutch is engaged, a stiffer spring is activated to simulate the stiffness of the knee during stance phase. When the clutch is disengaged, the knee becomes less stiff to simulate free swing phase.

1.2.3.7.2 **Cullell at el.** [32]

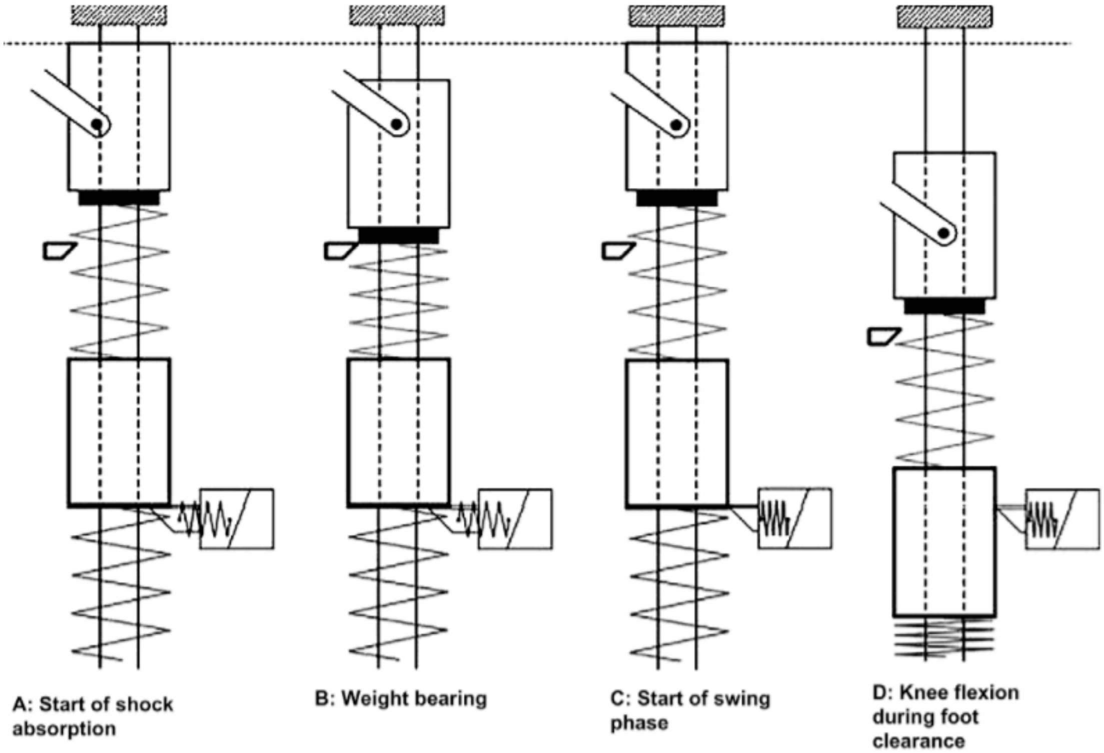

Figure 1-11: The dual-stiffness SCO developed by Cullell at el. [32]

Cullell at el. developed a stacked dual stiffness knee actuating system that mimics the stiffness of the knee in stance and swing phases. The conceptual design is shown in Figure 1-11. The triggering system includes gyroscopes and dual-axis accelerometers on the foot and shank, and an angular position sensor located at the knee. The SCO is bulky, and it has high power consumptions with only 2.5 hours battery life. This device is not yet commercially available.

1.2.3.7.3 Tian at el. [33]

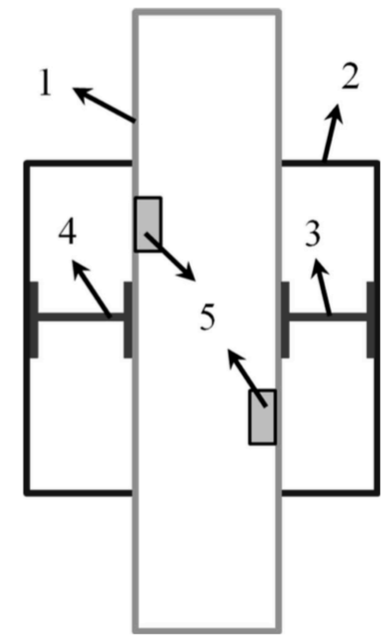

Figure 1-12: The conceptual design of the dynamic knee joint: 1) one part of the knee joint that is connected with the shank segment; 2) the other part of the knee joint that is connected with the thigh segment; 3) the actuator that combines a superelastic rod and a rotary spring in series; 4) the solenoid.

Tian at el. attempted to achieve the function of dual-stiffness knee using superelastic alloy in the belief that superelastic materials can better simulate the behavior on the knee. The conceptual design of the dynamic knee joint is shown in Figure 1-12. This research is still under simulation and conceptual design and no clinical results have shown yet.

1.3 DESIGN DIRECTIONS

The main functions of an ideal SCO are to resist flexion during stance while allowing for a free knee motion during swing. Research has demonstrated that SCOs improve the gait kinematic, user's energy consumption, and gait symmetricity compared to conventional locked-knee KAFOs [30], [34]–[37]. In addition to the two main functions of SCO, Terris et al. summarized a few features that are advantageous for any SCO designs. These include (reorganized from [21]):

1. **Assist knee extension in stance**: In addition to preventing knee flexion during stance, assist knee extension is advantageous in straightening the knee.
2. **Switch between stance and swing without needing to unload the knee:** This allows smoother switching between stance and swing modes. In most of the current designs, switching between the modes requires the knee extension moment to unload the joint. Although this could lead to a safer gait, the gait is less smooth. In a previous exoskeleton research, fully unloading and disengaging the knee was reported to be unrealistic and is

less energy efficient. Furthermore, patient with contracture may have difficulties unlocking the knee [27].

3. **Permit controlled knee flexion upon initial loading after foot strike:** Lack of knee flexion during foot strike causes abrupt impacts and disturbs the smooth progression of the COM of the body. Permitting knee flexion in the front leg during stance is advantageous for smoothing progression of the body COM and shock absorption [21], [38].
4. **Unlock the knee (allow flexion) at any knee and ankle angle:** Some SCOs that require specific knee or ankle angles to trigger unlocking may hinder sitting, stair ascent or descent motion. The ability to unlock at any ankle permits these motions.
5. **Lock the knee or resist knee flexion at any knee angle:** Locking the knee or resisting knee flexion at any knee angle rather than just at full knee extension is beneficial for standing with flexed knees, and walking in ascending or descending slope.

Currently, no technology yet exists that achieved all of the above specifications while maintaining low cost and weight. This thesis proposes a novel knee design (henceforth called artificial knee 100) in conjunction with an innovative supporting strategy. This novel artificial knee achieves aforementioned features number 1 to 4. It provides compliancy instead of an abrupt lock, which in the concept of energy is closer to the dual stiffness SCO. Rather than mechanically lock the knee by friction or any latch design, artificial knee 100 stores energy and utilizes the energy in other phases in the gait. Artificial knee 100 also provides a benefit that has been endured by users but no designer has previously come up with a solution – assists in toe clearance.

The objective here is to design an artificial knee (either a prosthetic knee or an orthotic knee) to exhibit the basic behavior of the human knee with no actuators, sensors and computers. If such knee becomes realizable, it can be used as a low cost artificial knee for various orthotic, prosthetic and exoskeleton applications.

This thesis presents a novel knee device that is designed to create support during the stance phase and assistance in the swing phases. A knee device has designed, fabricated, and tested with and without the exoskeleton system. This device has showed to enable paraplegics to walk. This knee is shown to be a good fit for certain paraplegics because it allows more freedom and provide adjustable support. It is highly modular and can also be attach in addition to other knee devices. The simple design has the potential to significantly decrease the manufacturing cost.

Chapter 2 presents the biomechanical analysis and develops the design requirements of the novel artificial knee. Chapter 3 introduces the mechanical design, the properties of this design, and develops a design process for this novel design concept. Chapter 4 presents quantitative evaluation of two paraplegics using artificial knee 100 in comparison to the wrap spring knee, and Chapter 5 shows qualitative usability results of artificial knee 100.

2 BIOMECHANICAL ANALYSIS

This chapter first introduces the biomechanical definitions of the body planes and angles followed by normal gait cycle the clinical gait analysis (CGA) data. In the second part, link-segment model is used to achieve the design requirements of artificial knee 100 by using knowledge of constraints, kinematics and kinetics.

2.1 HUMAN GAIT AND DEFINITION

2.1.1 Biomechanical Planes And Angles

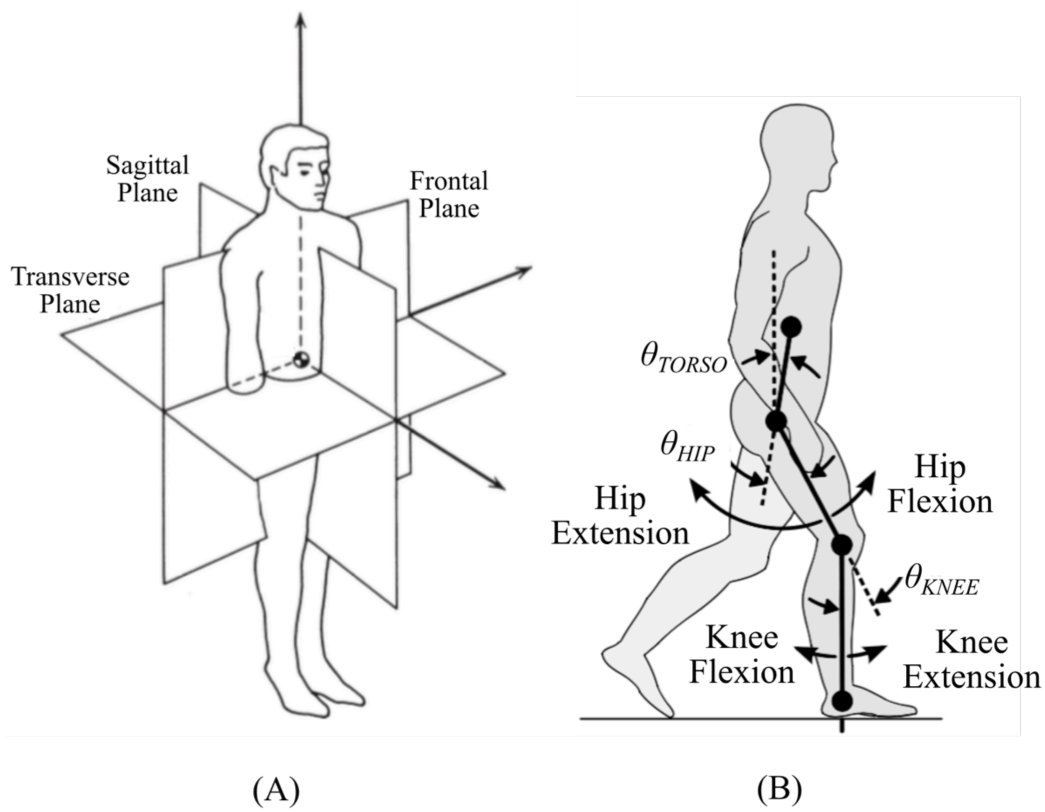

Figure 2-1: Biomechanical definition of (A) body planes (modified from [39]) (B) joint angles and directions [40].

Figure 2-1(A) shows three biomechanically defined body planes – sagittal, coronal, and transverse. Figure 2-1(B) shows the biomechanically defined joint angles and directions in the sagittal plane. The torso angle is defined relative to the ground; the hip angle is the angle of the thigh relative to the torso, and the knee angle the angle of the shank relative to the thigh. The direction of hip and knee flexion and extension are also defined in the figure.

2.1.2 Gait Cycle and Clinical Gait Analysis (CGA) Data

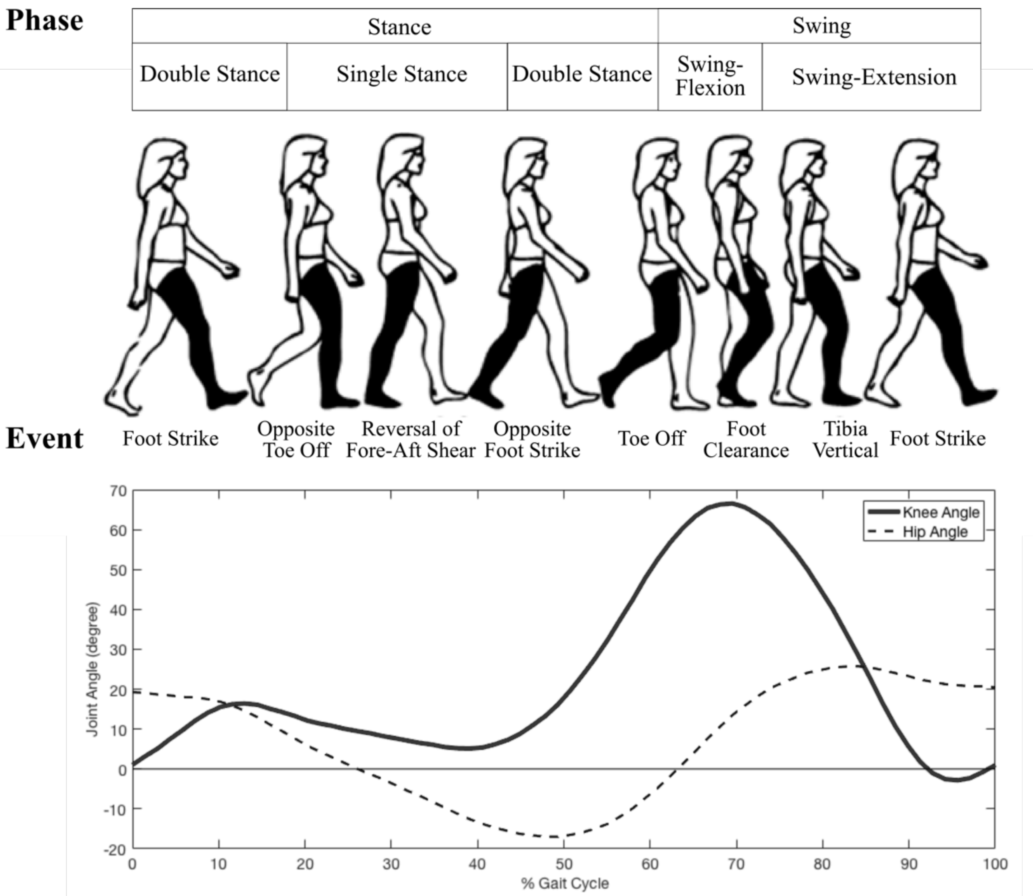

Figure 2-2: The events and phases in a gait cycle and the clinical gait analysis (CGA) data (figures modified from [41], [42]).

Figure 2-2 shows a gait cycle. There are two main phases in a gait cycle, stance phase and swing phase. The stance phase happens when the foot is on the ground, and the swing phase happens when the foot is off the ground. To be more specific, we can subdivide the stance phase into the single stance phase (SS) - when only one foot is on the ground, and the double stance phase (DS) - when both feet are on the ground. On the other hand, the swing phase can be subdivided into two phases: swing flexion - when the knee flexes, and swing extension - when the knee extends.

A gait cycle starts at foot strike, and begins with a double stance phase. Next, the single stance phase starts at opposite toe off. Then the second double stance takes place at opposite foot strike. Later, the gait enters the swing phase at toe off. Finally, the swing phase starts with a swing flexion phase, followed by the swing extension phases.

Figure 2-2 also shows the clinical gait analysis (CGA) data from Winter et. al. [42], [43]. At heel strike, the hip angle is around 20 degrees, then it starts decreasing and reaches at minimum about -20 degrees at opposite foot strike. After that the hip angle increases again to bring the leg forward for swinging. At the end of the swing, it decreases a little bit for foot strike. On the other hand, the knee angle starts at 0 degree at foot strike, increases a little bit during mid-stance, starts increasing significantly at around opposite foot strike, reaches maximum flexion at about 65 degrees in swing-flexion, and finally extends back to 0 degree before foot strike.

2.1.3 Design For Medical Application

The differences between normal walking and walking in knee-ankle-foot-orthoses (KAFOs), stance control orthoses (SCOs) or exoskeletons are somewhat considerably. One main essential feature of the KAFO, SCO or exoskeleton is the essentially fixed (or constrained) ankle. The effect of the fixed ankle helps the patients to be stabilized, but inhibits the ankle plantarflexor (foot moving downward), which is primarily used to accelerate the leg into swing during late stance [44]. The plantar flexion motion is also used to flatten the foot and to facilitate weight shifting during the stance phase. Because of the prohibition of this motion by the fixed ankles, allowing knee flexion right after foot strike has pointed to disburden the effort of progression in both orthosis and exoskeleton applications [30], [38].

2.2 KNEE TORQUE ANALYSIS

This article explores the feasibility of designing of a passive artificial knee 100 to help paraplegics walk by focusing on analyzing the knee torque in different phases of a gait. The first part of the analysis includes the postures when we need to prevent the knee from flexing. The second part includes when we want to flex the knee for swing. The third part includes a feature to assist toe clearance in the swing phase. Link segment kinematic [39] is used to model the human body. This method is proposed by Winter et. al. and is widely used for biomechanics and locomotion([39], [45]–[48]).

This study makes several assumptions for simplification. This analysis considers motion and force only in the sagittal plane. The hip, knee, and foot-ground contact are as pin joints rotating on the sagittal plane. The hip angle is controlled by a hip actuator, and the torso angle is controlled by some means of connections from the torso to the ground. This connection could be crutch, walker, or parallel bars that is controlled by the user, or by some mechanism connecting those directly to the torso. The rotating axes of two hips are aligned with each other.

2.2.1 Prevent Knee From Flexing

The knee is designed to buckling during static parallel standing, single stance (SS) and a split standing posture in double stance (DS). The body is modeled into linkages of torso, thigh, and shank, connected in serial with each other by pin joints. To get clearer insight of the effect of body weight, the mass is simply focused on the center of mass (COM) on the torso.

2.2.1.1 Single Stance (SS) (and Parallel Standing)

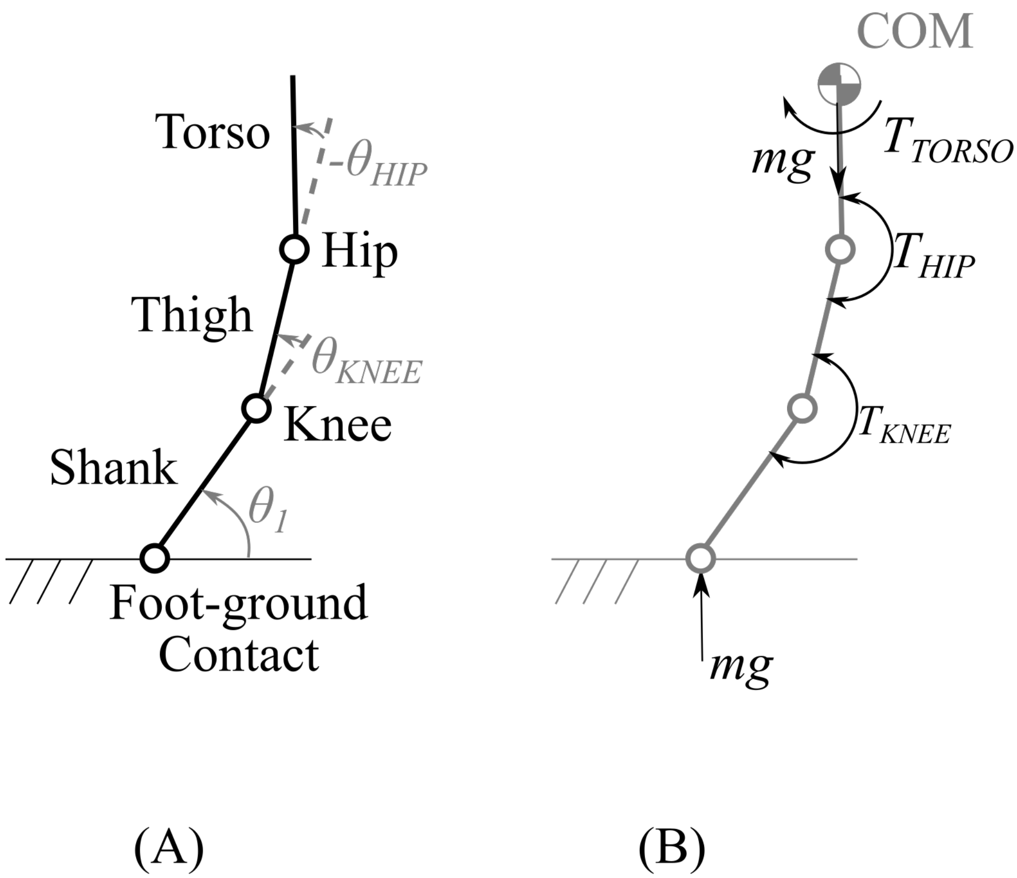

Figure 2-3: (A) The kinematic model in a stance posture (B) The force applying on each link segment and joint.

In a SS posture as shown in Figure 2-3(A), the body is analogous to an open kinematic chain that has 3-degree of freedoms (DOFs). This kinematic chain is confined by two constraints: the hip angle and torso angles. This kinematic chain has one DOF, which means the body segments are underdetermined. The body segments can move to anywhere, including flexing the knee. Therefore, the following section provides estimations of torque generated from the body weight (BW) in this posture. This estimation is useful as to design how much torque is needed on the knee to keep the posture stable.

This estimation is under a quasi-static condition. The constraints on the hip and torso angle generate torque on the hip T_{HIP} and torso T_{TORSO}, respectively. Without any knee torque, the BW will cause the kinematic chain to move. Assume a torque T_{KNEE} on the knee that balances the whole system. This torque is equal but in opposite direction to the torque on the knee generated from the BW.

2.2.1.1.1 Knee Torque Estimation

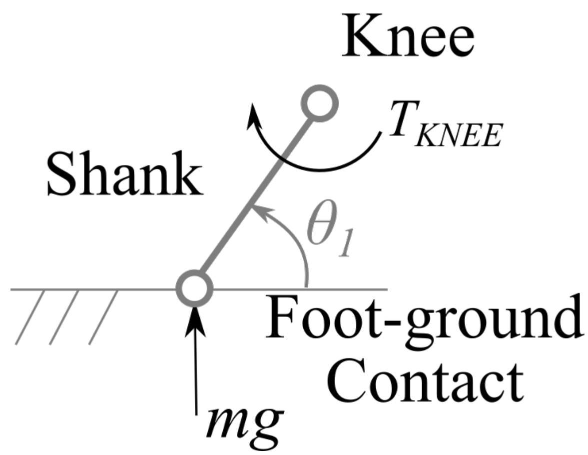

Figure 2-4: Model of the shank segment.

From Figure 2-4, we know that the

$$T_{KNEE} = -mgl_{SHANK}\cos(\theta_1) \tag{1}$$

where m is the BW, g is the gravitational constant, θ_1 is the angle between the ground to the shank, l_{SHANK} is the length of shank (i.e., distance from knee to the ground contact). We first assume the foot-ground contact is on the heel, and will soon introduce a modification concerning contacting on the toe.

It is crucial for a knee design to have a hyperextension stop to prevent the knee from hyperextension because this motion is harmful for paraplegics especially when they do not have muscle to counterbalance the force on the joint. The hyperextension stop can provide huge flexion torque when the knee is at zero degree. In this analysis the author concerns on postures that generate flexion torque because it buckles the knee.

The below equation gives us an insight of when we need an extension toque to prevent knee flexing:

$$\begin{cases} T_{KNEE} < 0 & \text{, if } \theta_1 < 90^\circ \\ T_{KNEE} > 0 & \text{, if } \theta_1 > 90^\circ \end{cases} \tag{2}$$

These equations tell that to keep force equilibrium, the mechanism is required to provide extension torque if the knee is ahead of the foot-ground contact (BW generates flexion torque), and provide flexion torque if the knee is behind the foot-ground contact (BW generates extension torque).

2.2.1.1.2 Modified Knee Torque Estimation

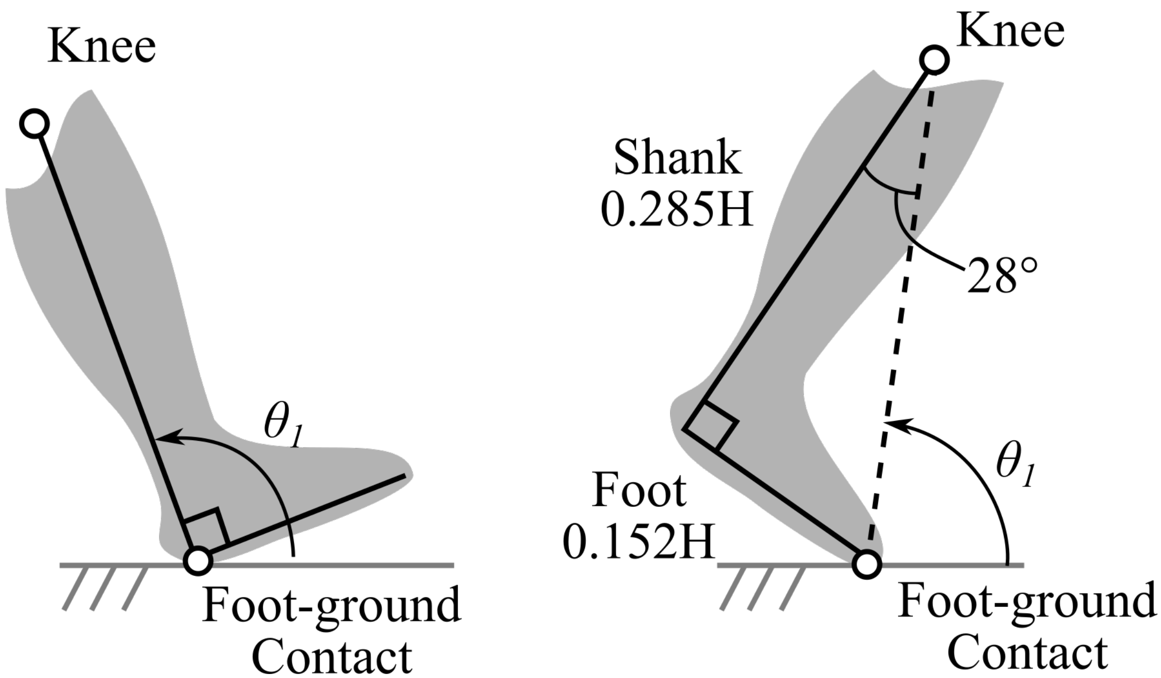

Figure 2-5: Modified Knee torque estimation considers the contact of the toe that requires offset of *θ_1* *by 28 degrees. H represents the body height.*

In our previous estimation, we assume the ground-foot contact is on the heel. In reality, when the θ_1 (the angle between the ground to the shank) is smaller than 90 degrees, the foot-ground contact point is on the toe. Considering the ankle angle is generally fixed in exoskeleton applications (i.e. Rewalk, Ekso, Phoenix), we assume the ankle is perpendicular to the foot. From anthropology data [39], the knee angle needs to be offset by 28 degree (as shown in Figure 2-5) to move the contact point from the heel to the toe, which gives us equations:

$$\begin{cases} T_{KNEE} = -mgl_{SHANK}\cos(\theta_1 + 28^\circ) & \text{, if } \theta_1 < 90^\circ \\ T_{KNEE} = -mgl_{SHANK}\cos(\theta_1) & \text{, if } \theta_1 > 90^\circ \end{cases} \tag{3}$$

These infer that

$$\begin{cases} T_{KNEE} < 0 & \text{, if } \theta_1 < 90^\circ - 28^\circ = 62^\circ \\ T_{KNEE} > 0 & \text{, if } \theta_1 < 90^\circ - 28^\circ = 62^\circ \end{cases} \tag{4}$$

From Eq. (4), we know that BW does not cause the knee to flexion if θ_1 is larger than 62 degrees. From the biomechanical view, in the beginning of the SS, heel strike normally lands at θ_1 more than 90 degrees, and becomes smaller in the mid-stance. Toward the end of the SS as opposite foot strikes, θ_1 is normally around 70 degrees.

Now let's consider walking with a bent knee. This is commonly observed in pathological gait and may cause flexion torque on the knee. We pinpoint three instance in the SS: foot strike (θ_{HIP}

=20 degrees), mid-stance (θ_{HIP} =0 degrees), and (θ_{HIP} =-20 degrees). Assume the torso angle is zero during the SS.

From Figure 2-3, we know that

$$\theta_1 = 90^{\circ} + \theta_{HIP} - \theta_{KNEE} \tag{5}$$

Combining Eq. (3) with Eq. (5), we can calculate T_{KNEE} under different knee angle θ_{KNEE} and in different subject BW. The torque generating from the BW extends the knee when hip angle is 0 and 20 degrees and knee angles ranges from 0 to 20 degrees. When hip angle is -20 degrees, the torque on the knee for an 80 kilograms subject is extension torque when knee angle is smaller than 8 degrees. The torque increases drastically to 40 newton-meter when knee angle is 15 degrees. The knee could be flexed in these conditions. However, keep in mind that this moment in time is also when the knee is about to be flexed, so this biomechanical advantage actually encourages knee flexion.

2.2.1.2 Parallel Standing

Another common posture in exoskeleton use, parallel standing, can be modeled in the same way. The only difference is that both legs support the body weight instead of one single leg. It is obvious the knee torque that needs to support in standing is smaller than those in single stance because both legs share the body weight. Therefore, the torque that prevents knee flexion in SS should also prevent knee flexion in parallel standing.

2.2.1.3 Double Stance (DS) (a Split Standing Posture)

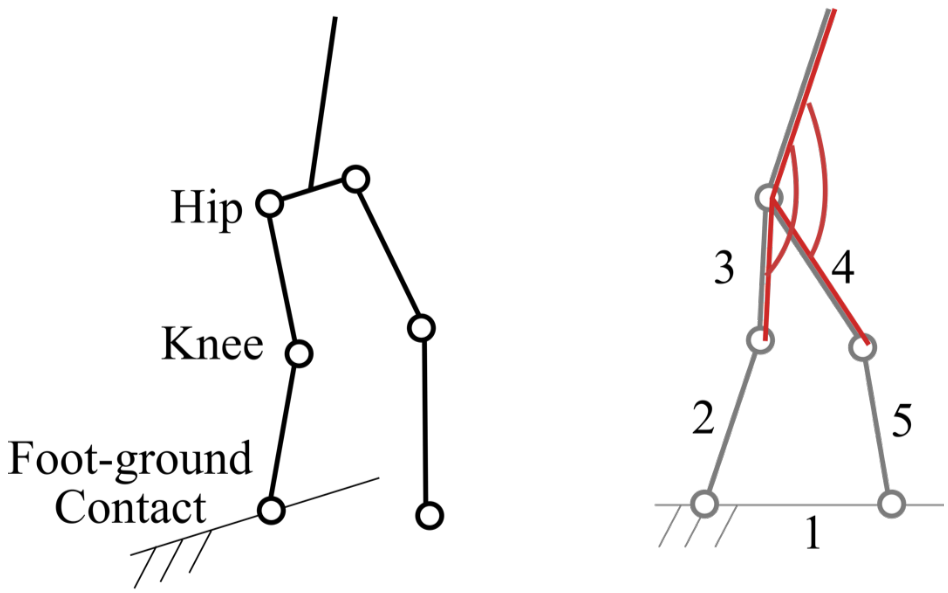

Figure 2-6: Model of a double stance posture.

DS is a 5 bar linkages closed kinematic chain (2-DOFs) plus one open kinematic chain (1-DOF), which has totally 3-DOFs, with three constraints (one torso angle and two hips control) as shown in Figure 2-6. The 5-linkages kinematic chain and its linkage numbers are shown in black, and the constraints are shown in red. The kinematic chain is fully defined. Therefore we do not need additional constraint on the knee to prevent knee from flexing.

Note that when either one or both knees reach full extension and are constrained by an overextension stopper, the system is overly constrained. In that case we need to release one or two constraints to avoid confliction. Therefore, we are able to deduce that if either one leg is constrained by the overextension stopper, the user does not need to use the crutches to hold their torso, but the system will keep the balance. In another case, if the torso is connected mechanically to the ground, either one constraint (torso or hip motors) needs to compensate to others.

On the other hand, if both knees are constrained by the overextension stoppers, the DOF of the kinematic chain is minus two. This indicates that two controls should be reduced, otherwise some compromise of joint angles should be observed due to the confliction of all the controls.

2.2.2 Allow The Knee To Flex

At some instances of the exoskeleton use, we need to allow the knee to flex. This includes the end of the stance phase.

2.2.2.1 At the end of the stance phase

At the end of the stance phase when the back leg is about to flex the thigh and bend the knee for toe off, the posture has smallest θ_1, which helps bend the knee. Although we have biomechanical advantages over flexing the knee, we want to make sure that the resistive torque that we designed for preventing knee from flexing does not hinder knee flexion at the end of the stance phase.

Assume the hip actuator that provides huge torque on the hip. From the kinematic chain view, the knee can definitely be bent. However if the knee torque is high as well, realistically another joint may break – the foot-ground contact, it may slip. Therefore the friction force on the foot-ground contact must be able to break the knee before the foot starts slipping. The maximum torque generating on the knee from the body weight and the friction before slipping is:

$$T_{KNEE} = -\%mgl_{SHANK}\cos(\theta_1) - \mu_S\%mgl_{SHANK}\sin(\theta_1) \qquad (6)$$

where $\%mg$ is the portion of the body weight on the back foot; μ_S is the maximum static friction.

Assume the coefficient of static friction is one, only 30% of the body weight is on the back foot, and the torso angle is zero. For an 80-kilograms subject at the end of the stance phase when the hip angle is -20 degrees, the knee torque ranges from (flexion torque) 80 to 130 newton-meters when knee angle ranges from 0 to 30 degrees. This results shows that the body weight and friction force is advantageous to create high flexion torque on the knee at the end of the stance phase..

2.2.3 Assist In Toe Clearance

Toe clearance is one of the most important factors that correlate to walkability in many orthoses, prosthetics or exoskeleton applications. Toe clearance is the distance between the toes to the ground when the leg swings forward. During the swing phase, the lower leg acts like a double pendulum. It is common knowledge that during the swing phase, most of the energy comes from the hip actuation. Therefore many orthoses, prosthetics or exoskeleton applications, the knee joint is free during the swing phase.

The benefits of these free-swing knees are simple design and low cost. However, toe clearance is compromised due to the loss of knee control. This loss of toe clearance may result in foot drag during gait.

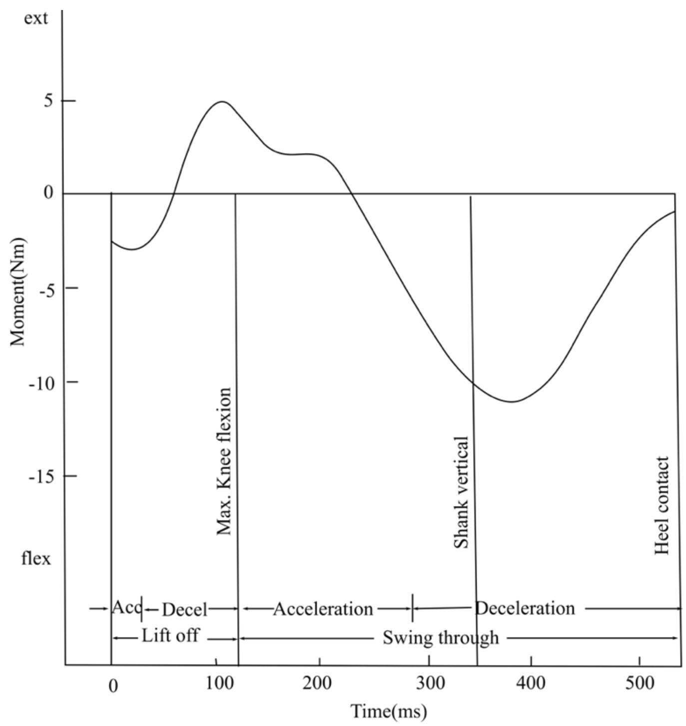

Figure 2-7: Predicted muscle torque around the knee (modified from [49]).

Normal gait was studied in order to understand the torque around the knee and their functions. Winter et al. [49] proposed a dynamic model that predicted the muscle moment around the knee of a normal, level ground walking gait by studying the knee acceleration. The normalized results are shown in Figure 2-7. The results suggest that the muscle provides flexion from 0~50 milliseconds in order to produce enough toe clearance; from 50~220 milliseconds, the knee muscles create an extension torque which accelerates the swing motion to get a faster gait; from 220~500 milliseconds, the muscles provide a flexion torque that decelerates the lower leg to smooth the knee extension. Overall, the torque from 0~50 milliseconds provides higher toe clearance, and the torque from 50~500 milliseconds provides a smoother gait.

From the above discussion, the artificial knee should provide flexion torque at the beginning of the swing phase. During the rest of the swing phase, artificial knee 100 does not provide any torque. The free swing-extension concept had been commonly practice in many orthoses or prosthetics in the market.

2.2.3.1 Dynamic Model of Swing

A model of dynamic swing leg is built to evaluate the effectiveness of the hypothesis. This dynamic model is similar to the aforementioned link segment model, with different constraints and utilizing Lagrangian dynamics for kinetic analysis. Toe clearances are calculated when the knee is a free joint and when the knee is applied by a flexion torque when knee angle is smaller than a threshold. The modeling detail is shown in the Appendix.

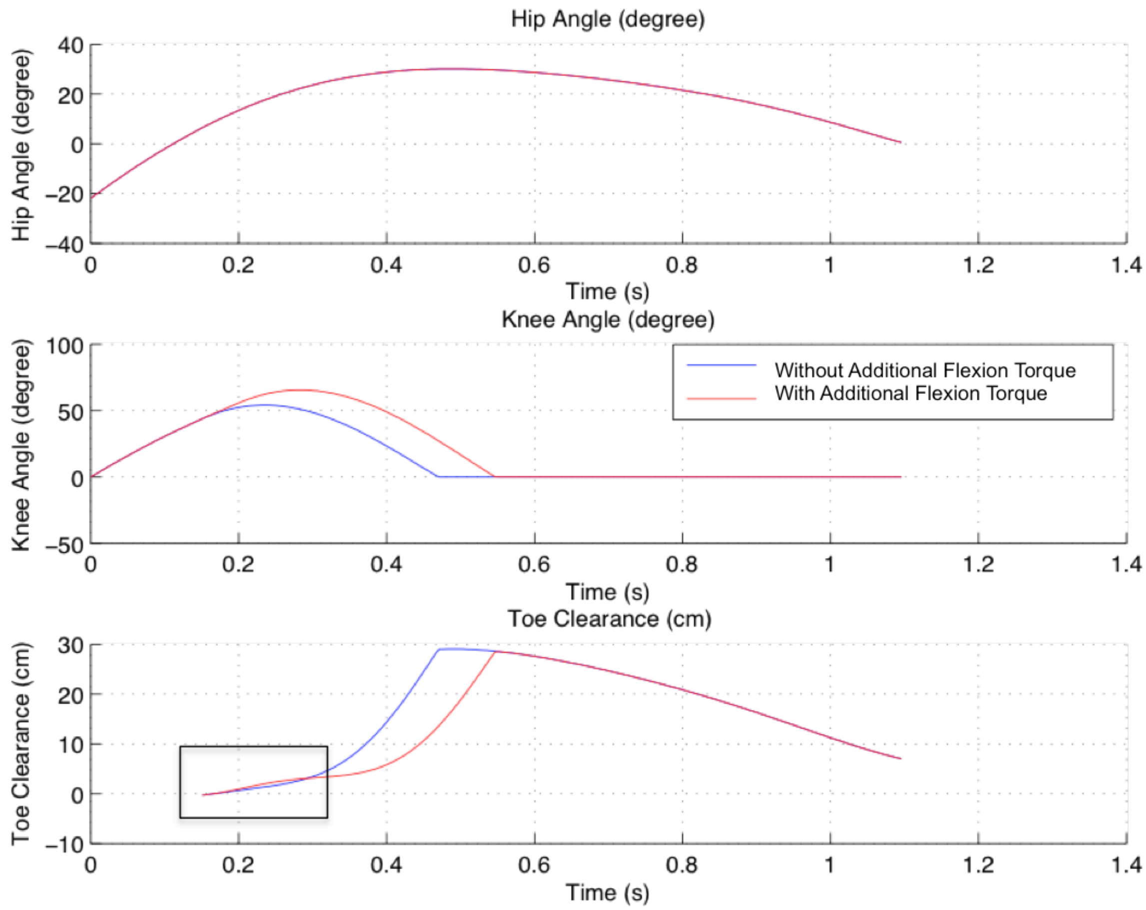

Figure 2-8: The results of the dynamic swing model: a slightly higher toe clearance is observed with an additional flexion torque in a period of time in the swing flexion phase.

Figure 2-8 shows the result of the model. Toe clearance related to tripping and falling is around the time when the knee is at its maximum flexion. In the model, it is when the time is between 0.2 and 0.3 seconds. With additional flexion torque, the knee angle is increased and the time when knee starts extend is delayed. This combination results in a higher toe clearance in this time range that relates to tripping.

2.3 REMARKS

These biomechanical analyses provide useful insights into a novel knee design. To the author's knowledge, no passive knee devices setup their design criteria based on the kinematics as a system. This research considered the systematic kinematic chain and the constraints on the system and established the design criteria that are different than all the other knee devices. Artificial knee 100 is also the first knee device that tried to tackle the problem of toe clearance.

To summary the above discussions, the body weight help extends the knee during the single stance phase if the knee angle is small. The body weight facilitates knee flexion at the end of the stance phase when the knee is about to flex. During the double stance, the system is fully defined by the kinematic chain with controlled hips. This infers that with controlled hip and extended knee in stance, little help is required on the knee to create ambulation. However, considering pathological gait differences, muscle resistance, or environmental influences, it is safer to have a mechanism that prevents the knee from flexing during the majority of the stance phase (i.e. before the knee is ready to flex). Next, a flexion torque in swing-flexion phase is hypothesized to increase toe clearance, which is a desire goal. Finally, free swing extension without resistive torque should be considered because the knee can extend as a result from the inertia of the lower limb. The free-swing-extension concept had been commonly practice in many orthoses and prosthetics in the market.

3 MECHANISM

3.1 DESIGN REQUIREMENTS

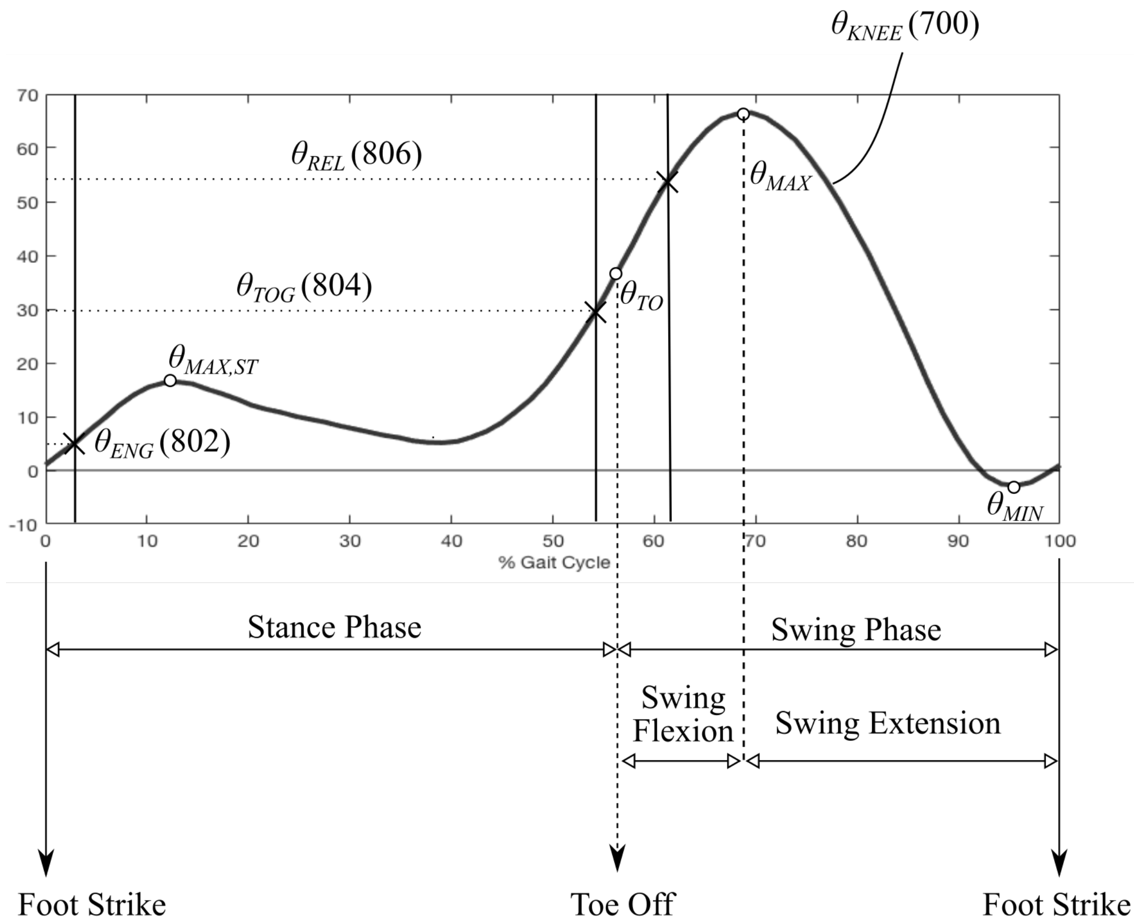

Figure 3-1: The function of the knee mechanism reflecting on Winter's CGA data.

As can be seen in Figure 3-1, human knee angle, during the entire walking cycle, flexes twice: once during the stance phase and once during the swing phase. During the stance phase the knee angle increases (flexes) to $\theta_{MAX,ST}$ During the swing phase, the knee reaches maximum knee flexion θ_{MAX}. θ_{TO} represents the knee angle during the toe off. The knee reaches the minimum knee angle θ_{MIN} toward the end of swing phase. Although there are variation from the plot shown in Figure 3-1, generally the human knee goes through two flexions: a small flexion during the stance phase and a large one during the swing phase. The small flexion is in response to the person's weight while the larger flexion provides toe clearance during the swing phase.

The objective here is to design an artificial knee (either a prosthetic knee or an orthotic knee) to exhibit the basic behavior of the human knee with no actuators, sensors and computers. If such knee becomes realizable, it can be used as a low cost artificial knee for various orthotic, prosthetic and exoskeleton applications. Artificial knee comprises thigh link 102, shank link 104, rotatably coupled to each other at knee joint 140. Based on the observation described above in Chapter 2, the objective is to design an artificial knee 100 that exhibits three behaviors:

1. Artificial knee 100 should resist the knee flexion during the stance phase. This means artificial knee 100 helps the human during the stance phase to support a portion of user's weight.
2. Artificial knee 100 should encourage knee flexion during the swing phase to assist in toe clearance during the swing flexion phase.
3. Artificial knee 100 should allow free swing extension in the swing extension phase.

The three specifications above mean that the artificial knee 100 will support the user during the stance phase, but it is free during the swing extension. It further encourages the knee flexion right at the early swing phase. An important aspect of this invention is that all of the above specifications are achieved passively without the use of actuators, computers and/or sensors.

According to above, artificial knee 100 should produce an extension torque from engagement angle 802 (represented by θ_{ENG} in Figure 3-1) to toggle angle 804 (represented by θ_{TOG} in Figure 3-1). This means that artificial knee 100 resists flexion and assists the user during the stance phase to support at least a portion of the user's weight.

Artificial knee 100 further should provide flexion torque from toggle angle 804 (θ_{TOG}) to release angle 806 (represented by θ_{REL} in Figure 3-1). This means artificial knee 100 encourages knee flexion during the swing phase to assist in toe clearance. θ_{TOG} represents a knee angle that torque in the artificial knee switches (toggles) from being an extension torque to a flexion torque. The extension torque is needed to support the weight, while the flexion torque is needed to clear the ground. Once the knee has accomplished the above two specifications faithfully, it then needs to freely extend and get ready for foot strike as shown in Figure 3-1. This means the mechanism that created flexion and extension torques should become ineffective when the knee is extending before foot strike. In summary, artificial knee 100 should first provide extension torque (from engagement angle θ_{ENG} 802 to toggle angle θ_{TOG} 804) and then should provide flexion torque (from toggle angle θ_{TOG} 804 to release angle θ_{REL} 806). Artificial knee 100 does not need to provide any other torque in any other phase of the knee trajectory.

The state when artificial knee provides extension torque is called the "extension support state", and flexion torque the "flexion support state".

One must specify angles θ_{ENG}, θ_{TOG}, θ_{REL} (represented by 802, 804, and 806) so that artificial knee 100 behaves as described above. The range limits of angles 802, 804, and 806 are defined by the three inequalities below:

$$\begin{gathered}\theta_{MIN} < \theta_{ENG} < \theta_{MAX,ST} \\ \theta_{MAX,ST} < \theta_{TOG} < \theta_{TO} \\ \theta_{TO} < \theta_{REL} < \theta_{MAX}\end{gathered} \tag{7}$$

Where, as shown in Figure 3-1, θ_{MIN} is the minimum knee angle during the gait, $\theta_{MAX,ST}$ is the maximum knee angle in the stance phase, θ_{TO} is knee angle at toe off, and θ_{MAX} is the maximum knee angle throughout the gait.

If $\theta_{ENG} > \theta_{MAX,ST}$, artificial knee 100 provides no resistance during some portion of stance phase. If $\theta_{REL} < \theta_{TO}$, toe clearance will not be encouraged. Ideally we want to select θ_{TOG} (804) exactly the same as the knee angle at toe off so we can start generating flexion torque as soon as toe off takes place. However, it is difficult to know when toe off will take place without sensors. To prevent any extension torque after toe off (because it might hinder knee flexion), we select θ_{TOG} (804) to be smaller than the average knee angle at toe off. Extension torque after toe off will prevent knee flexion needed for ground clearance. From our observations, the knee angle at toe off is around 35 degrees. Therefore in one embodiment, we aimed to choose θ_{TOG} (804) to be 30 degrees. On the other hand, conceptually we prefer to make θ_{ENG} (802) as small as possible and θ_{REL} (806) as large as possible to create more supportive torque. However (θ_{REL} - θ_{ENG}) needs to be within the range of normal knee operation range. This means

$$(\theta_{REL} - \theta_{\mathrm{ENG}}) < (\theta_{MAX} - \theta_{MIN})$$

From observations, θ_{MIN}, $\theta_{MAX,ST}$ and θ_{MAX} are around 0, 20 and 65 degrees, respectively. Considering various gaits for different individuals, in some embodiments, we aimed to design artificial knee 100 such that θ_{ENG} (802) and θ_{REL} (806) to be 5 and 55 degrees, respectively.

3.2 PROPOSED MECHANISM

3.2.1 Basic Architecture

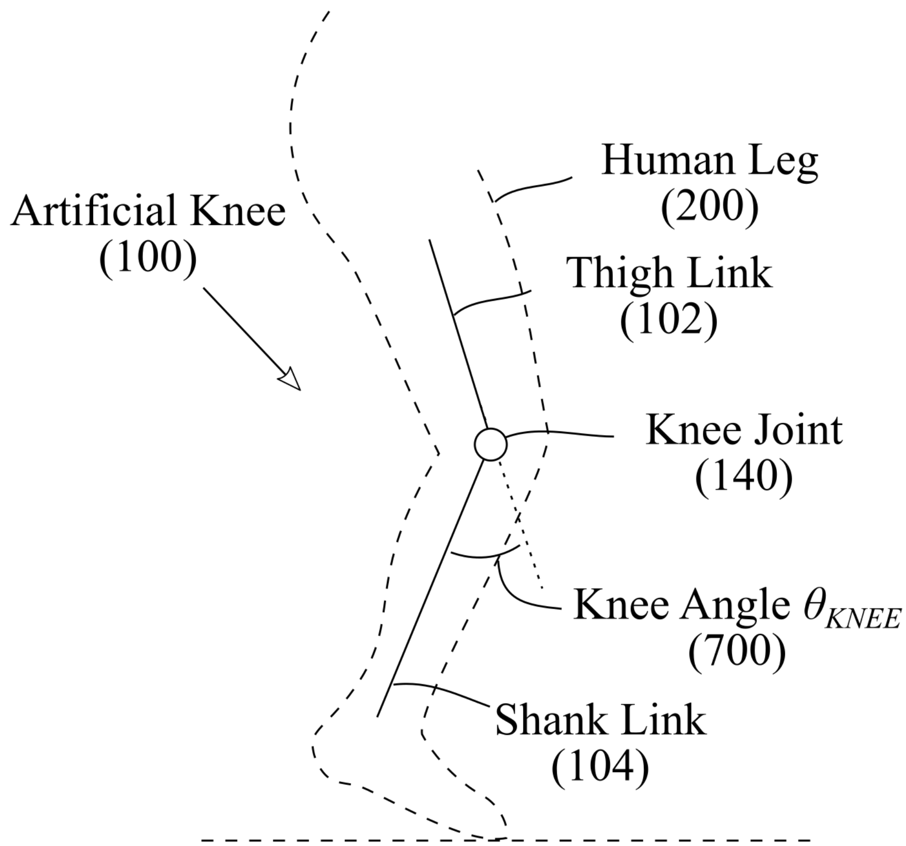

Figure 3-2: The schematic artificial knee includes a thigh link 102 and a shank link 104 rotating about at knee joint 140.

Figure 3-2 shows the schematic artificial knee 100 and knee angle 700. It comprises of thigh link 102, and shank link 104 rotating about a knee joint 140. The thigh and shank link is designed to move in unison with the human's thigh and shank. The knee joint 140 is approximately aligned with the person's knee. Knee angle θ_{KNEE} (700) represents the angle between shank link 102 and thigh link 104.

3.2.2 *The Four Bar Linkage*

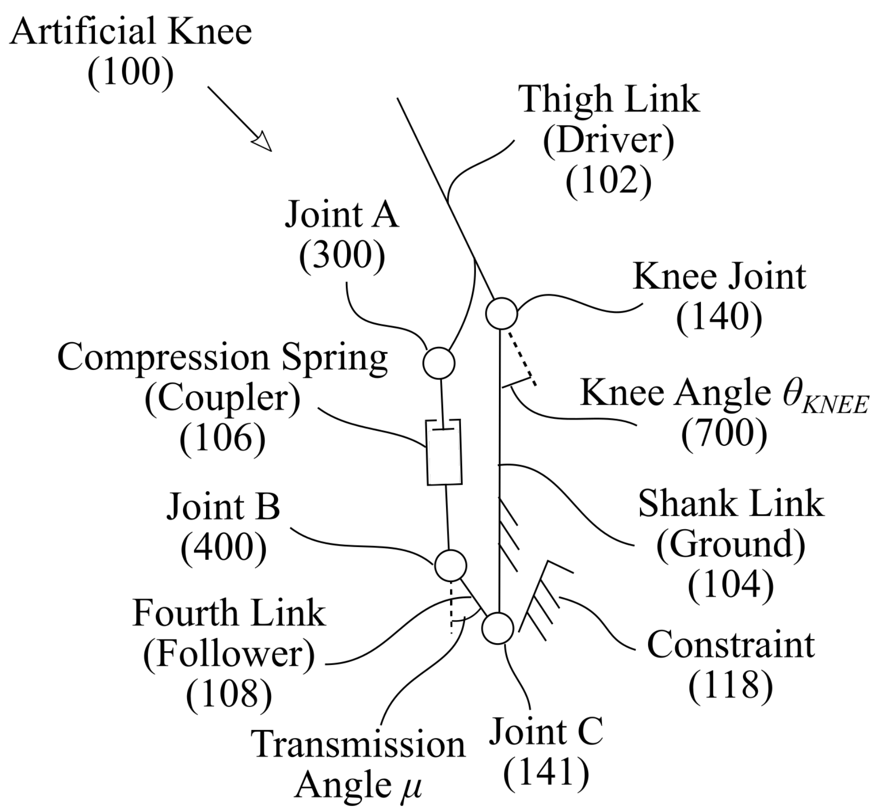

Figure 3-3: The proposed artificial knee 100 is in a form of four bar linkage.

Figure 3-3 shows that artificial knee 100 further comprises compression spring 106 rotatably coupled to thigh link 102 from its first end. In addition, artificial knee 100 further comprises fourth link 108 rotatably coupled with the second end of compression spring 106. Compression spring 106, fourth link 108 in addition to shank link 104 and thigh link 102, form a four bar linkage as shown in Figure 3-3.

3.2.3 *Utilizing Singular Points to Switch Between Configurations*

Below describes how this four bar linkage achieves the three design requirements mentioned above. To further understand the design method, one can consider thigh link 102 and shank link 104 as the *driver link* and *ground link* of the four bar linkage respectively. Furthermore, compression spring 106 and fourth link 108 are considered the *coupler link* and *follower link* of the four bar linkage

The transmission angle μ is defined by the angle between fourth link 108 and compression spring 106 as shown in Figure 3-3. When compression spring 106 is not compressed and it acts like a rigid link, this mechanism is a rocker-rocker four-bar linkage, which means that both driver link (thigh link 102) and follower link (fourth link 108) have a reciprocating motion.

As shown in Figure 3-3, constraint 118 is fixed on shank link 104 to stop fourth link 108 (follower) at certain angles. This constraint 118 can simply be a hard stop. For convenience, we assume constraint 118 to be parallel with follower 108 when it blocks follower 108.

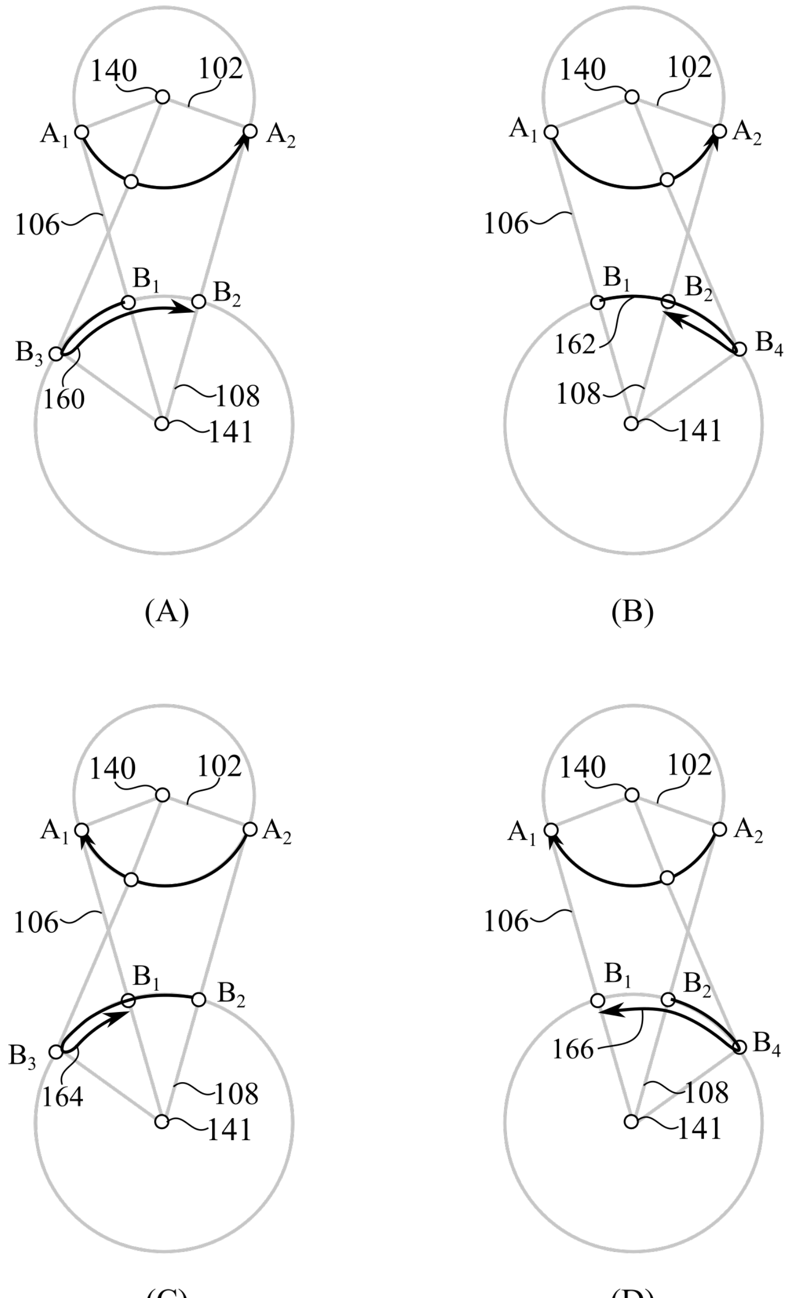

Figure 3-4: A 0π double-rocker mechanism moving from one singular point to another. (A) and (B) show driver 102 moving anti-clockwise from A_1 to A_2 while follower 108 is initially perturbed (A) to anti-clockwise following trajectory 160 (B) to clockwise following trajectory 162. (C) and (D) show driver 102 moving clockwise from A_2 to A_1 while follower 108 is initially perturbed (C) to anti-clockwise following trajectory 164 (D) to clockwise following trajectory 166.

When compression spring 106 is not compressed, artificial knee 100 forms a 0π double-rocker classified by Murray et al. [50] as shown in Figure 3-4. The range of motion of thigh link 102 (driver link for the four bar linkage) is defined by the singular points where compression spring 106 (coupler link for the four bar linkage) aligns with fourth link 108 (i.e., transmission angle μ is 0 or 180 degrees).

Figure 3-4(A) shows artificial knee 100 when thigh link 102 moves from one singular configuration A_1 to another singular configuration A_2. At each singular configuration, fourth link 108 has two options to move: can either follow trajectory 160 in Figure 3-4(A) or follow trajectory 162 shown in Figure 3-4(B). Singular configurations are the only points that fourth link 108 has these two options.

Figure 3-4(A) and Figure 3-4(B) show configurations where thigh link 102 moves from A_1 anti-clockwise to A_2. Fourth link 108 is initially located at singular point B_1. If fourth link 108 is perturbed to start moving anti-clockwise as shown in Figure 3-4 (A), then trajectory 160 shows how fourth link 108 moves from B_1 to B_2. Figure 3-4 (B) shows the same mechanism where thigh link 102 moves from A_1 to A_2 however fourth link 108 is initially perturbed to a clockwise direction. The fourth link 108 move from B_1 to B_2 along trajectory 162.

Similarly, Figure 3-4(C) and Figure 3-4(D) show configurations where thigh link 102 moves from A_2 clockwise to A_1. Fourth link 108 is initially located at singular point B_2. If fourth link 108 is perturbed to start moving anti-clockwise as shown in Figure 3-4(C), then trajectory 164 shows how fourth link 108 moves from B_2 to B_1. Figure 3-4(D) shows the same mechanism where thigh link 102 moves from A_2 to A_1 however fourth link 108 is initially perturbed to a clockwise direction. The fourth link 108 move from B_2 to B_1 along trajectory 166.

Now we consider configuration Figure 3-4(B) and Figure 3-4(C) only. As shown in Figure 3-4(B), fourth link 108 is perturbed to move along trajectory 162 at point B_1. As thigh link 102 moves from A_1 to A_2, fourth link 108 (follower) moves from B_1 to B_2 then to B_4 and back to B_2. As shown in Figure 3-4(C), fourth link 108 is perturbed to go along trajectory 164. As thigh link 102 moves from A_2 to A_1 in clockwise direction, fourth link 108 moves from B_2 to B_1 and to B_3 and back to B_2. Figure 3-4(B) and Figure 3-4(C) show how the four bar linkage operates for an entire cycle of thigh link 102, if fourth link 108 is perturbed at point B_1 and B_2 along trajectories 162 and 164.

The range of motion of follower 108 in this mechanism is defined when the thigh link 102 (driver link) aligns with coupler 106, i.e., when thigh link 102 is at point A_1 and A_2 in Figure 3-4.

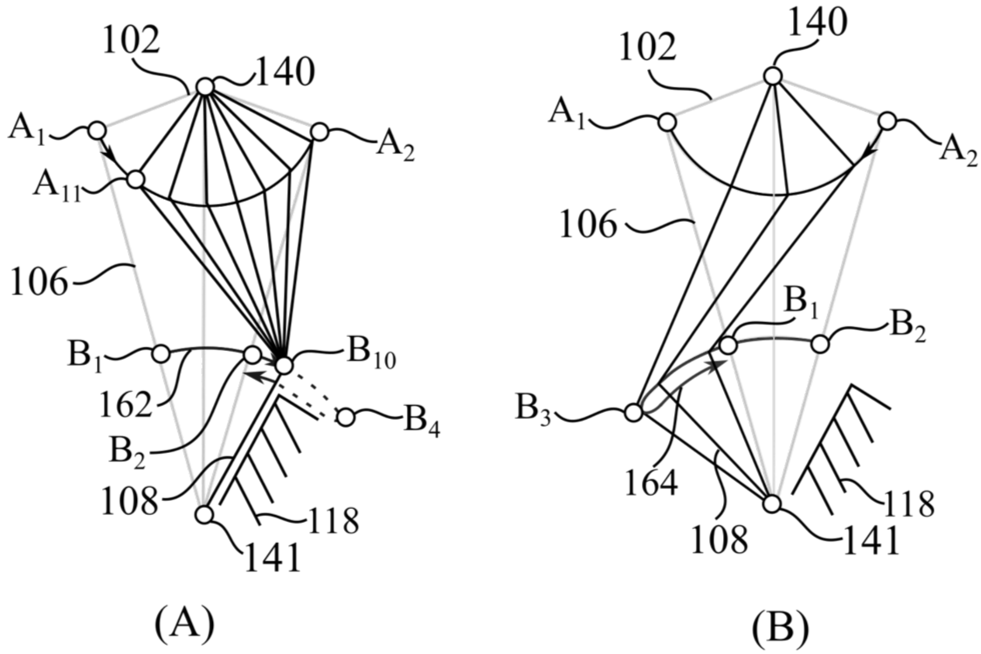

Figure 3-5: Constraint 118 blocks the fourth link 108 between B_2 and B_4 such that (A) when thigh link 102 moves from A_1 to A_2 compressive spring 106 is compressed, and (B) when thigh link 102 moves from A_2 to A_1 compressive spring 106 is not compressed.

Now we place constraint 118 that blocks fourth link 108 between B_2 and B_4 shown in Figure 3-5. Figure 3-5(A) represents artificial knee 100 when thigh link 102 rotates anti-clockwise from A_1 to A_2. Figure 3-5(B) represents artificial knee 100 when thigh link 102 rotates clockwise from A_2 to A_1.

When thigh link 102 moves from A_1 to A_2 counterclockwise, constraint 118 blocks fourth link 108 as shown in Figure 3-5(A). Since coupler link (compression spring 106) is compressible, as thigh link 102 continues to move, coupler link (compression spring 106) gets compressed and resists the rotation of thigh link 102 relative to shank link 104. When thigh link 102 approximately reaches point A_2, fourth link 108 gets released. A small torque applying on the fourth link 108 pushes fourth link 108 away from constraint 118. At this time, when thigh link 102 moves back from A_2 to A_1 clockwise, fourth link 108 moves along trajectory 164 with no constraint as shown in Figure 3-5(B). This means thigh link 102 moves from A_2 to A_1 with no resistance. Once thigh link 102 reaches point A_1, another small torque pushes fourth link 108 to be on trajectory 162. This behavior represents a situation where when thigh link 102 moves from A_1 to A_2, it will face resistance; however, from A_2 to A_1 thigh link 102 will not face any resistance.

The above-mentioned characteristics allow artificial knee 100 to have different configurations during operation, i.e., artificial knee 100 is a mechanism with variable configurations (MVTs). The singular points are important because they are the transition points between configurations.

This design is different from any other four-bar linkage to the author's knowledge. In general, operations close to singular points should be avoided because they reduce the driver link's efficiency regarding in controlling the follower. However in this implementation, driver link 102 is not fully controlled, but rather relies on the hip to indirectly control driver link 102. Therefore, instead of a normal four-bar linkage design where driver link 102 provides motion to the whole system, this mechanism utilizes coupler 106 to give support torque to driver link 102. In other words, the compressive spring 106 provides torque at specific instances to support knee joint 140.

In total, artificial knee 100 passes through two singular points in one gait cycle: one to transit the transmission angle μ from positive to negative, and another one to transit back to positive. At singular points, some source of torque applied to the follower is required to break the singular points because driver link 102 loses the ability to control the four bar linkage The direction of this torque determines the configuration as shown in Figure 3-5.

3.2.4 Toggle Switch

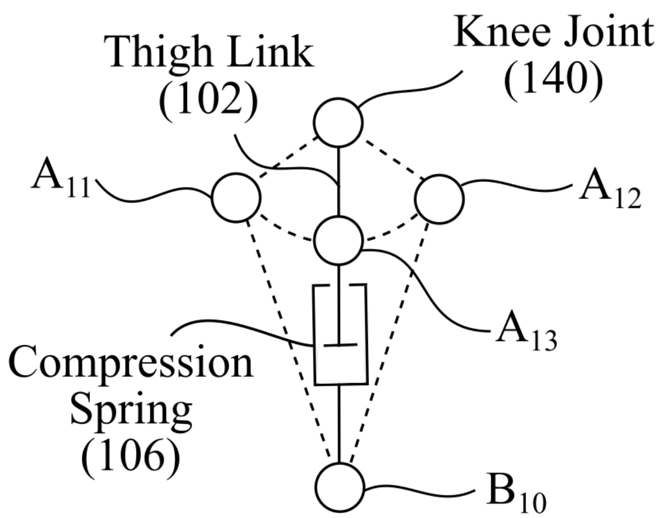

Figure 3-6: when fourth link 108 is blocked by constraint 118, artificial knee form a toggle switch.

When follower108 is constrained, coupler link 106 (compression spring 106) in this setup creates a toggle switch. As shown in Figure 3-6, the mechanism is at a toggle point when driver link 102 aligns with coupler link 106 (compression spring 106), at which point coupler link 106 is at its shortest length. The toggle point is an unstable equilibrium point at which point the coupler link 106 provides torque that pushes driver link 102 away from the toggle point.

3.2.5 Operation In The Gait

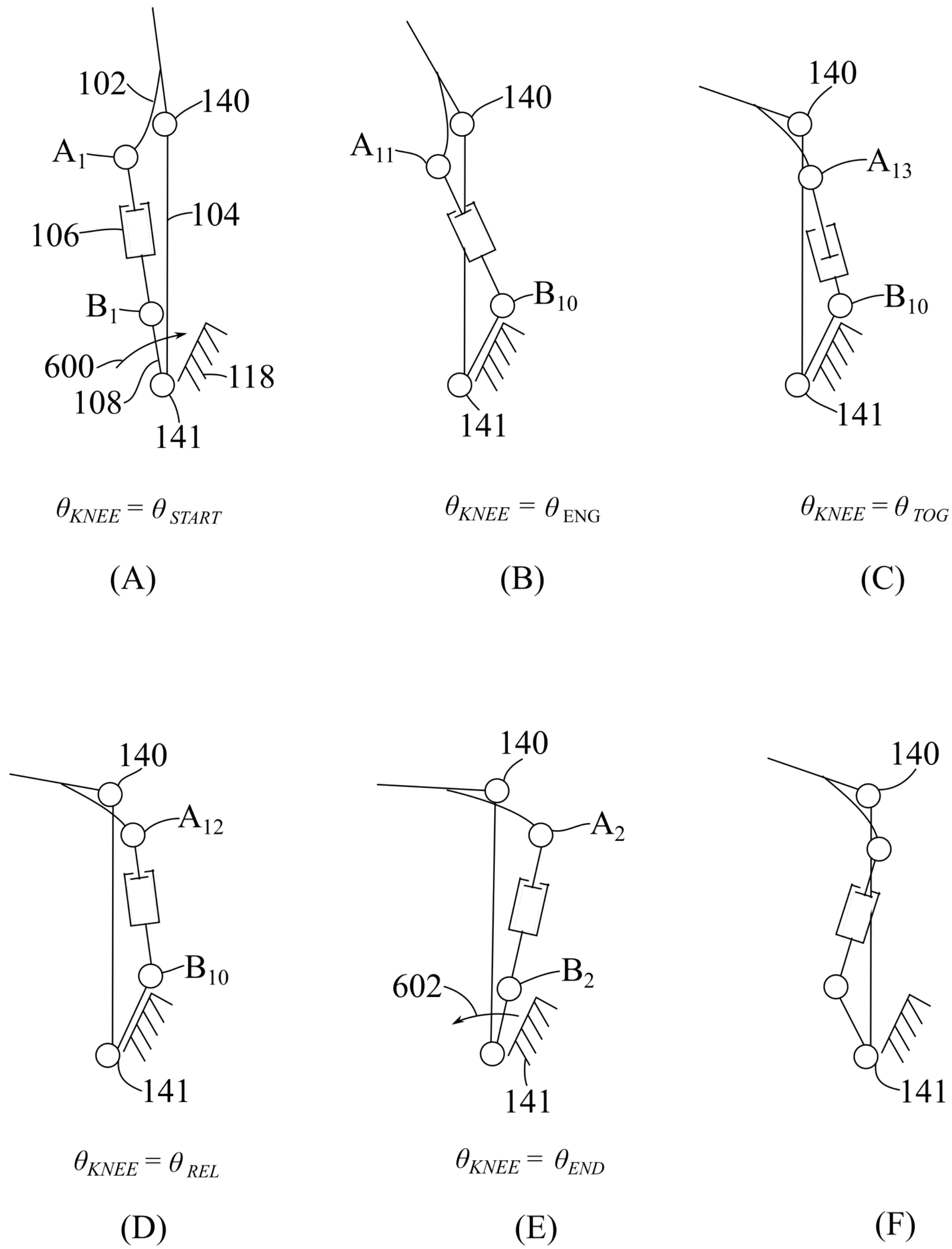

Figure 3-7: Operation of artificial knee 100 in a gait cycle.

The operation of artificial knee 100 in a gait cycle is shown in Figure 3-7. Figure 3-7(A) shows that the mechanism is at a singular point where coupler link (compression spring 106) aligns with the follower link (fourth link 108) when the knee is at virtually full extension (a very small degree of flexion). The knee angle at this instance is defined as start angle θ_{START} (800). With the application of a small torque along direction 600 on follower link 108, follower link 108 moves clockwise to break away from singular point and ultimately transitions the transmission angle μ to a negative value. As the knee flexes, follower link 108 rotates toward constraint 118 until follower link 108 encounters constraint 118 as shown in Figure 3-7(B). At this point, compression spring 106 begins to provide an extension torque as artificial knee 100 continues to flex. Knee angle θ_{KNEE} (700), at this instance is called engagement angle θ_{ENG} (802). This instant is also when the extension support state starts.

When thigh link 102 continues to rotate, there is a point where thigh link 102 aligns with coupler link (compression spring 106) as shown in Figure 3-7(C). At this point, the torque generated by coupler link 106 switches its direction and becomes a flexion torque. This point where the torque generated by compression spring toggles is referred to as toggle point. The knee angle θ_{KNEE} (700) at this instance is at toggle angle θ_{TOG} (804) when the flexion support state starts.

The flexion torque exists until coupler link 106 reaches its original length as shown in Figure 3-7(D). Knee angle θ_{KNEE} (700), at this point, is defined as the release angle θ_{REL} (*806*).

The thigh link 102 continues to rotate counterclockwise until it reaches another singular point when knee angle θ_{KNEE} (700) is at the end angle θ_{END} (808) as shown in Figure 3-7(E). At this point, a small torque on the follower 108, along direction 602, causes follower link 108 to rotate away from constraint 118. Transmission angle μ at this time switches from negative to positive.

During knee extension as shown in Figure 3-7(F), driver link 102 rotates clockwise, and follower link 108 rotates away from constraint 118. No torque resists driver link 102.

When driver link 102 keep rotating clockwise (knee extension) and returns back to Figure 3-7(A), artificial knee 100 is again at a singular point at which the transmission angle μ is on the verge of shifting signs.

The state of artificial knee 100 between Figure 3-7(E) and Figure 3-7(A) is where we call the first free state. The state of artificial knee 100 between Figure 3-7(A) and Figure 3-7(B) is the second free state. The state of artificial knee 100 between Figure 3-7(B) and Figure 3-7(C) is extension support state. The state of artificial knee 100 between Figure 3-7(C) and Figure 3-7(D) is the flexion support state. The state of artificial knee 100 between Figure 3-7(D) and Figure 3-7(E) is the third free state.

3.2.6 *Mechanism States In Gait Cycle*

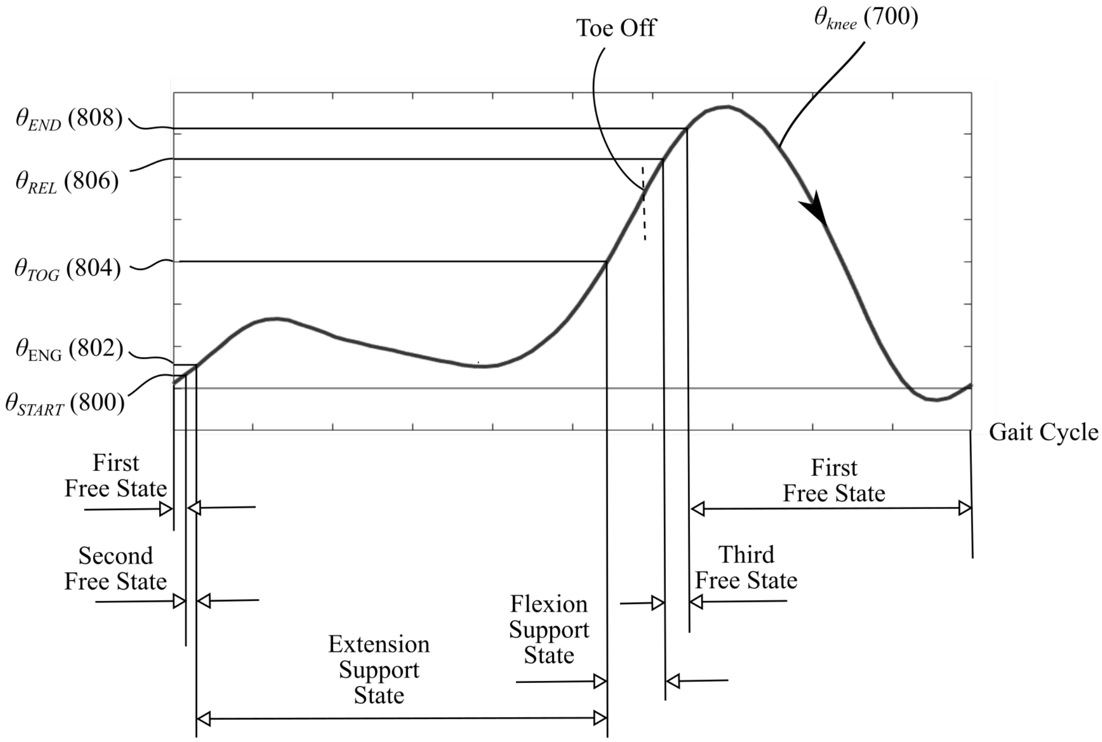

Figure 3-8: The states of the artificial knee 100 corresponding to the knee angle θ_{KNEE} (700) in the CGA data.

Figure 3-8 depicts the states of the artificial knee 100 corresponding to the knee angle θ_{KNEE} (700) in the CGA data. Artificial knee 100 is in the first free state as the gait starts as knee angle θ_{KNEE} (700) is not larger than start angle θ_{START} (800). Artificial knee 100 is in the second free state when knee angel θ_{KNEE} (700) is between start angle θ_{START} (800) and engagement angle θ_{ENG} (802). Artificial knee 100 is in the extension support state when knee angle θ_{KNEE} (700) is between engagement angle θ_{ENG} (802) and toggle angle θ_{TOG} (804). Artificial knee 100 is in the flexion support state when knee angle 700 is between toggle angle θ_{TOG} (804) and release angle θ_{REL} (806). Artificial knee 100 is in the third fee state when knee angle θ_{KNEE} (700) is between release angle θ_{REL} (806) and end angle θ_{END} (808).

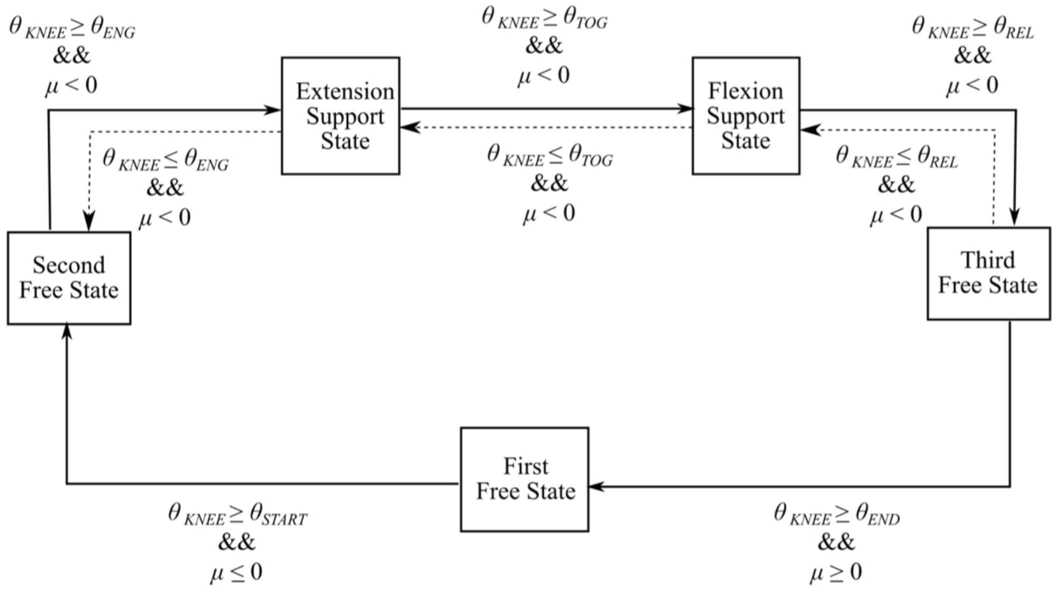

Figure 3-9: States of artificial knee 100.

Figure 3-9 depicts the states of artificial knee 100. The solid lines show when artificial knee 100 is operated normally as the knee angles θ_{KNEE} (700) follows the CGA data as shown in Figure 3-8. The dashed line shows the mechanism state flow if the knee angle does not perform normally. The mechanism in extension support state, flexion support state, or third free state could return to its previous state. However, the mechanism cannot return to its previous state once it passes the singular angle, that is, starting angle θ_{START} (800) and end angle θ_{END} (808).

3.2.7 Reset Range $\Delta\theta_{RESET}$ and Supportive Range $\Delta\theta_{SUP}$

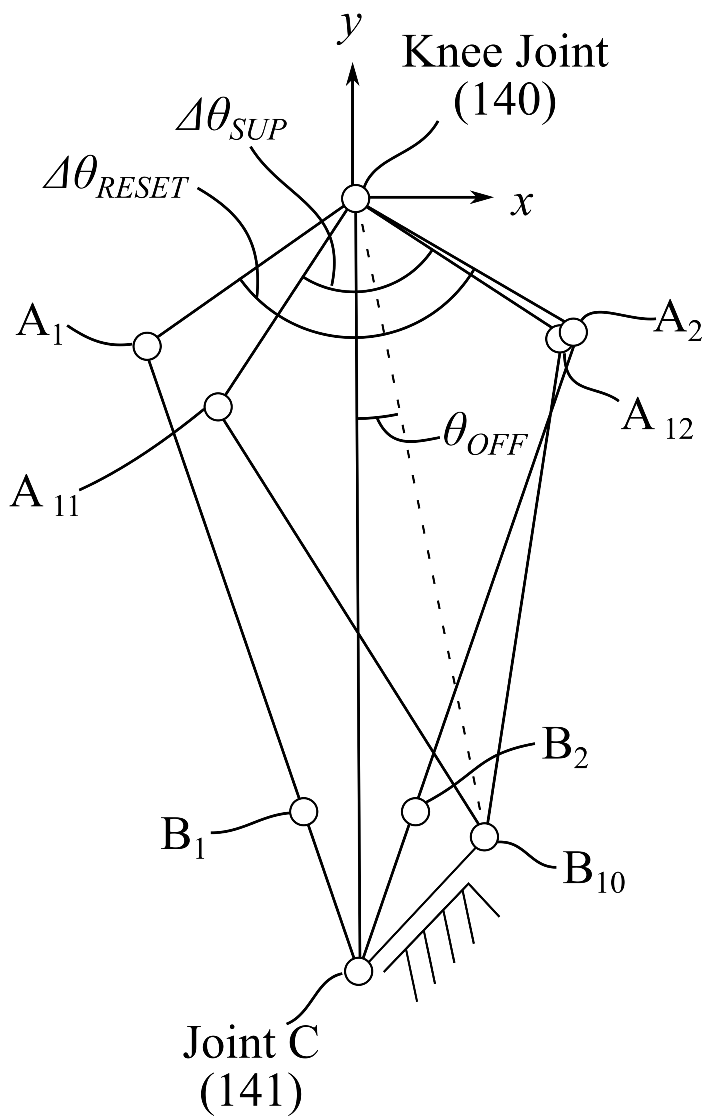

Figure 3-10: Superimposition of the operation of mechanism shows the supportive range $\Delta\theta_{SUP}$ and reset range $\Delta\theta_{RESET}$.

Figure 3-10 shows the superimposition of Figure 3-10. We defined reset range $\Delta\theta_{RESET}$ and supportive range $\Delta\theta_{SUP}$ as the following:

$$\begin{aligned} \Delta\theta_{SUP} &= \theta_{REL} - \theta_{ENG} \\ \Delta\theta_{RESET} &= \theta_{END} - \theta_{START} \end{aligned} \tag{8}$$

The geometrics of these ranges are shown in Figure 3-10. These ranges will be critical when designing the geometry parameters.

Intuitively, in our application the reset range $\Delta\theta_{RESET}$ should be as small as possible so that the mechanism can run in a smaller range; the supportive range $\Delta\theta_{SUP}$ should be as large as possible so that the mechanism can offer more torque, therefore be more effective. The reset range also confines the range of motion of the knee. We will tackle the problem by introducing an extension link later in this article.

3.2.8 Position of the Constraint

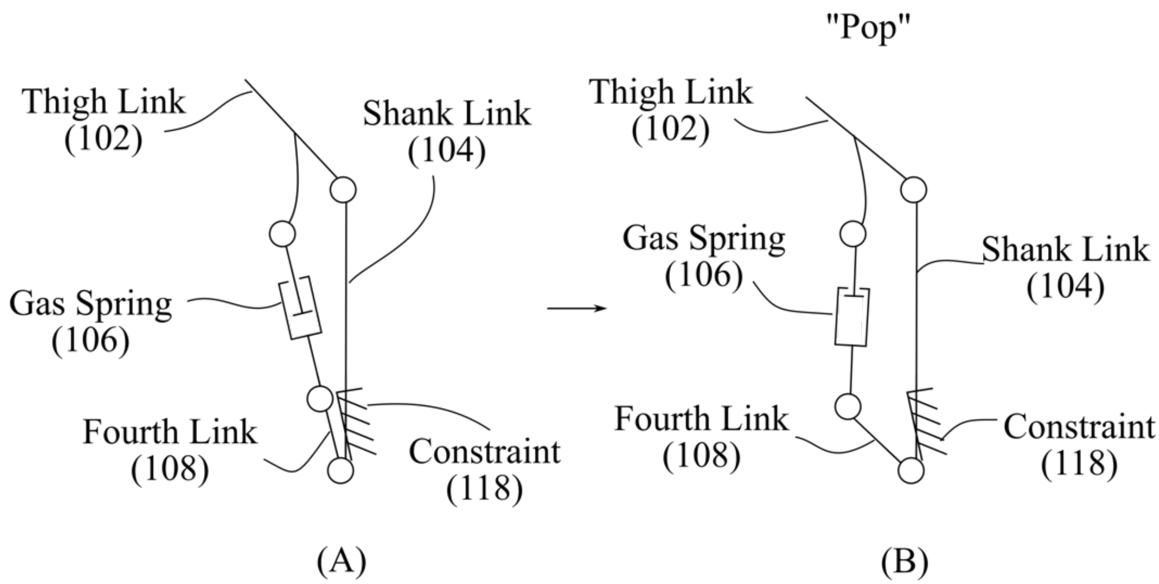

Figure 3-11: A popping motion takes place when the constraint aligns with the gas spring while the spring is still engaged. (A) shows the instant before the pop and (B) shows when the gas spring pop out.

Position of the constraint is important. The constraint should be positioned between B_2 and B_4 as mentioned in Figure 3-5. If the constraint is not positioned between B_2 and B_4 but between B_1 and B_2, a "popping" motion will take place. The "popping" motion is caused from disengaging the spring before the spring returns to its original length as shown in Figure 3-11(A) and (B). The linear force on the spring is designed to push the follower toward the constraint. However in Figure 3-11, the constraint is positioned that the spring 106 aligns with the follower while the spring is still in compress. As the driver rotates anti-clockwise, the spring force pushes the follower away from the constraint and causes the "popping" motion.

The "popping" motion is not ideal for the gas spring as a complete release of load all at once could cause internal damage to the gas spring. From an energy perspective, this is not ideal in our application either because we prefer to collect that energy in the spring to assist in flexing the knee. Therefore, in our design we make sure there is no popping motion, i.e., there is no instance when the constraint would align with the spring while the spring is in compression.

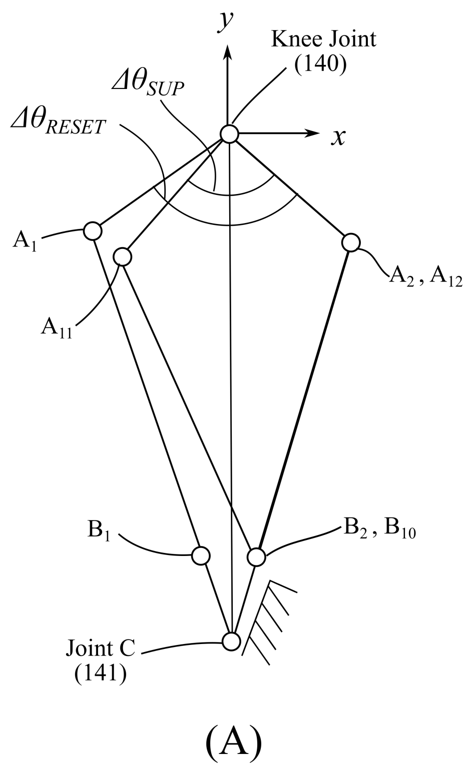

Figure 3-12: Rotating constraint 118 from (A) to (B) causes a decrease in the supportive range.

In the range of B_2 and B_4, constraint 118 should be positioned such that fourth link 108 is constrained close to B_2, because constraining closer to B_2 increases the supportive range $\Delta\theta_{SUP}$. As shown in Figure 3-12(A), the supportive range $\Delta\theta_{SUP}$ largest when B_{10} overlaps with B_2. In another case shown in Figure 3-12(B), the supportive range $\Delta\theta_{SUP}$ decreases as B_{10} is designed away from B_2. Based on the principle of maximizing the supportive range $\Delta\theta_{SUP}$ in our implementation, the constraint is designed so that it constrains fourth link 108 at a location very close B_2, but leaves a small clearance to prevent tolerancing issues that might cause popping out.

3.2.9 Energy Storage

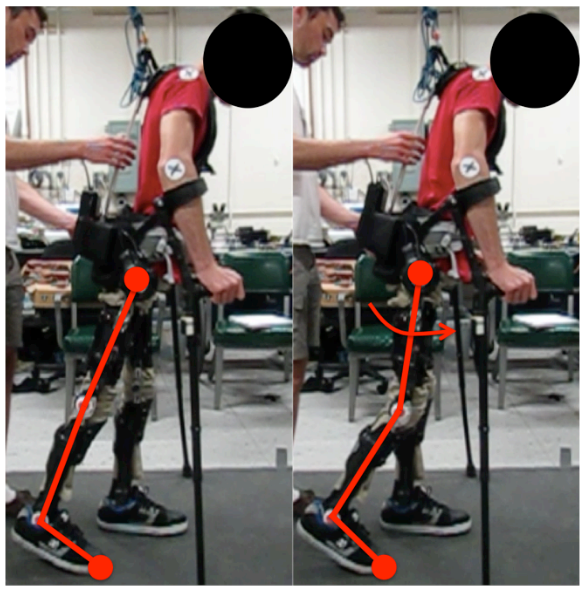

(A) (B)

Figure 3-13: Biomechanical advantage ensures knee flexion and energy storage.

How is it possible to ensure that the knee can continue to flex while experiencing a resistive (extension) torque from a compression spring? We had shown in Chapter 2 that the amount of torque on the knee generated by the body weight can be comparably large when the hip starts to flex as shown in Figure 3-13(A) and (B). Conceptually, we utilize this motion to compress the spring and store energy in it.

Let us recall the condition we briefly discussed in Eq.(7) – artificial knee 100 should already have passed the toggle point at toe off. This is because the energy storage method we have here utilizes the ground reaction force to flex the knee. In order to ensure that knee flexion continues, the energy storing state must finish before toe off.

3.2.10 Adding Extension Link to Expand Range of Motion

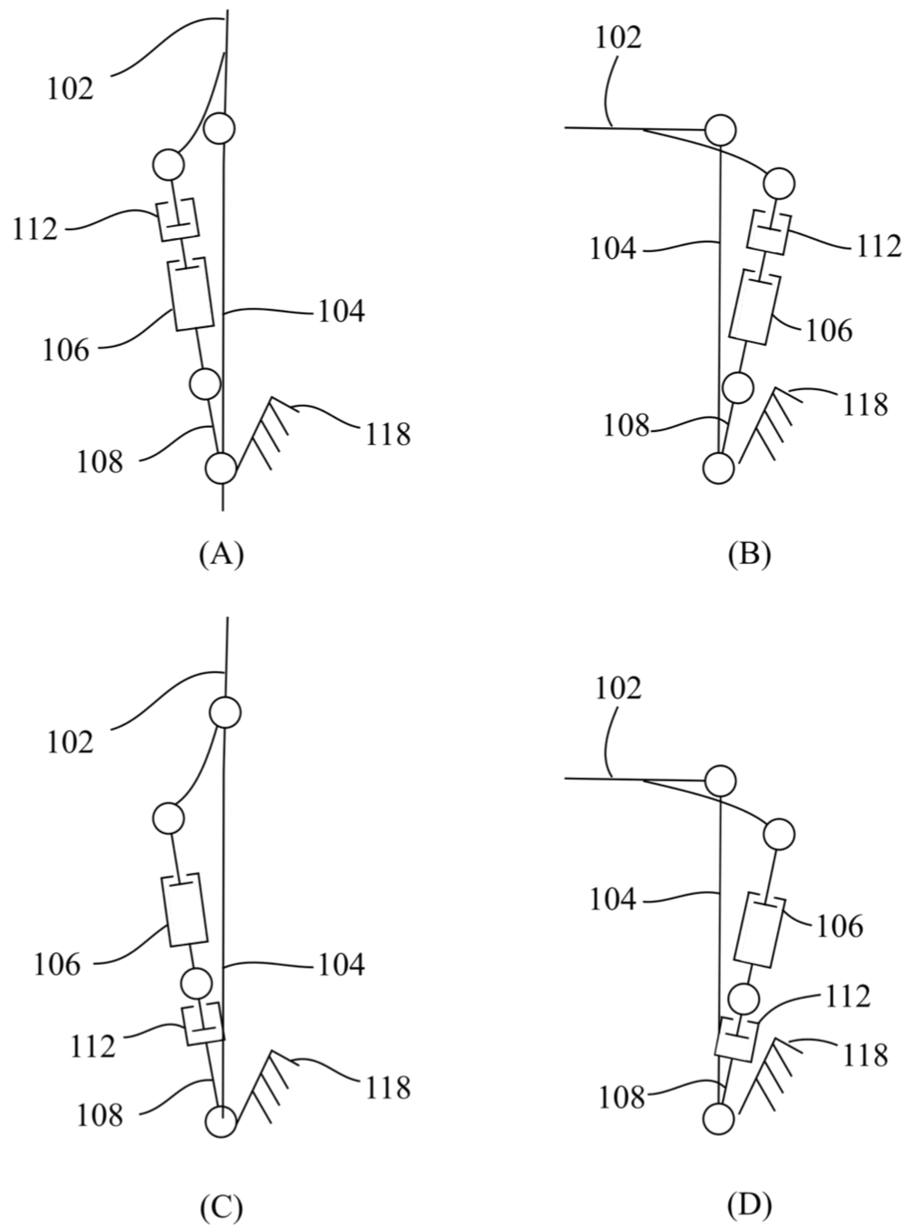

Figure 3-14: Extension link expands the range of motion without interfering with the operation. (A) and (B) show one embodiment of extension link 112. (C) and (D) show another embodiment of extension link 112.

Figure 3-14 depicts how artificial knee 100, in one embodiment, has an extension link 112 that allows knee angle θ_{KNEE} (700) to expand larger than the knee angle at the singular configurations, i.e., starting angle θ_{START} (800) and than end angle θ_{END} (808). In one embodiment, extension link 112 can be an extension spring that is capable of lengthening the coupler but always tends to return the coupler to its shortest length. Extension link 112 acts as a rigid link when it is not pulled so the aforementioned operation is not affected, but becomes extendable when the knee reaches outside the boundary of singular configurations.

Figure 3-14(A) and Figure 3-14(B) show one embodiment of artificial knee 100 with extension link 112, where the first end of extension link 112 is rotatably coupled to thigh link 102, and the second end of extension link 112 is linearly coupled to the first end of compression spring 106. Figure 3-14(A) depicts artificial knee 100 with extension link 112 that allows the knee angle θ_{KNEE} (700) to be about 0 degree. Figure 3-14(B) depicts artificial knee 100 with extension link 112 that allows the knee angle θ_{KNEE} (700) to be about 90 degree.

Figure 3-14(C) and Figure 3-14(D) show another embodiment of artificial knee 100 with extension link 112, where the first end of extension link 112 is rotatably coupled to the second end of compression spring 106, and the second end of extension link 112 is linearly coupled to follower 108. Figure 3-14(C) depicts artificial knee 100 with extension link 112 that allows the knee angle θ_{KNEE} (700) to be about 0 degree. Figure 3-14(D) depicts artificial knee with extension link 112 that allows the knee angle θ_{KNEE} (700) to be about 90 degree.

3.2.11 Preventing Overextension

It is critical to prevent the knee from overextending because it can be harmful to the patient's knees. This could be done with a simple hard stop on the shank link to stop the relative motion of the thigh link.

3.3 SIMULATION TORQUE PROFILE

3.3.1 Torque Calculation

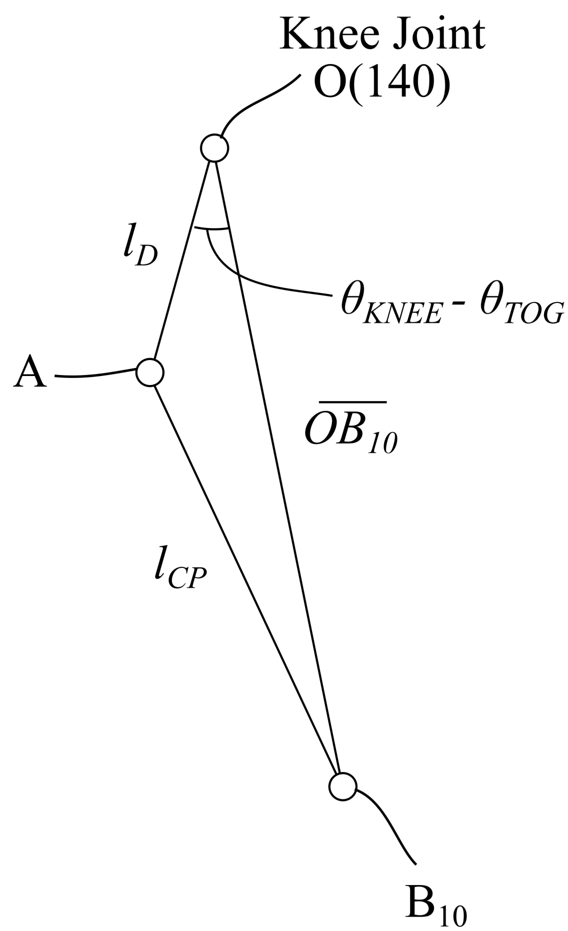

Figure 3-15: The triangle OAB_{10} defines the torque generated by the spring.

Figure 3-15 shows triangle OAB_{10} at an instance when the fourth link 108 is constrained. The torque generated by the spring can be formulated by:

$$\begin{aligned} T_{MECH} &= F_{SPRING}\overline{OB_{10}}\sin\angle OB_{10}A \\ &= F_{SPRING}\overline{OB_{10}}\sin(\theta_{KNEE}-\theta_{TOG})\frac{l_D}{l_{CP}} \end{aligned} \tag{9}$$

And engagement angle and release angle are:

$$\theta_{ENG} = \theta_{TOG} - \cos^{-1}\left(\frac{l_D^{\ 2} + \overline{OB_{10}}^{\ 2} - l_{CP0}^{\ 2}}{2 l_d \overline{OB_{10}}}\right)$$
$$\theta_{REL} = \theta_{TOG} + \cos^{-1}\left(\frac{l_D^{\ 2} + \overline{OB_{10}}^{\ 2} - l_{CP0}^{\ 2}}{2 l_D \overline{OB_{10}}}\right) \tag{10}$$

The maximum torque from the mechanism is

$$T_{MECH,MAX} = F_{SPRING} \overline{OB_{10}} \sin(\theta_{REL} - \theta_{TOG}) \frac{l_D}{l_{CP}}$$
$$= F_{SPRING} \overline{OB_{10}} \sin(\Delta\theta_{SUP}) \frac{l_D}{l_{CP0}} \tag{11}$$

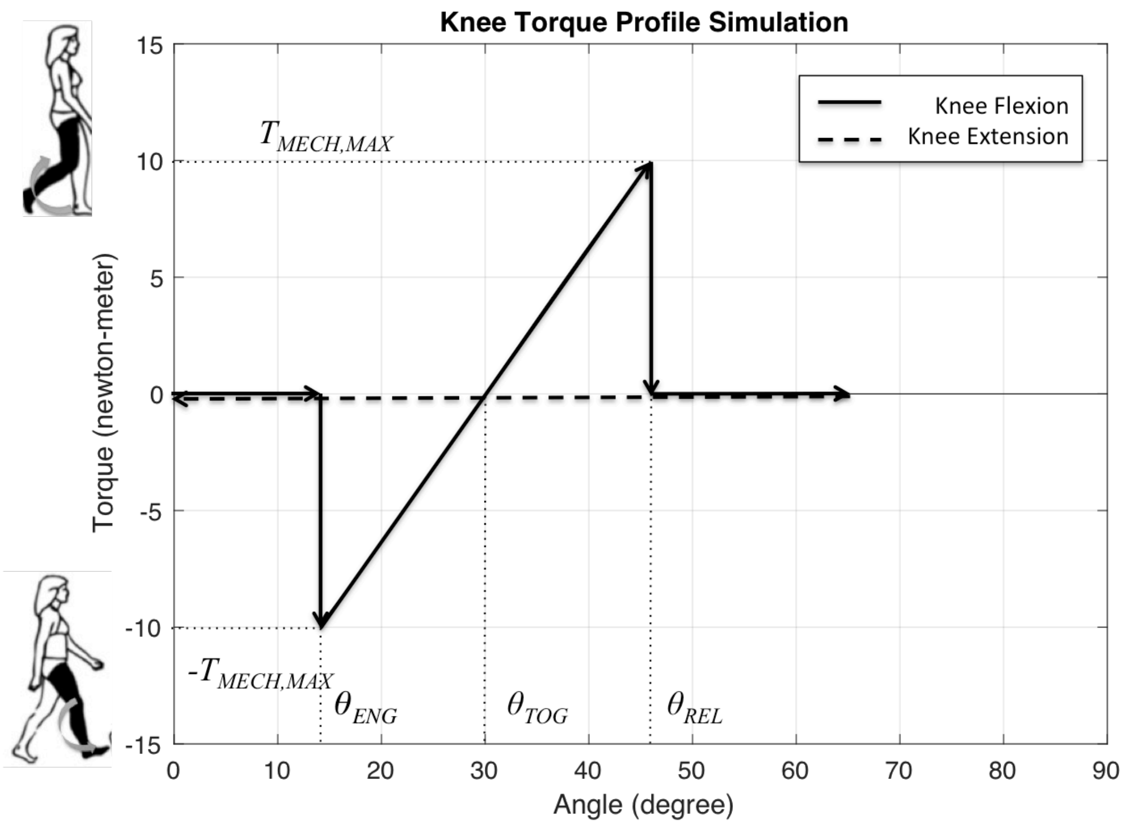

Figure 3-16: Simulation torque profile.

Figure 3-16 shows a simulation torque profile. The force of the gas spring is assumed to be constant for simplification, with the general agreement that the gas spring force is rather consistent throughout the stroke (with respect to the coil spring). With this assumption, the torque is opposite and mirrored with respect to the toggle angle. As the knee flexes from 0 degree to 90 degrees, the mechanism follows the solid line that provide torque in the supportive range – first an extension torque followed by a flexion torque. The torque outside the supportive range is zero. As the knee extends, the mechanism does not provide any torque as shown in the dashed line.

3.3.2 Parameters Of A Torque Profile

The design parameters for the aforementioned torque profile are

1. θ_{TOG}
2. $\theta_{REL} - \theta_{ENG}$ (i.e. supportive range $\Delta\theta_{SUP}$)
3. $T_{MECH,MAX}$

Figure 3-17 shows a few torque profiles with various aforementioned design parameters: θ_{TOG} in Figure 3-17(A), $\theta_{REL} - \theta_{ENG}$ in Figure 3-17(B), and $T_{MECH,MAX}$ in Figure 3-17(C). We could select these parameters based on the design requirements we discussed in earlier this chapter, and from the torque estimation we obtained from Chapter 2.

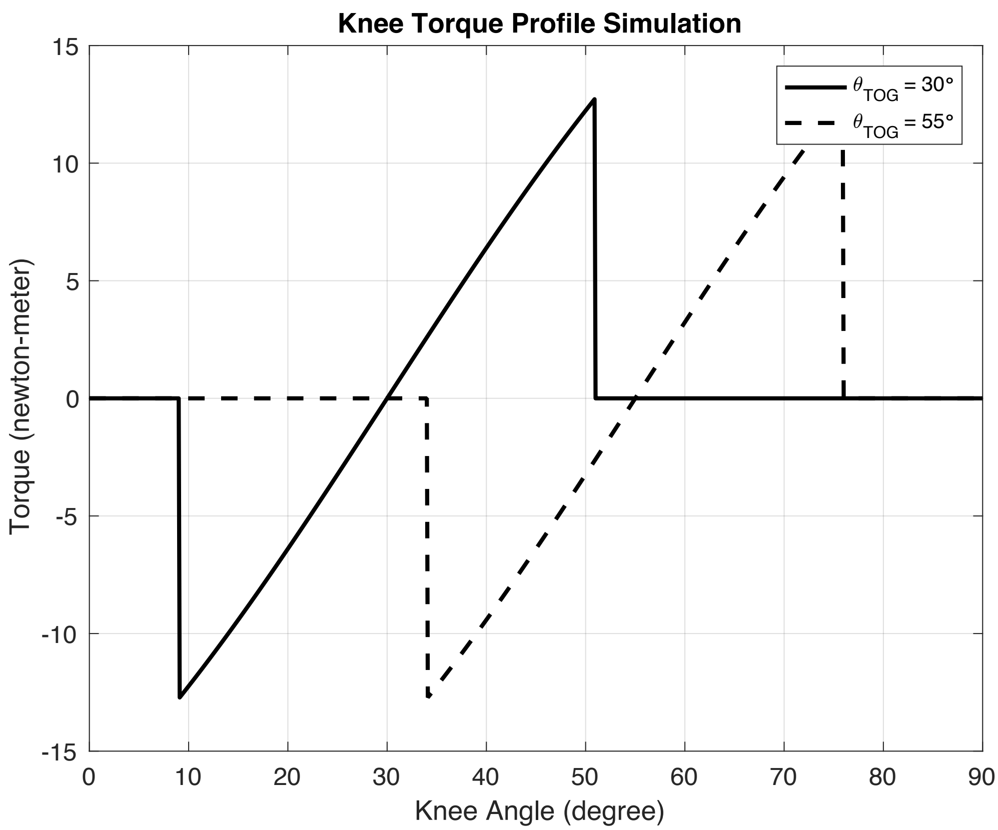

(A)

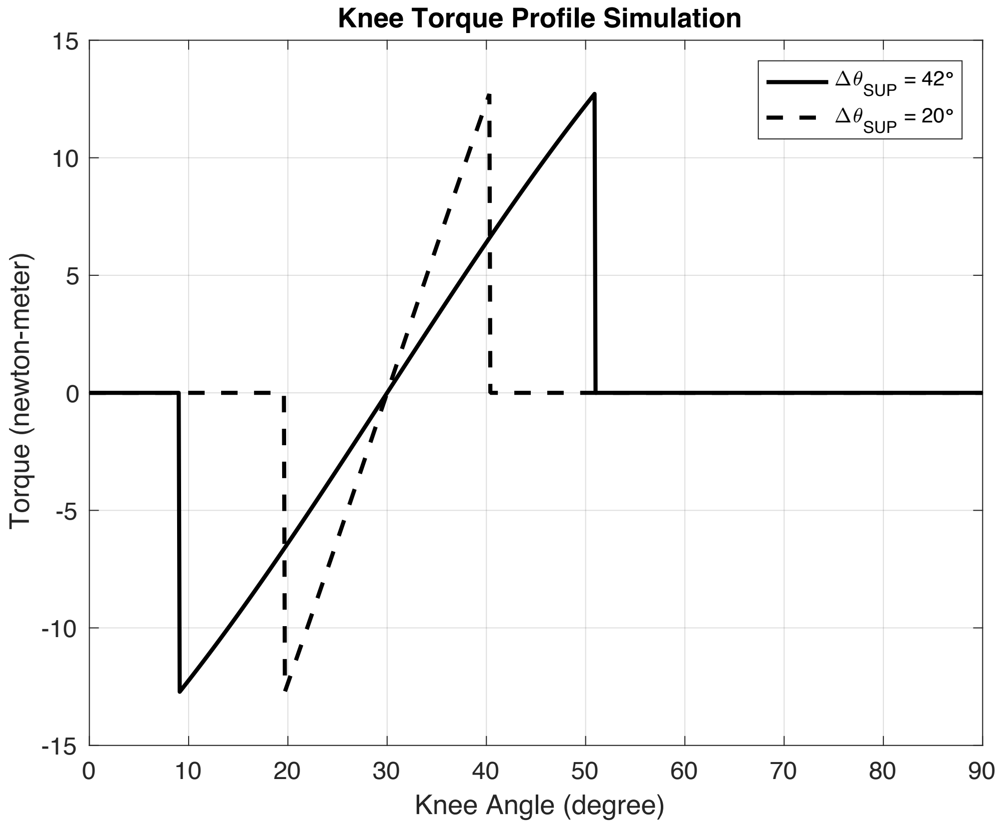
Knee Torque Profile Simulation
$\Delta\theta_{SUP}$ = 42°
$\Delta\theta_{SUP}$ = 20°
Torque (newton-meter)
Knee Angle (degree)
15
10
5
0
-5
-10
-15
0
10
20
30
40
50
60
70
80
90

(B)

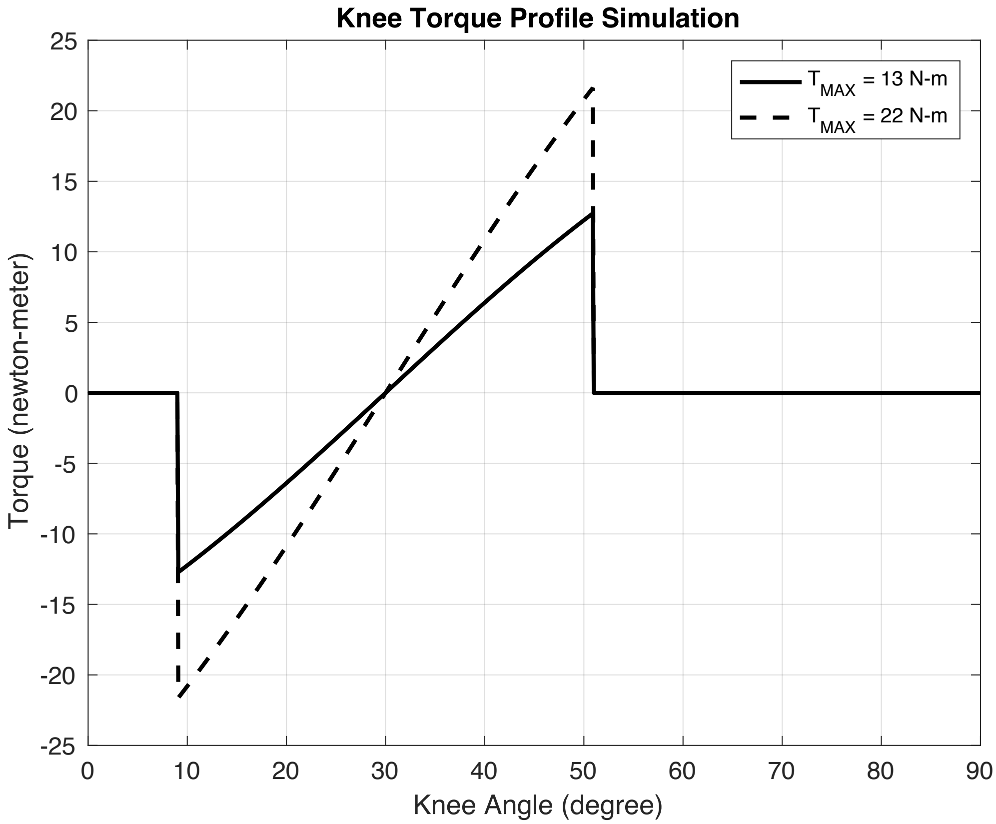

(C)

Figure 3-17: Torque profiles with various (A) θ_{TOG} (B) $\Delta\theta_{SUP}$ (C) $T_{MECH,MAX}$.

3.4 DESIGN PROCESS

3.4.1 The Designed Parameters and the Unknown Parameters

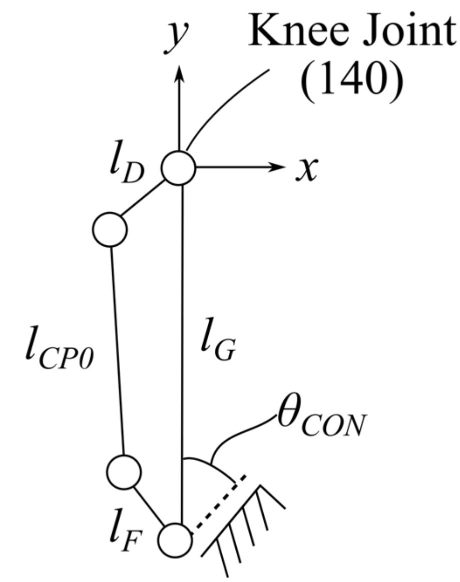

Figure 3-18: The parameters that form a specific design.

Based on the previous discussion, we propose a design process for this type of mechanism. To design such a four bar linkage as shown in Figure 3-18, the unknown parameters are:

1. l_D Length of driver link 102

2. l_G Length of ground link 104

3. l_F Length of follower link 108

4. θ_{CON} Angle between ground link 104 and follower 108 when follower 108 is constrained

And the designed and known parameters are:

1. l_{CP0} Original length of coupler 106; this is usually set by the manufacturer

2. F_{SPRING} Force of the spring. This is usually set by the manufacturer

3. $T_{MECH,MAX}$ Maximum designed torque of the mechanism

4. θ_{START} The smaller knee angle when artificial knee 100 is at the singular configuration

5. θ_{END} The larger knee angle when artificial knee 100 is at the singular configuration

6. θ_{ENG} The smallest knee angle when fourth link 108 is constrained

7. θ_{REL} The biggest knee angle when fourth link 108 is constrained

From these known parameters, we also know the following numbers (refer to Figure 3-10),

1. $\Delta\theta_{RESET} = \theta_{END} - \theta_{START}$

2. $\Delta\theta_{SUP} = \theta_{REL} - \theta_{ENG}$

3. $\theta_{TOG} = \dfrac{\theta_{REL} + \theta_{ENG}}{2}$

4. $\theta_{OFF} = \theta_{TOG} - \dfrac{\theta_{END} + \theta_{START}}{2}$

3.4.2 Design Process in Three Steps

Step 1: Get l_D (and $\overline{OB_{10}}$) by the following equations:

$$\begin{cases} l_{CP0}{}^2 = l_D{}^2 + \overline{OB_{10}}^2 - 2 l_D \overline{OB_{10}} \cos(\dfrac{\Delta\theta_{SUP}}{2}) \\ T_{MECH,MAX} = F_{SPRING} \overline{OB_{10}} \sin(\dfrac{\Delta\theta_{SUP}}{2}) \dfrac{l_D}{l_{CP0}} \end{cases} \tag{12}$$

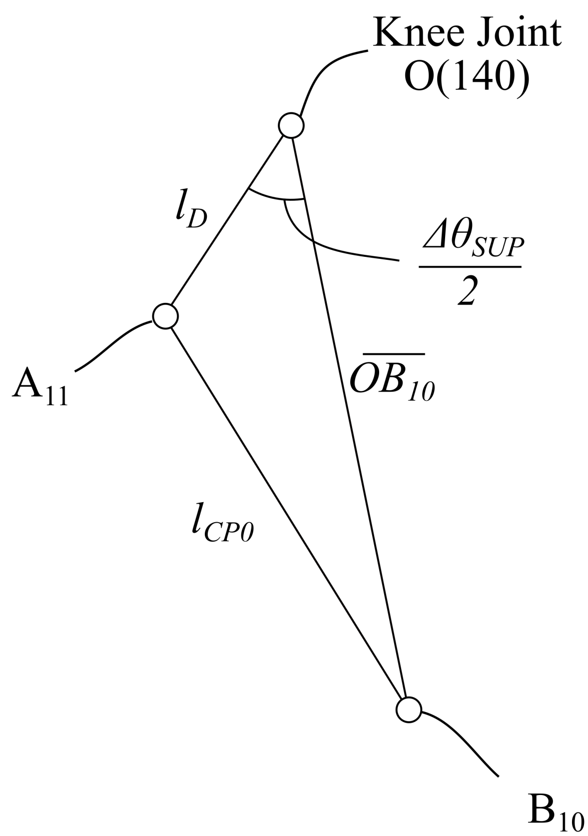

Figure 3-19: The geometry constraints for design process step 1.

We obtain these equations from the triangle $OA_{11}B_{10}$ as shown in Figure 3-19.

Step 2: Get l_F, l_G, and θ_{CON} by the following equations:

$$
\begin{cases}
(l_{CP0}+l_F)^2 = l_D{}^2 + l_G{}^2 - 2l_D l_G \cos(\dfrac{\Delta\theta_{RESET}}{2}) \\
l_F{}^2 = l_G{}^2 + \overline{OB_{10}}^2 - 2l_G \overline{OB_{10}} \cos\theta_{OFF} \\
\dfrac{\sin\theta_{OFF}}{\sin\theta_{CON}} = \dfrac{l_F}{\overline{OB_{10}}}
\end{cases} \tag{13}
$$

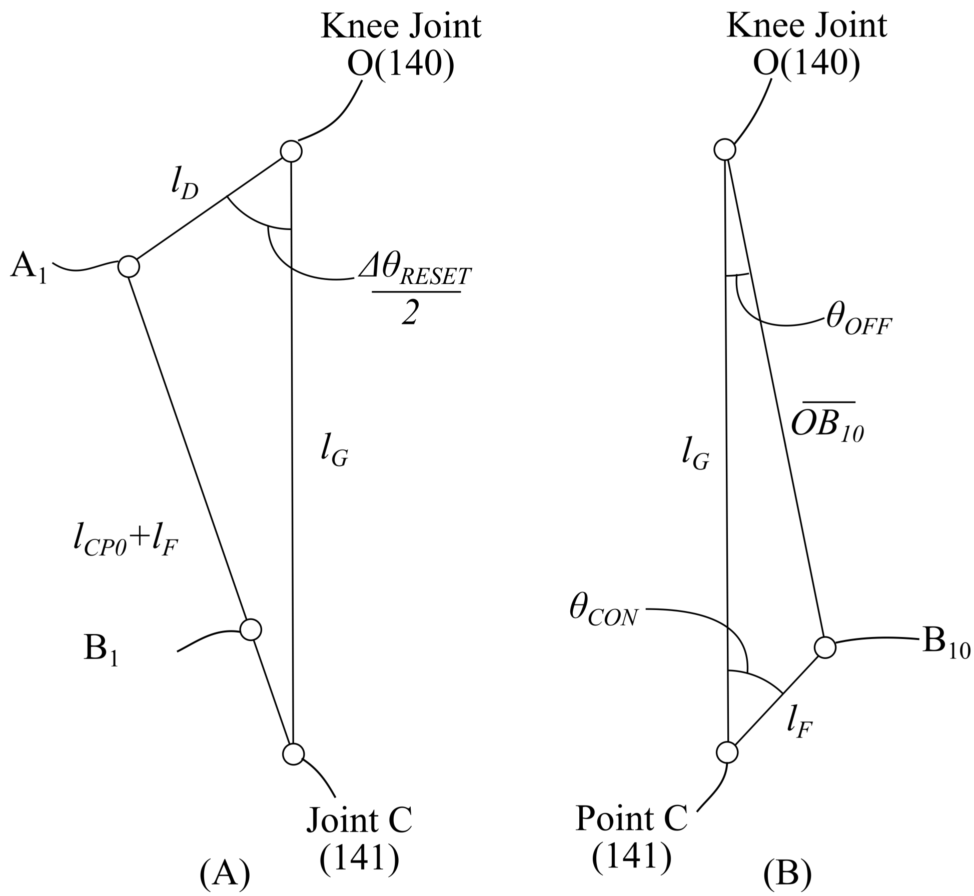

Figure 3-20: The geometry constraints for design process step 2.

The above equations can be obtained by the triangle OA_1C and $OB_{10}C$ as shown in Figure 3-20.

<u>Step 3</u>: Define the thigh and shank links, and if necessary, rotate them.

Now that we have obtained all the linkage lengths and the constraint angle, let us figure out where is the thigh link and shank link. The angle between the thigh and the driver, $\theta_{THIGH,D}$, and the angle between the shank and the ground link $\theta_{SHANK,G}$ (as shown in Figure 3-21) are:

$$\begin{cases} \theta_{THIGH,D} = \dfrac{\theta_{END} + \theta_{START}}{2} - \theta_{ROTATE} \\ \theta_{SHANK,G} = \theta_{ROTATE} \end{cases} \tag{14}$$

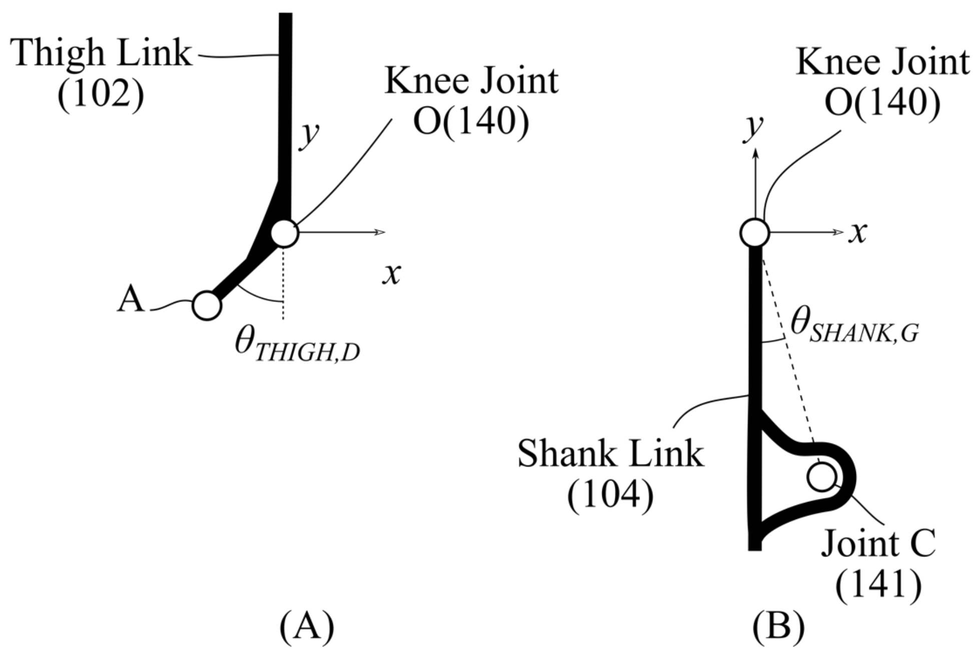

Figure 3-21: Positions of joint A and joint C in relation with the thigh link and shank link.

Now we can design a mechanism that meets the requirements. On top of that, we can expand the design by rotating the whole design. Rotation is useful the mechanism gets connected to any other parts of the exoskeleton, because there might exist a physical interference with another mechanism. In such a case we can rotate the design to avoid confliction.

3.4.3 Full Design Process

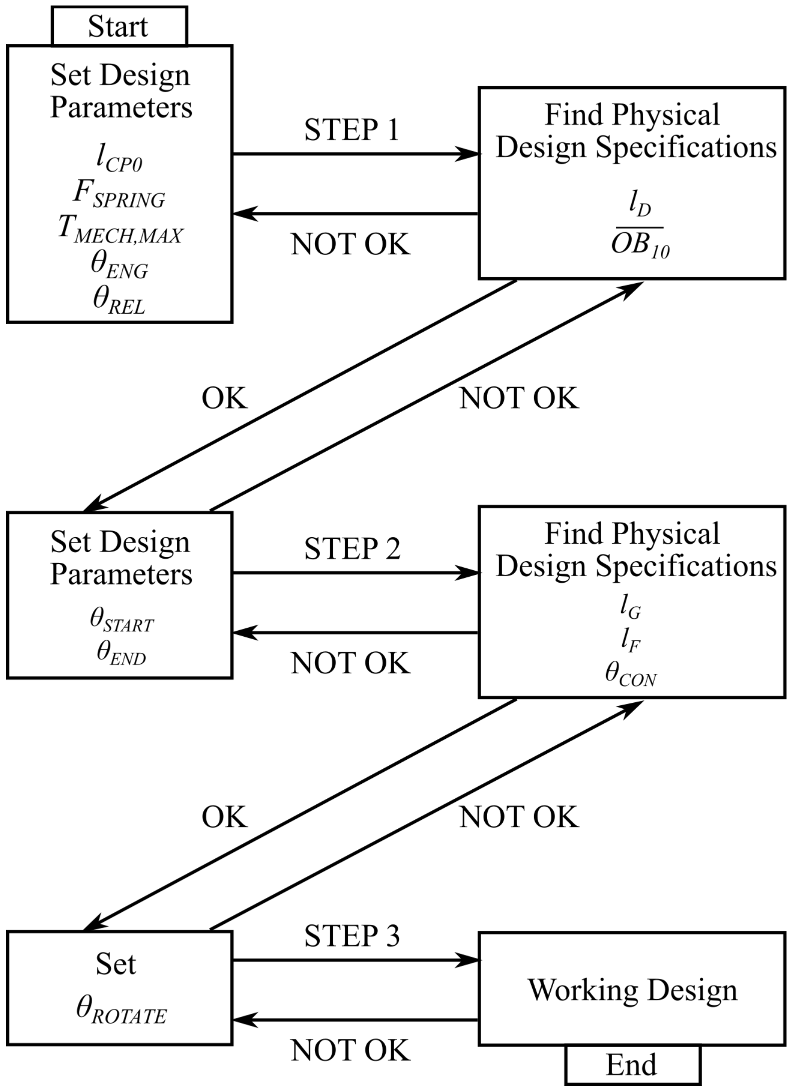

Figure 3-22: The full design process

Now we have devised an approach to create a mechanical design that meets the above three design requirements shown above. The actual design process is actually not as easy as it looks, because we need to consider the physical constraints including the stress and fatigue, material, tolerance, machinability and assembling process, etc. The design parameters that we have assigned might not reach a feasible mechanical design at all. Therefore we need to go back and forth to fine-tune design parameters that could lead to a feasible and robust design. The whole design process in a flow chart is shown in Figure 3-22.

3.5 PHYSICAL DESIGN

3.5.1 *Specifications*

A set of parameters that we reach through this process is shown in Table 3-1.

Table 3-1: The final design parameters and the physical design specifications

Design Parameters	Physical Design Specifications
$l_{CP0} = 5.69$ centimeters $F_{SPRING} = 1000$ Newton $T_{MECH,MAX} = 15$ Newton-meter $\theta_{START} = 1^{\circ}$ $\theta_{ENG} = 5^{\circ}$ $\theta_{REL} = 55^{\circ}$ $\theta_{END} = 55^{\circ}$	$l_D = 2.54$ centimeters $l_G = 9.65$ centimeters $l_F = 1.78$ centimeters $\theta_{CON} = 9^{\circ}$

According to Baker's classification, this four bar linkage is a class 1 rocker-rocker-rocker [51]. According to Murray's classification, it is a *0π* double-rocker [50].

3.5.2 *Adjustability*

As we mentioned in Chapter 2, with fixed ankles, enabling knee flexion after toe off facilitates progression of the body weight. In a previous research, unlocking the knee at foot strike and providing a resistive torque later to support stance had proven to be able to smoothly transfer the weight forward [30], [38]. The aforementioned strategy used a time-based controller. In this design, we can control when to start the resistance by using the engagement angle θ_{ENG}. Therefore, in addition to the aforementioned design, we make the supportive range $\Delta\theta_{SUP}$ (which directly affects the engagement angle θ_{ENG}) adjustable so that it can provide more options for different gait.

We achieve this by designing a fine tuner that can adjust l_G. It is noticed that by changing the l_G value by only 0.2 centimeters changes the supportive range $\Delta\theta_{SUP}$ by about 20 degrees. This characteristic can minimize the size of the physical design because the adjustment range for l_G could be really small.

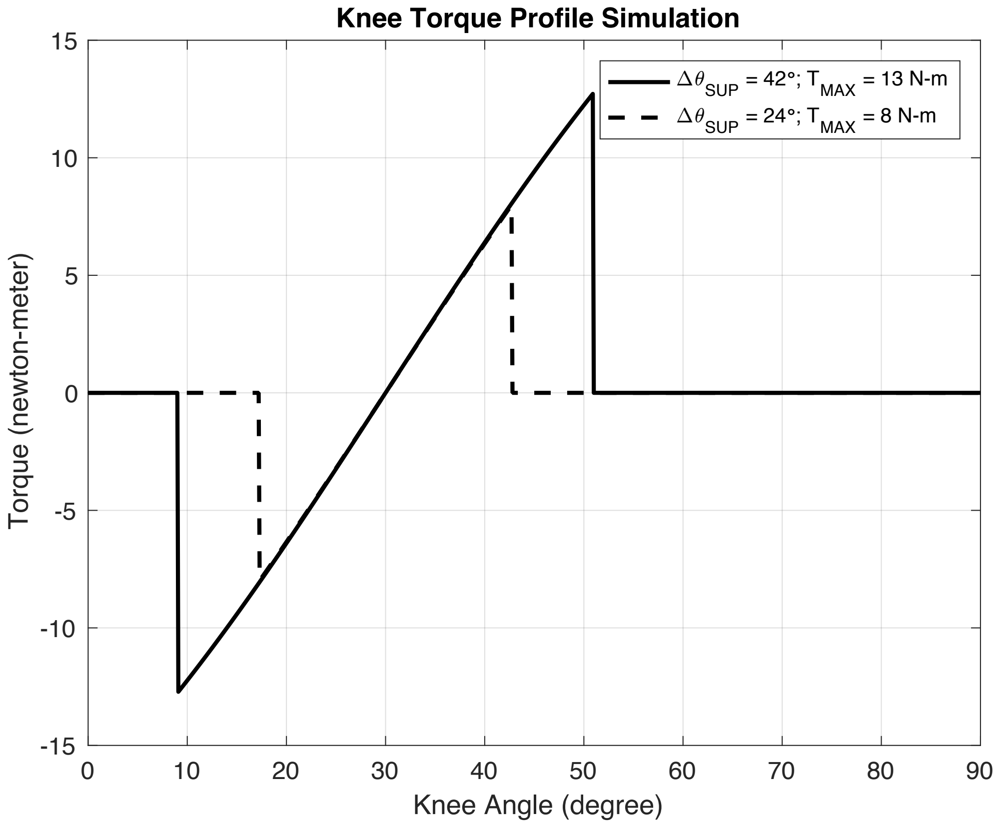

Figure 3-23: The adjustability on the supportive range $\Delta\theta_{SUP}$ of the mechanism.

Note that the torques in the supportive range $\Delta\theta_{SUP}$ is a function of $\overline{OB_{10}}$ as in Eq.(11), which interferes with l_G as in Eq. (13). Therefore when changing l_G we should get two different curves in the supportive range $\Delta\theta_{SUP}$. However, because l_G varies little, these two curves are nearly the same. Changing l_G essentially changes the supportive range $\Delta\theta_{SUP}$ but torque curve stays nearly the same as shown in Figure 3-23. In another word, adjusting l_G changes the supportive range $\Delta\theta_{SUP}$ and the maximum torque $T_{MECH,MAX}$ together, following nearly identical torque curves.

3.5.3 Physical Design

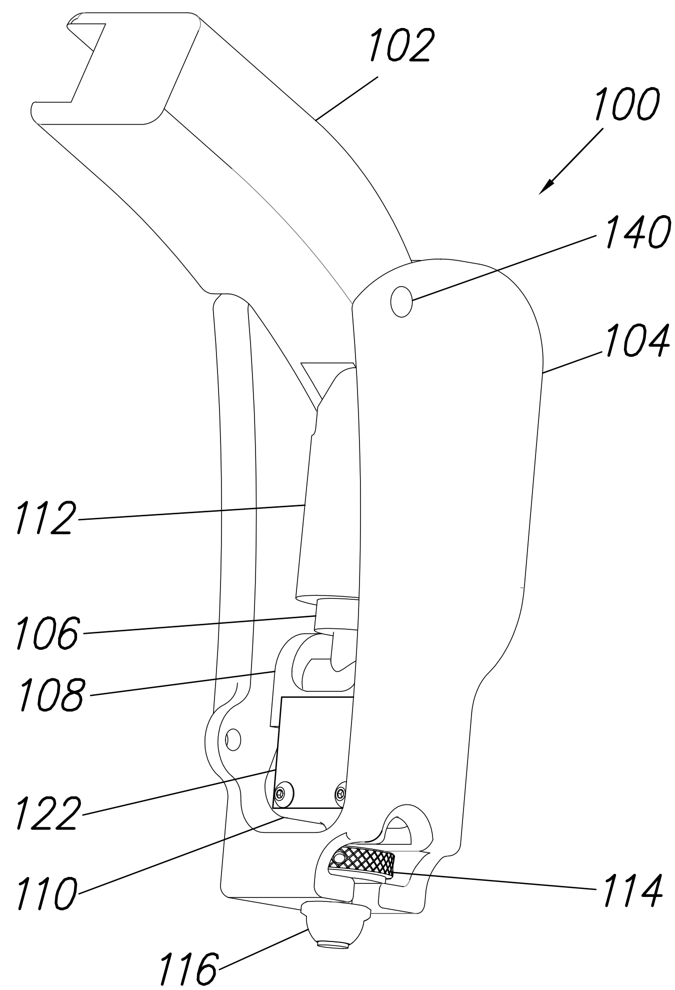

(A)

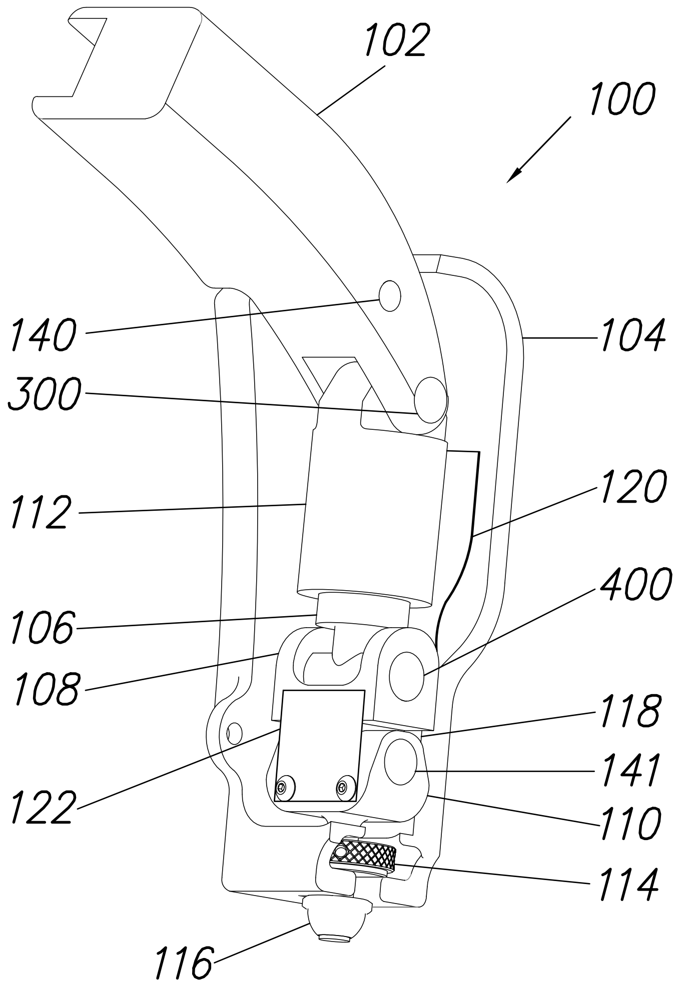

(B)

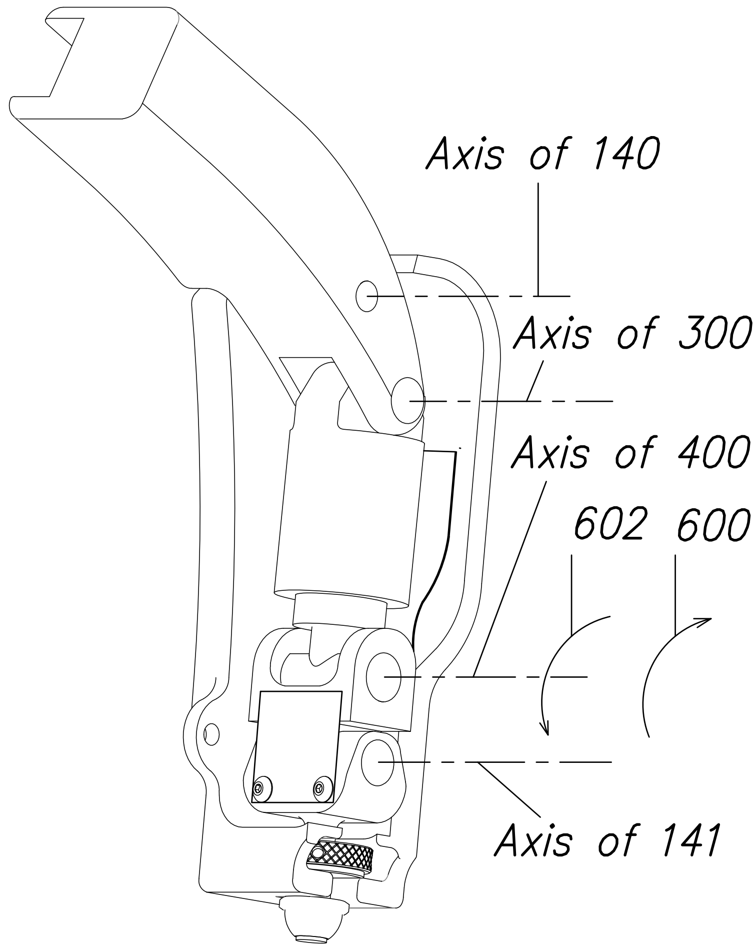

(C)

Figure 3-24: Schematic of the actual design in (A) normal view (B) cross-sectional view, and (C) another cross-sectional view.

The stance control toe clearance assistive device 100 is shown in Figure 3-24.The thigh link 102 rotates with the shank link 104 about the knee joint 140. The extension link 112 is rotatably coupled with the thigh link 102 about joint A (300), and linearly coupled with the gas spring 106. The gas spring 106 is rotatably coupled with the fourth link 108 about joint B (400). The fourth link 108 is rotatably coupled with adjuster 110 about joint C (141). Adjuster 110 is fixed on the shank link 104 during operation, but can be adjusted by a thumb nut 114 and a lock nut 116. Figure 3-24 (B) and (C) show cross-sectional views of artificial knee 100.

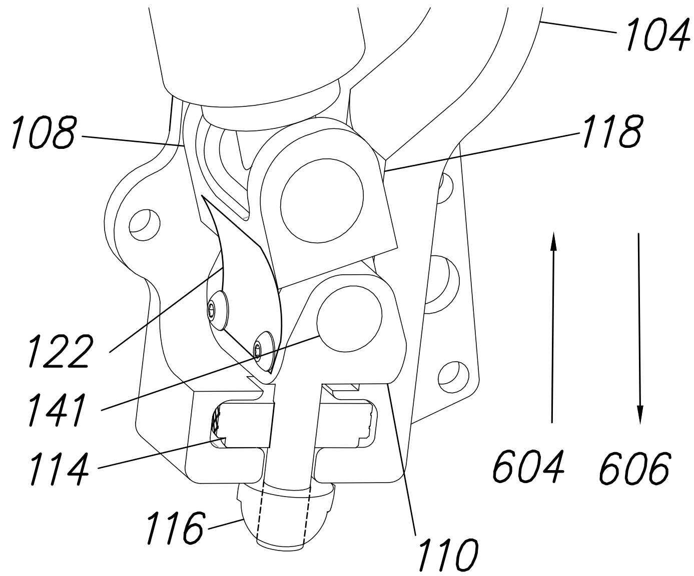

Figure 3-25: A cross-sectional view with a closer look at the adjustment mechanism.

Figure 3-25 shows another cross-sectional view with a closer look at the adjustment mechanism. The adjustment 110 has external threads going through the thumb nut 114 and the lock nut 116. When the two nuts are brought together, they clamp down a part of shank link 104, which creates an extension force on the external thread of the adjustment 110 and fix the adjustment 110 with respect to the shank link 104.

In this embodiment as shown in Figure 3-25, artificial knee 100 further comprises an adjustment mechanism to change the length between knee joint (140) and joint C (141). In other words, the adjustment mechanism allows the user to change the length of ground link 104. It will be explained later how this adjustment allows various behaviors for artificial knee 100. The adjustment mechanism comprises adjuster 110 with external threads. Adjuster 110 external threads match the internal threads of a hole in shank link 104. The adjustment mechanism further comprises thumb nut 114 and lock nut 116. By turning thumb nut 114, adjuster 110 moves along direction 604 and 606 relative to shank link 102. This means that the rotary joint between ground link 104 and follower link 108 can be adjusted. The combination of thumb nut 114 and lock nut 116 secures adjuster 110 to shank link 104. An ordinary person skilled in the art can develop various adjustment mechanisms to change the length of ground link 102.

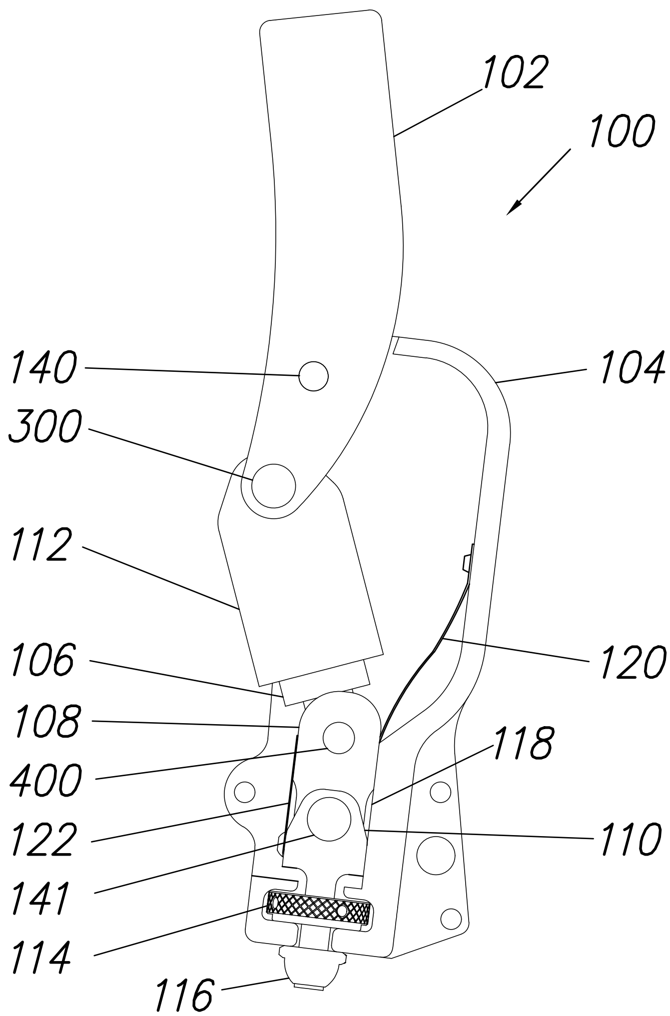

Figure 3-26: A cross-sectional view of artificial knee 100 when the knee is at engagement angle.

Figure 3-26 (similar to Figure 3-24, but with a better view of leaf springs 120) depicts a cross-sectional view of the mechanical configuration in Figure 3-24(B). In this embodiment, artificial knee 100 further comprises leaf spring 120. The first end of leaf spring 120 is coupled to shank link 104, and the second end of leaf spring 120 is able to provide torque in direction 602 on follower 108. Leaf spring 120 causes fourth link 108 (follower link) to move along trajectory 164 as shown in Figure 3-5(B). Artificial knee 100 further comprises a leaf spring 122. The first end of leaf spring 120 is coupled to shank link 104, and the second end of leaf spring 120 is able to provide torque in direction 600 on follower 108. Leaf spring 122 causes fourth link 108 (follower link) to move along trajectory 162 as shown in Figure 3-5(A). In some embodiments, leaf spring 120 and leaf spring 122 can be combined into one single spring, or other type of torque generators such as magnet. The objective of leaf spring 120 and leaf spring 122 is to create torques causing follower link 108 to move along trajectories 164 and 166.

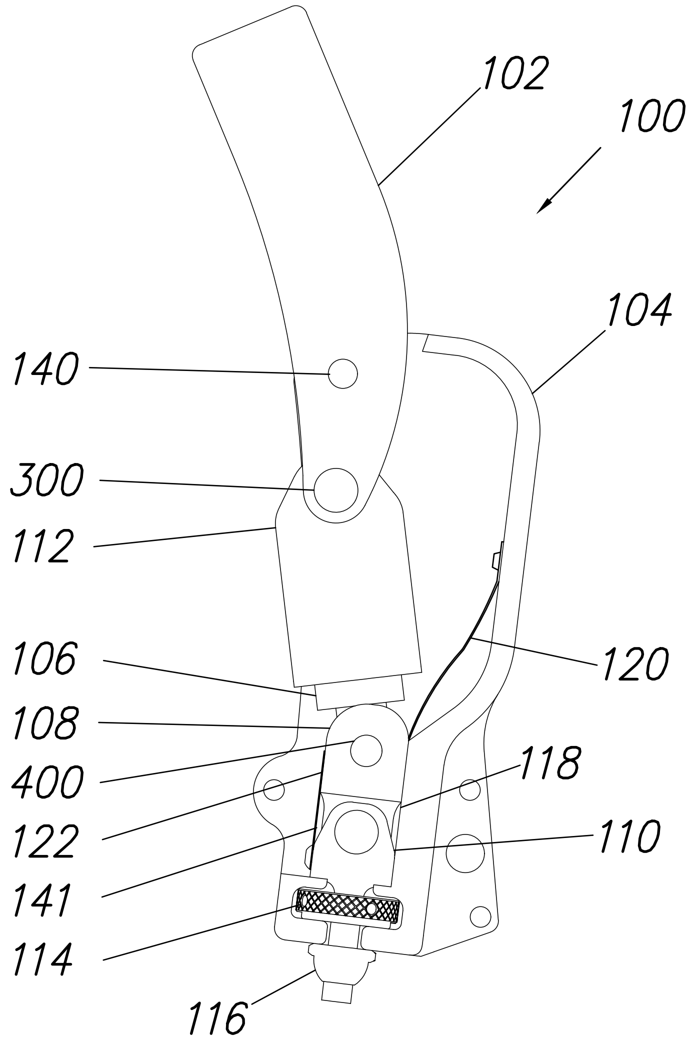

Figure 3-27: A cross-sectional view of artificial knee 100 when the knee is at the engagement angle. Comparing to Figure 3-26 the adjuster moves away from the knee joint, which increases the engagement angle

Figure 3-27 shows how turning the adjustment mechanism can affect engagement range. In Figure 3-27 adjuster 110 moves in direction 606 from the setup shown in Figure 3-26; this results in an increase in the length of the ground link, and further increases the engagement angle θ_{ENG} (802).

Figure 3-28: The actual mechanism

The aforementioned mechanism is fabricated and assembled as shown in Figure 3-28. The gas spring weighs 0.06 kilograms and the full assembly weighs 0.73 kilograms.

3.5.4 Experimental Torque Profile

Experimental torque profile are plotted to evaluate the effectiveness of the simulation. We measure the torque and ankle using a force sensor and a resistor. The thigh link is pulled and pushed from 0 degree to 90 degrees and then back to 0 degree while the shank link is fixed. The knee axis is perpendicular to the ground to eliminate gravity factor. This process is conducted slowly to minimize dynamic effect.

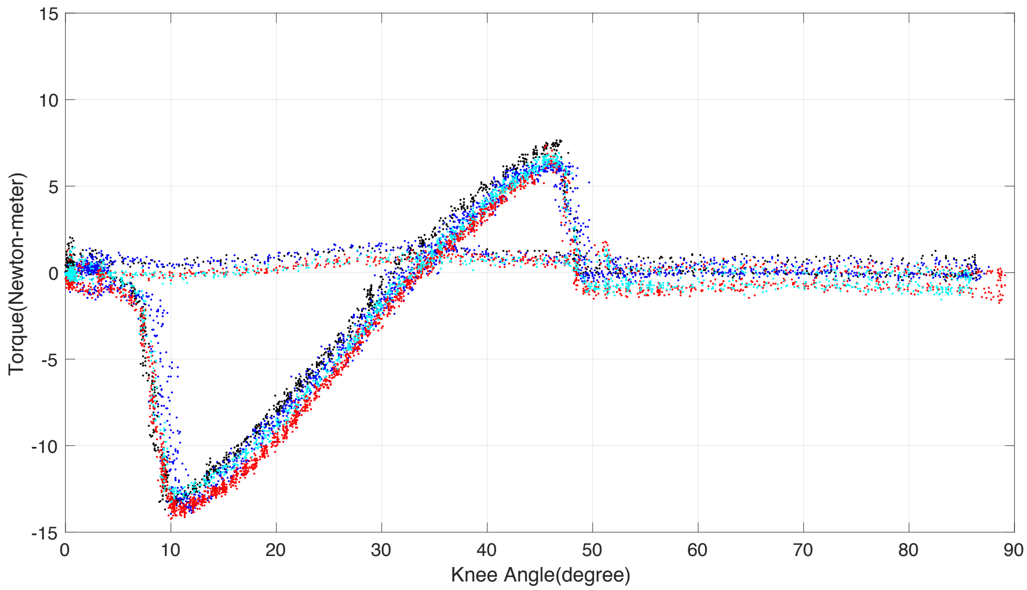

Figure 3-29: Experimental torque profile.

Figure 3-29 shows the experimental torque profile of a pair of knees. When the engagement angle θ_{ENG} is around 10 degrees, the maximum torque $T_{MECH,MAX}$ is about 13 Netwon-meter . This is close to the simulation torque profile. An offset of the toggle angle is observed, which was designed at 30 degrees but was measured at 35 degrees. This might be a consequence of the static friction as we flex the knee. In addition to that, the maximum torque and ranges are also smaller on the flexion (positive) side comparing to the extension side (negative). This might be a combination consequence of the friction, the asymmetric property of the gas spring (the gas spring generates more force in compression than in extension), and the small torque T_F applying on the fourth link. As a consequence, the energy (the area under the curve) storing in the spring has noticeable differences to the energy releasing from the spring. The curved experimental data comparing to the rather linear simulation might also be an outcome of the gas spring force not being exactly constant.

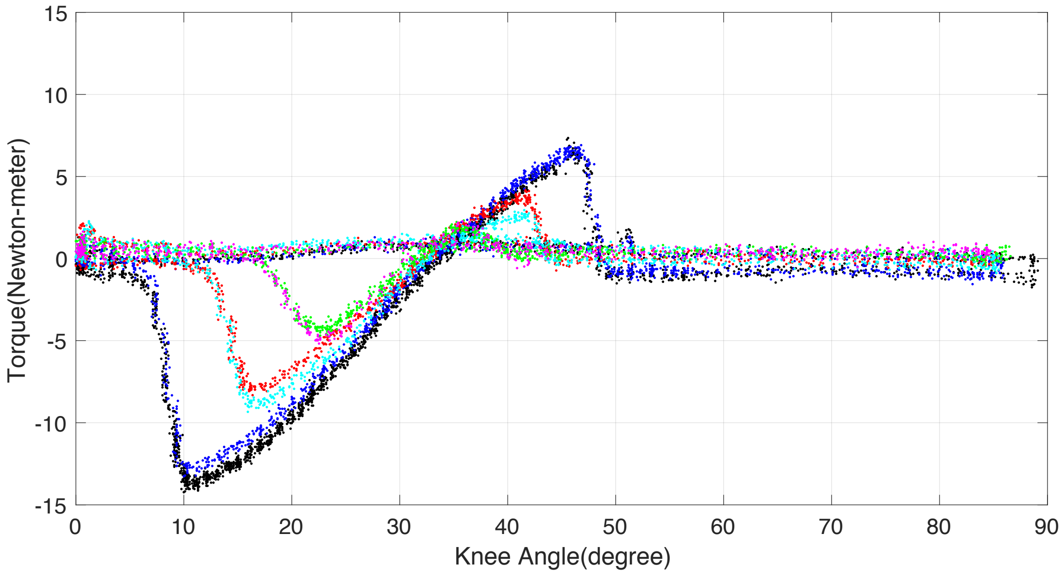

Figure 3-30: Experimental torque profiles of different supportive ranges.

Figure 3-30 shows the torque profiles of different supportive ranges $\Delta\theta_{SUP}$. The torque profiles follow almost the same curve in the supportive range $\Delta\theta_{SUP}$ as we observed in the simulation. We also notice that there is a small flexion torque when the knee extends back to 0 degree. This is caused by the second spring 122 that resists the fourth link 108 from rotating in its first direction 150 as the knee extends. This torque is small and not in the same order of magnitude relative to the designed torque, so it should not cause significant effect.

4 EVALUATIONS

In this section, two case studies with paraplegics were conducted using Phoenix's exoskeleton to evaluate the effectiveness of artificial knee 100.

4.1 CASE I: COMPLETELY PARALYSIS

The subject is a 29-year-old male subject with height 1.83 meters and weight 49 kilograms. He has T10 spinal cord injury with ASIA grade A, which means complete absence of motor and sensory function below the level of injury. This subject has used the exoskeleton for over 5 years. He has no spasticity nor contracture, which means that he does not have notable joint or muscle resistance.

4.1.1 Method

10-Meter-Walk-Tests (10MWTs) were conducted to evaluate the performance of gait using both artificial knee 100 and the wrap spring knee. 10MWT is a well-established functional mobility assessment tool commonly used in the clinical community to evaluate persons with neurological mobility impairment such as Parkinson's disease, stroke, and spinal cord injury [52], [53]. It measures the walking speed in meters per second over a short distance to evaluate functional mobility, gait, and vestibular function.

Figure 4-1: Video analysis tool tracker is used to fetch kinematic data.

In addition to the time results of the 10MWT, video-tracking tool Tracker© was also used for gait analysis (as shown in Figure 4-1). Videos from a sagittal plane were taken by a Nikon D600 with 1080p (1920×1080) full HD camera, recording at 30 fps. Hip, knee and ankle positions were tracked and translated into hip and knee angles using MATLAB.

This case study followed a standard regulation of the 10MWT. The subject was instructed to walk at a comfortable speed. The result was the time measured between the instants when the subject passed 2-meters and 8-meters lines. Three trials were collected for each knee setup. The subject was using crutches during the tests.

Three knee setup: wrap spring knee, two different torques of an older version of artificial knee 100 (toggle angle 30 degrees, engagement angle θ_{ENG} 5 degrees, Stronger artificial knee has maximum torque at 3.8 Newton-meter, weaker artificial knee has maximum torque at 2.8 Newton-meter) were tested individually. Stronger and weaker knee in this setup has the same engagement angle and toggle angle but uses different gas springs to achieve different torque output.

4.1.2 Results

The subject reported that he had to consciously put weight on the about-to-swing leg in order to flex artificial knee 100 through the toggle point. Table 4-1 shows data of the 10MWT. The subject walks faster when he was using artificial knee 100 than using the wrap spring knee. The time that the subject took to walk is reduced by 14.9% with the stronger artificial knee 100, and 10.4% with the weaker artificial knee 100.

Table 4-1: The 10MWT results for the first case study subject

Knee Setup	Time (second)			
	Test 1	*Test 2*	*Test3*	*Average*
Controlled group: Wrap Spring Knee	23.04	21.99	22.77	22.60
Experimental group 1: Strong artificial knee 100	18.55	19.31	19.82	19.23 *(-14.9%)*
Experimental group 2: Weak artificial knee 100	21.01	20.29	19.47	20.26 *(-10.4%)*

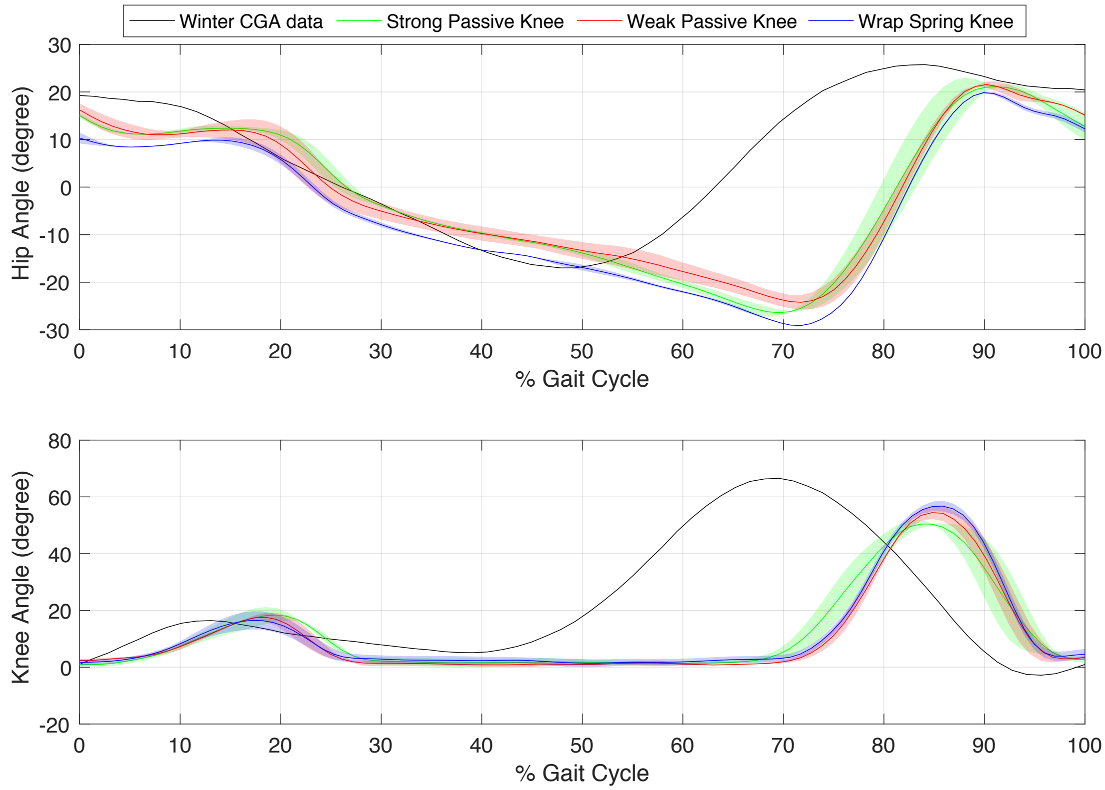

Figure 4-2: The gait analysis data of the 10MWT for the first case study subject.

The hip and the knee data were shown in Figure 4-2, superimposing with Winter's clinical gait analysis (CGA) data as a comparison with the normal gait. The solid lines show the average of the video analysis results, and the shaded areas show errors.

The results shows that the percentage of the stance phase is significantly larger in an exoskeleton gait than in the normal gait. A normal hip flexion starts at 50% of a gait cycle, while in an exoskeleton hip flexion starts at about 75% of a gait cycle. Both hip and knee data had a slightly increase of the angle from gait cycle 10% to 25% as the pilot shifted the body weight forward. In the current setup, the wrap spring knee enables the front knee to flex right after foot strike by unlocking the knee for a short period of time as shown in Figure 4-3 (A) and (B).

The subject's knee is fully extended during mid-stance from gait cycle 25% to 70%. This forms a good posture for not buckling the knee during single stance. The subject reported that he felt the leg was flexed at toe off when using the artificial knee 100, but the influence is little such that it is hard to tell if this flexion torque assisted toe clearance.

4.1.3 Discussion

It appears that the prolonged stance phase is due to the walking strategy and physical constraints associated with the exoskeleton. For example, since paraplegics could not fully control the limbs, they tended to pause and made sure the posture was stable before they took the next step. During the pause, they found balance based on their upper body position and crutch placement which might also result in longer stance time.

(A) (B) (C) (D)

Figure 4-3: Sequence of the gait.

Allowing knee flexion during weight acceptance was suggested to be able to shift the subject’s weight forward easier [30], [38]. This feature was reported to be a desirable feature for both wrap spring knee and artificial knee 100. No recognizable toe clearance improvement was observed between the two knee systems, though. This might be because the torque assisting on the knee was too small to make noticeable difference.

One important fact is that the artificial knee 100 controls the resistance torque based on the angle, whereas the wrap spring knee controls the lock and unlock motion based on time. The subject was not used to the angle-based control at first, but preferred over a time-based control at the end of the testing. He reported that angle-based control is more intuitive because he could take time to adjust his posture during or between steps.

The subject reported that he needed to be more cautious about the gait and posture, as the knee is not fully locked. Artificial knee 100 is designed under the assumption that the torso angle is controlled, which is controlled by the subject in these tests. If there exists a technology that automatically controls the torso angle, it should reduce the level of consciousness that the subject is required to control the torso angle.

Overall, the kinematic outputs of both stronger and weaker artificial knees 100 are very similar to that of the wrap spring knees. The subject reported satisfaction with the performance of artificial knee 100. Although the subject stated that he was more conscious of the foot positioning and weight distribution using artificial knee 100, his comfortable gait speed was faster using artificial knee 100 than using the wrap spring knee.

4.2 CASE II: INCOMPLETE PARALYSIS

The second subject is a 36 year-old male. He weighs 88 kilograms and is 1.87 meters tall. He had L1 incomplete spinal cord injury for 2 years. He has no contracture or spasticity (Modified

Ashworth Scale is 0). He had used the Phoenix exoskeleton with the wrap spring knee for 8 days. The first testing was conducted right after the subject walked in the wrap spring knee for about half an hour. The subject has partial control on the lower limb, and was able to walk with the walker without any leg braces.

4.2.1 Method

Similar to the previous tests, 10MWTs were conducted with this subject using artificial knee 100 and the wrap spring knee. The author conducted one iteration of 10MWT with each knee setup. The subject was asked to walk in his comfortable speed. The engagement angle θ_{ENG} was setup at 10 degrees. In addition to the walking speed, total number of steps and cadence were also measured during the 10MWT.

Figure 4-4: Video tracking method is used to collect kinematic data.

Same video analyzing method was used to get kinematic data from the 10MWT (shown in Figure 4-4). In addition to the previous described hip and knee data, additional data of the toe clearance was also collected by the same tracking method with a closer focus on the foot trajectory (shown in Figure 4-5). The toe clearance is measured by the height of the toe when the toe is at its maximum horizontal velocity [54].

Figure 4-5: A closer record of the foot trajectory is used to get toe clearance data

In these tests, the wrap spring knee did not allow the knee to bend after foot strike. According to the other researchers, this feature was disabled because they figured that for certain patients that have muscle resistance, unlocking the knee after foot strike might cause the subject to walk with bent knees. This circumstance is not ideal because it created large torque on the knee that may exceed the torque that the machine can resist. In addition, a flexed knee in single stance lowered the whole body and made it harder to create enough toe clearance. To fit in a wider variety of patients, other researchers disable this feature. Therefore the wrap spring knee does not unlock after foot strike during these tests.

4.2.2 Results

After about 10 minutes of training, the subject was able to walk with the artificial knee 100 using crutches, and he experienced gait difference once he walked with artificial knee 100. Some of his quotes include: *"Yeah, that is much better. That is a better feeling"*. *"You can control where the steps are on, and they are going nowhere else that they should".* The subject reported that he preferred the feature that he can have some control over the gait, but also have support when needed. He also reported that allowing knee flexion after foot strike facilitated him to shift weight.

The subject experienced assistance on the knee flexion in the beginning of the swing phase that helped him create more toe clearance. He was also able walk up a small incline (about 5 degree) much easier when using the artificial knee 100 than the wrap spring knee.

Similar to the other subject, this subject reported that he needed to be more cautious of the gait and the weight distribution. Because the subject had partial control on the leg, he described that he needed to "work harder" in order to walk. However he appreciated this because it helped him exercise his muscle, which could contribute regaining or improving functionality in his legs after the injury. After about 20 minutes of walking on the first day, the subject reported that he felt the muscle sore that night. The level of worked out in his legs was significantly higher with the artificial knee compare to the one with wrap spring knee (3 out of 10).

The walking speed, total number of steps and cadence results are shown in Table 4-2. The gait analysis results are shown in Figure 4-6. Toe clearance data were collected separately and sync with the hip and knee data in the swing phase shown in Table 4-3 and Figure 4-7.

Table 4-2: The 10MWT result for the second case study subject

	Wrap spring	Artificial knee 100
Total time	40.25 seconds	58.33 seconds
Total steps	17 steps	20 steps
Cadence	2.35 seconds per step	3.00 seconds per step

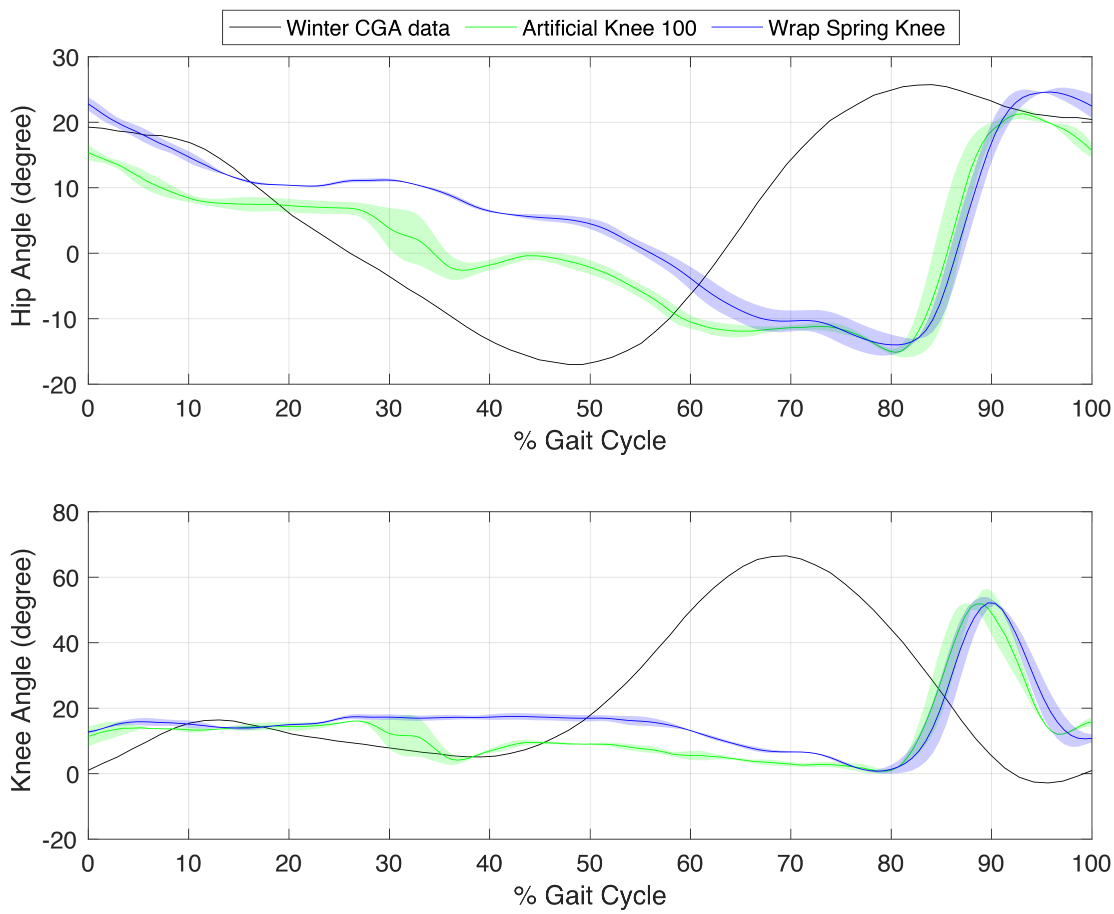

Figure 4-6: The gait analysis data of the 10MWT for the first case study subject.

Table 4-3: Results of the toe clearance measurement of using artificial knee 100, wrap spring knee, and normal gait for comparison.

	Toe Clearance	Standard deviation
Artificial knee 100	2.80 cm	0.31 cm
Wrap spring knee	2.48 cm	1.37 cm
Normal gait [54]	1.29 cm	0.4 cm

The average toe clearances of using artificial knee 100 and the wrap spring knee are 2.80 and 2.48 centimeters, respectively. The standard deviations of using artificial knee 100 and the wrap spring knee are 0.31 and 1.37 centimeters, respectively (sample size is 5). To give a general comparison, the toe clearance in a normal gait is 1.29 centimeters and variability is 0.4 centimeters [54].

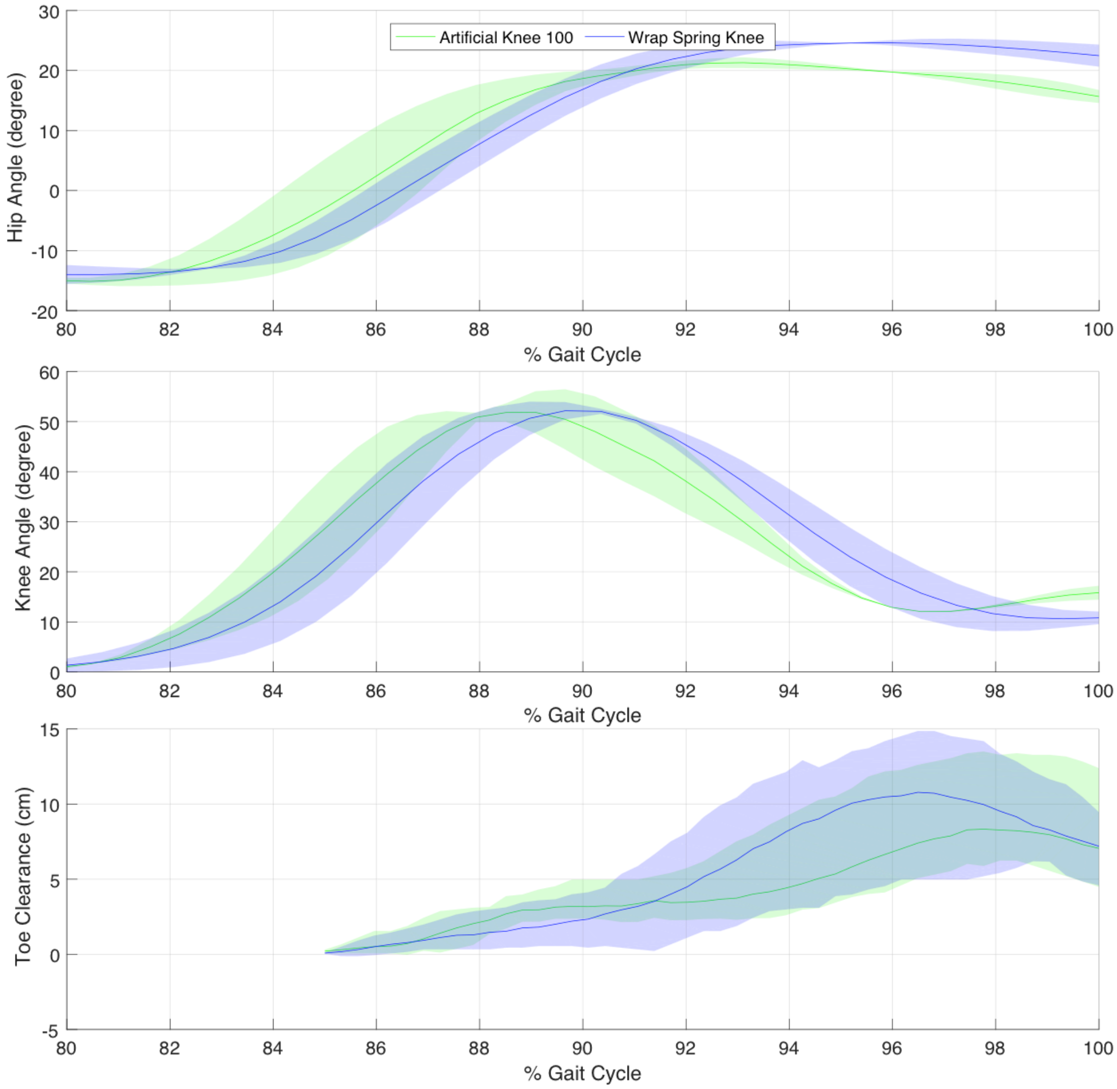

Figure 4-7: Toe clearance data are collected separately and synchronized with the hip and knee data in the swing phase.

4.2.3 Discussion

The results showed that the subject had slower gait and shorter step lengths when using artificial knee 100. The hip data shows a decreased maximum hip angle with artificial knee 100, and this is consistent with the shorter gait length. It appears that the shorter and slower gait is due to the pilot being more cautious about the gait.

The subject was observed to have a “kicking back” motion right before hip flexion starts that resulted in the ripple of the hip and knee data from 30% to 40% gait cycle. This might be caused by different reasons including fitting issues or walking habit. The subject did not fully extended the knee during stance in both cases, but the amount of flexion is small enough that the subject did not report any risk of buckling the knee during the stance phase.

The result shows that the subject had increased average toe clearance using both knees. This might be due to that the subject was concerned about tripping and thus create an increased average toe clearance. High variability was observed when the subject was using the wrap spring knee. This might be caused by less ability to precisely control the lower limb due to the constraints from the wrap spring knee.

4.3 CONCLUSIVE REMARKS

In this section two paraplegics tested on the artificial knee 100. Both subjects were able to walk with artificial knee 100 using crutches after about 10 minutes training using the parallel bars. For the first subject, the kinematic performance of artificial knee 100 is similar to that of the wrap spring knee. The 10MWTs shows subject walked faster in artificial knee 100. The second subject appeared to be more cautious and had shorter and slower gait with artificial knee 100. However, the subject likes the feature that artificial knee 100 allows him to have more control over the gait. The toe clearance was higher when using artificial knee 100, which is a desire outcome for prevention of tripping and falling. The subject felt that the gait with artificial knee 100 is more natural because it allows him to shift weight forward more easily. Moreover, the subject reported that he felt muscle sore after walking with artificial knee 100, which shows the effectiveness of working out using artificial knee 100, and unveils the capacity of artificial knee 100 in rehabilitation use.

5 QUALITATIVE EVALUATIONS

This section discloses some qualitative characteristics of using artificial knee 100 in different scenarios, which is useful to evaluate how feasible it could be to use artificial knee 100 in clinical setting.

5.1 SPLIT STAND

(A) (B) (C)

Figure 5-1: The subject experienced stability and cannot buckle the knee when shifting his weight in a split stand posture.

In a static split stand posture such as a weight-shifting instance during double stance, the subject in our first case study reported that this posture is stable and he could not buckle the knee by simply shifting his weight back and forth (as shown in Figure 5-1). This result is consistent to the conclusion we had in Chapter 2 (section 2.2.1.3). The body segments as a kinematic chain is fully defined by the control of the hip motors, thus theoretically the subject does not require control on the torso angle. In addition, the subject cannot move the posture if the hip motor fully defines the hip angles.

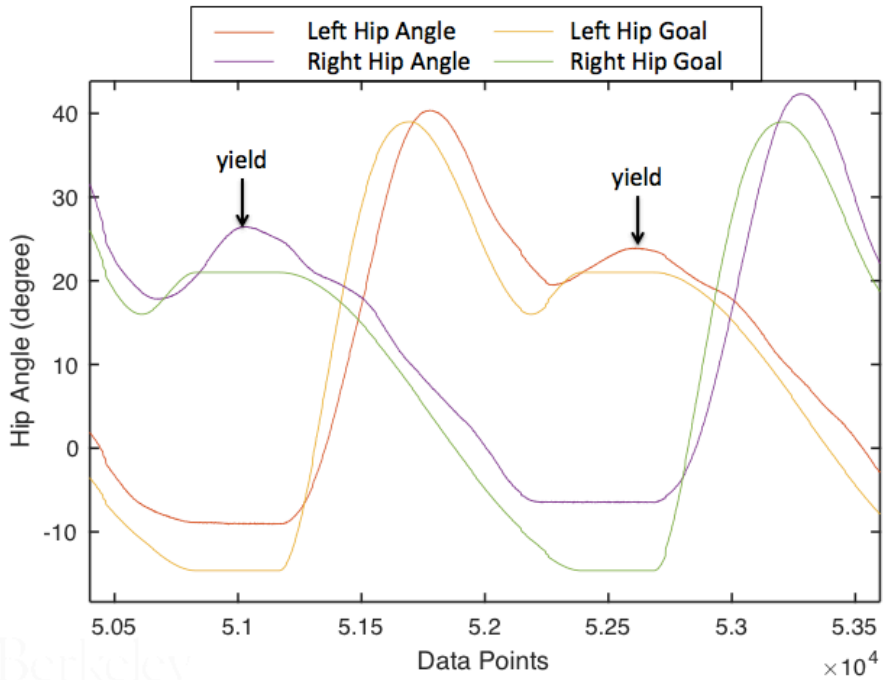

Figure 5-2: The hip data read from the hip encoder shows that during weight shift, the front hip yielded.

Nevertheless, the motor was not fully constrained but rather had some compliancy in practical. As the subject shifted the body weight forward (as shown in Figure 5-4), thigh angles yielded as observed from the hip data shown in Figure 5-2. This compliancy happened to facilitate the subject to shift weight forward.

(A) (B) (C)

Figure 5-3: The subject experienced stability and could not buckle the knee when shifting his weight back and forth in a split stand posture (θ_{ENG} = 10 degrees).

The subject in our second case study was balanced as well in split stand posture when the engagement angle θ_{ENG} is less than 15 degrees. He could not buckle his knee even by pulling himself to the ground.

(A) (B)

Figure 5-4: In a split stance posture during double stance, the subject reported that he could rest on the posture without much upper body strength.

With engagement angle θ_{ENG} less than 15 degrees, the subject felt the support that he could rest on the posture without much upper body strength. He stated that artificial knee 100 stopped flexing at the angle that he felt stable but still was able to freely control and flex his leg muscle. The subject was able to shift his weight more easily and that led to a smoother gait with foot flatten on the ground during weight acceptance as shown in Figure 5-4.

(A) (B)

Figure 5-5: The subject could buckle the knee when engagement angle is large (θ_{ENG} = 20 degrees).

However, when the engagement angle θ_{ENG} is larger (at 20 degrees), the subject reported that he could buckle the knees accidentally as shown in Figure 5-5. The subject experienced insecurity because the free range of the knee was too much. This result shows that the resistance on the knee is crucial as it prevent knee from accidentally buckling. Overall, the subject preferred the engagement angle θ_{ENG} at 15 degrees because the free range allowed him to exercise his muscle, and provided a smoother gait, while maintaining the stable postures.

5.2 PARALLEL STAND

(A) (B)

Figure 5-6: The subject experienced stability during standing

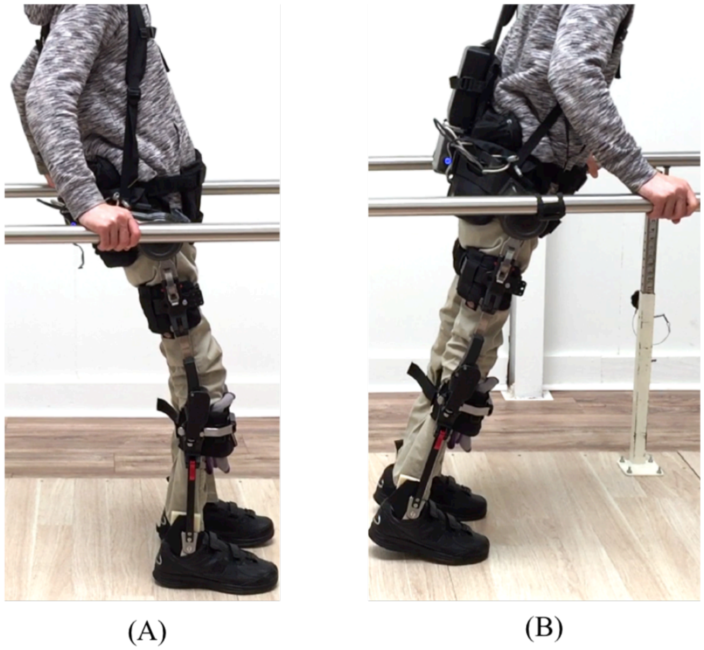

Figure 5-7: The knee did not buckle when the subject moved the torso back and forth in parallel stand.

During parallel stand, the subject experienced stability and comfort (as shown in Figure 5-6). He could not buckle the knee when leaning back and forth (as shown in Figure 5-7). He felt safe resting in it during parallel stand.

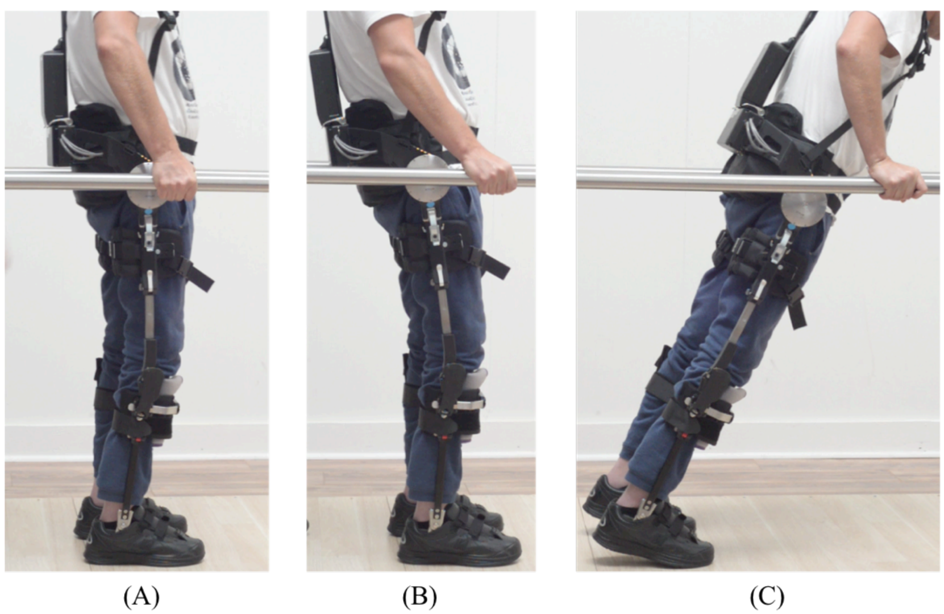

Figure 5-8: The subject in parallel stand tried to buckle the knee by (A) pulling himself down using parallel bars (B) leaning backward (C) leaning forward (θ_{ENG} = 10°).

When the engagement angle θ_{ENG} is smaller than 15 degrees, during parallel stand as shown in Figure 5-8, the subject could not buckle the knee even if he tried pulling himself downward using parallel bars, leaning backward, or leaning forward.

5.3 STANDING UP

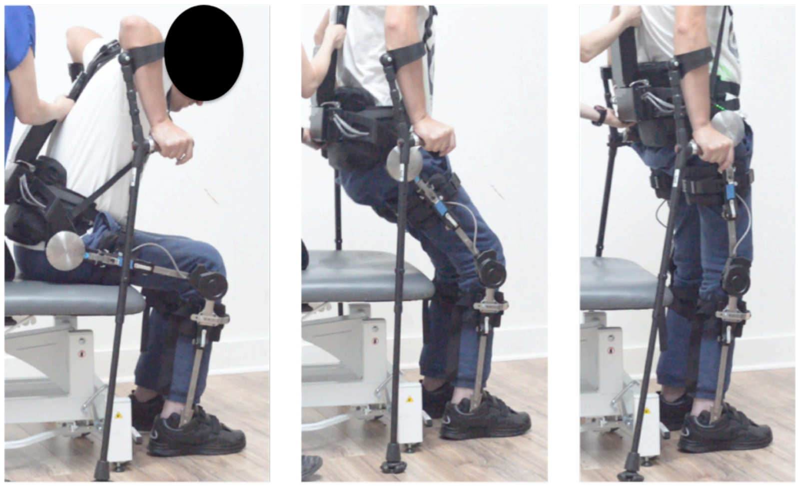

(A) (B) (C)

Figure 5-9: Standing up with wrap spring knee.

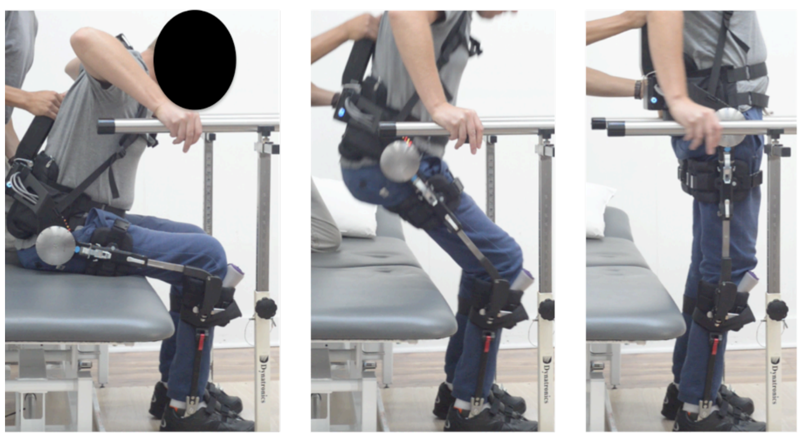

(A) (B) (C)

Figure 5-10: Standing up with artificial knee 100.

The kinematic of standing up using the artificial knee 100 was very similar to that in the wrap spring knee as the author expected (Figure 5-9 and Figure 5-10). In both cases, the subject was required to push his body up by using crutches, walker, or parallel bars. The subject did not experience any difference in his arm between using the wrap spring knee and artificial knee 100 during the process of standing up.

5.4 SITTING DOWN

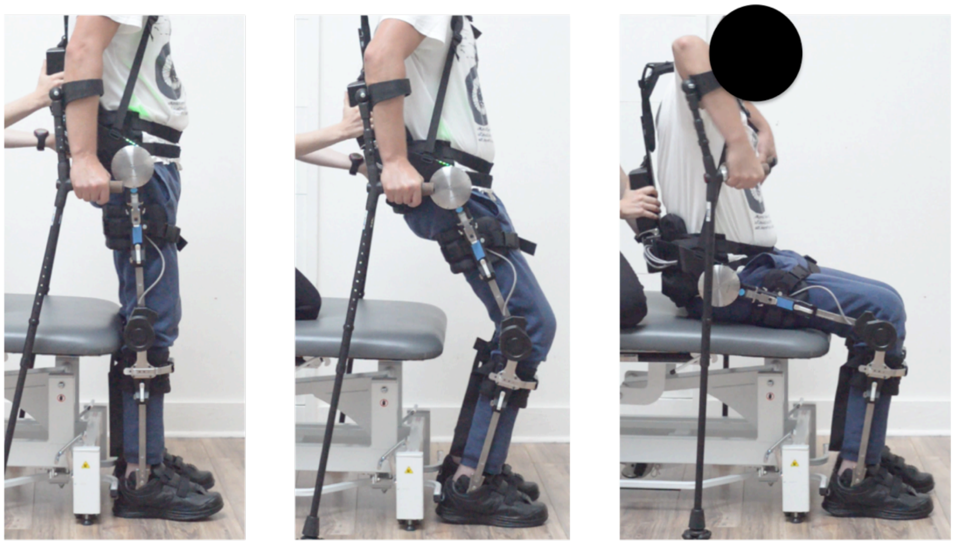

(A) (B) (C)

Figure 5-11: Sitting down with wrap spring knee.

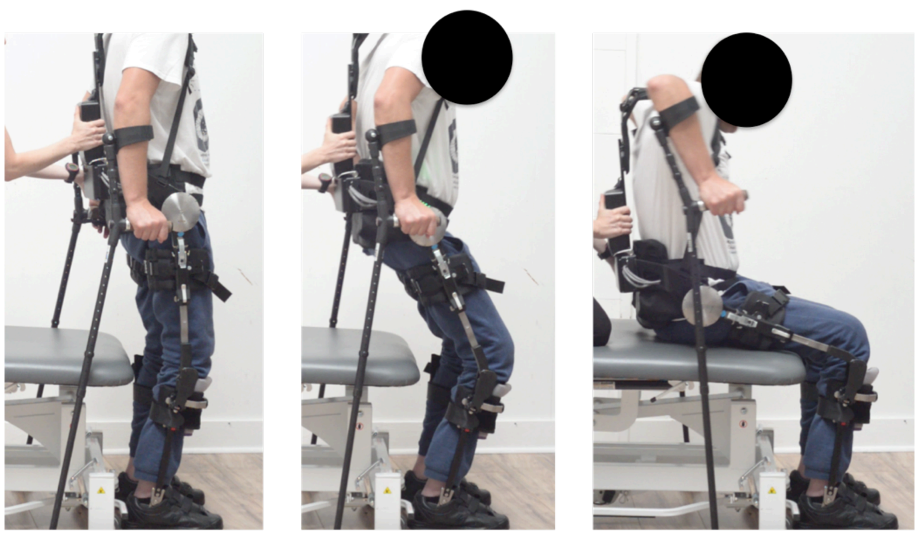

(A) (B) (C)

Figure 5-12: Standing up with artificial knee 100.

During sitting down, artificial knee 100 would provide resistant in flexion, and then assist in flexion when the knee angle is larger than the toggle angle. This is different from the wrap spring knees, which provide no assistance or resistance in either direction during sitting down right when it is unlocked.

The subject experienced resistance in the beginning of the sitting down process when using artificial knee 100. He stated that this resistance smoothened the sitting process. After the toggle angle, he was able to sit down with the assistant flexing torque on the knee. The subject reported that he preferred the artificial knee 100 over the wrap spring knee during sitting down because the wrap spring knee had abrupt dropping motion when the knee was suddenly unlocked.

5.5 TURNING AROUND

(A) (B) (C)

Figure 5-13: Turning motion could bend the knee.

With the current design, the outcome of turning motion could be improved. As shown in Figure 5-13 (tested with a healthy subject), the knee could be bent when the subject turned. The knee provides no resistance of flexion when the knee angle is larger than the toggle angle. This may lead to an unsafe situation for paraplegic subjects.

5.6 POPPING NOISE

When the knee did not fully extended in the early stance phase, the artificial knee 100 created a popping noise as the knee flexes during weight bearing. This sound is similar to the popping motion we described in Chapter 2 in that it is caused from the gas spring that releases at a time. Nevertheless, this popping noise was a result of that the fourth link 108 was not securely constrained by constraint 118 as the knee angle is not sufficiently smaller than the starting angle. The compression spring 106 is charged as the fourth link 108 was held by the friction rather than by the constraint 118. Therefore the compression spring 106 "pops" as the knee flexes. This condition created unnatural sound and was bothersome for both safety and cosmetic reasons. The popping noise could be minimized by increasing the engagement angle θ_{ENG}.

5.7 CONCLUSION REMARKS

Combining all the testing results, the author organized few pros and cons of using artificial knee 100 on an exoskeleton.

Pros:

1. The subject claimed more muscle is worked out after using artificial knee 100. This indicates that artificial knee 100 is potentially a better solution for subjects who prefer more rehabilitating work out or more control over the gait.
2. Artificial knee 100 encourages flexion during the swing-flexion phase, which is able to assist in toe clearance for some subjects.
3. Artificial knee 100 allows the front knee to flex after foot strike, which was reported to be a favored feature for both paraplegics subjects
4. Artificial knee 100 is able to support body weight and provide security during parallel standing and split standing.
5. Artificial knee 100 can be adjusted it to fit subjects with different injury levels by providing more support or more freedom.
6. Artificial knee 100 allows standing up and sitting down.
7. Artificial knee 100 is triggered by the knee angle, which eliminates the requirements of sensor from the foot or ankle. Therefore, unlike those dorsiflexion-driven SCOs, this invention does not reject users who have ankle mobility problems.

Cons:

1. Subjects have preferences in engagement angle θ_{ENG} during standing and walking. Although artificial knee 100 could be easily adjusted within 30 seconds, it was still unrealistic to adjust the range every time the subject wanted to switch between stand and walk.
2. The "popping" motion is hard to completely avoid and is bothersome for both safety and usability reasons. Although the engagement angle θ_{ENG} can be tuned to minimize the noise, users who require the confidence of a locking device might not tolerate this.
3. Subject using artificial knees 100 requires being more cautious on the gait compared to using the wrap spring knees.

6 CONCLUSION

Combining the concept of mechanism with variable topologies (MVTs) and the toggle switch, multiple functions were merged into one simple passive design that helped create ambulation. Artificial knee 100 stores energy in the stance phase, utilizes the energy to help clear the ground, and allows the knee to freely extend during swing. Unlike wrap spring knee or other dorsiflexion-triggered knee devices that is requires signals from the hip or ankle data, the artificial knee 100 estimates the phases of the gait by using purely knee angles. This feature allows artificial knee 100 to be highly modular and is flexible to be attached on an assistive device without the need of any other trigger. The author utilizes the kinematic and kinetic constraints to minimize the required knee torque for ambulation. Instead of fully locking the knee during stance phase, artificial knee 100 provides compliant torque to support body weight. An important aspect of this design is that all the above specifications are achieved passively without the use of any computers, sensors and motors.

The implementation of artificial knee 100 is particularly broad. From orthotics, prosthetics to exoskeleton, artificial knee is highly modular and could be easily implemented. Because of the compliancy, the artificial knee 100 can also be attached in addition to other knee devices to achieve certain tasks, say, assist in toe clearance as reported in the author's master thesis [55]. The concept of artificial knee 100 is not limited to knee devices but may also be valid to other applications especially in assistive devices because locomotion is mostly repetitive and with multiple phases.

Artificial knee 100 was shown to be a good fit for certain paraplegics because it allows more freedom and provides adjustable support such that it was suggested to be more effective toward rehabilitation. More clinical studies of this device are critical to gain experience in usage of artificial knee 100, and to find the criteria for suitable subjects. Because of its simple planar machinery design, this simple yet highly functional design has the potential to significantly decrease the manufacturing cost. This research opens a design paradigm of a novel design method for knee devices.

References

[1] National Spinal Cord Injury Stataistical Center, “Spinal Cord Injury Facts and Figures at a Glance,” Birmingham, AL, 2017.

[2] Steward Thomas P, “The Physiological Aspects of Immobilization and the Beneficial Effects of Passive Standing,” *Altimate Med.*, pp. 47–48, 2006.

[3] Christopher and Dana Reeve Foundation, *Paralysis Resource Guide*, 3rd ed. Christopher and Dana Reeve Foundation Paralysis Resource Center, 2009.

[4] P. J. Manns and K. E. Chad, “Components of quality of life for persons with a quadriplegic and paraplegic spinal cord injury.,” *Qual. Health Res.*, vol. 11, no. 6, pp. 795–811, 2001.

[5] A. Esquenazi, M. Talaty, A. Packel, and M. Saulino, “The ReWalk Powered Exoskeleton to Restore Ambulatory Function to Individuals with Thoracic-Level Motor-Complete Spinal Cord Injury,” *Am. J. Phys. Med. Rehabil.*, vol. 91, no. 11, pp. 911–921, 2012.

[6] R. J. Farris, H. A. Quintero, and M. Goldfarb, “Preliminary Evaluation of a Powered Lower Limb Orthosis to Aid Walking in Paraplegic Individuals,” *IEEE Trans. Neural Syst. Rehabil. Eng.*, vol. 19, no. 6, pp. 652–659, 2011.

[7] E. Strickland, “Good-bye, wheelchair,” *IEEE Spectr.*, vol. 49, no. 1, pp. 30–32, 2012.

[8] “Rex Bionics.” [Online]. Available: http://www.rexbionics.com/. [Accessed: 14-Apr-2015].

[9] M. G. Mckinley, “Design of Lightweight Assistive Exoskeletons For Individuals with Mobility Disorders,” University of California, Berkeley, 2014.

[10] “Ekso Bionics.” [Online]. Available: http://www.eksobionics.com/. [Accessed: 14-Apr-2015].

[11] “ReWalk-More than Walking.” [Online]. Available: http://www.rewalk.com/. [Accessed: 14-Apr-2015].

[12] “Cyberdyne.” [Online]. Available: http://www.cyberdyne.jp/english/products/HAL/. [Accessed: 01-Feb-2015].

[13] “Indego-Power People Forward.” [Online]. Available: http://www.indego.com/indego/en/home. [Accessed: 14-Apr-2015].

[14] B. Tita, “Parker Hannifin ’ s Robotic Exoskeleton Gets FDA OK for Personal Use,” 2016.

[15] S. Brewster, “This $40,000 Robotic Exoskeleton Lets the Paralyzed Walk,” *MIT Technology Review*, 2016.

[16] H. M. & C. Parker Hannifin Corporation, *Indego Therapy Brochure*. 2017.

[17] “Fillauer LLC | Orthotics and Prosthetics Manufacturer.” [Online]. Available: http://fillauer.com/. [Accessed: 01-Aug-2017].

[18] “Becker Knee Joint Catalog.” [Online]. Available: http://www.beckerorthopedic.com/Catalog/BeckerCatalog.htm. [Accessed: 08-Jan-2017].

[19] F. Tian, M. S. Hefzy, and M. Elahinia, “State of the Art Review of Knee–Ankle–Foot Orthoses,” *Ann. Biomed. Eng.*, vol. 43, no. 2, pp. 427–441, 2015.

[20] K. a Bernhardt, S. E. Irby, and K. R. Kaufman, “Consumer opinions of a stance control knee orthosis.,” *Prosthet. Orthot. Int.*, vol. 30, no. 3, pp. 246–256, 2006.

[21] T. Yakimovich, E. D. Lemaire, and J. Kofman, “Engineering design review of stance-control knee-ankle-foot orthoses,” *J. Rehabil. Res. Dev.*, vol. 46, no. 2, pp. 257–268, 2009.

[22] “UTX ® Stance Control KAFOs,” 2016. [Online]. Available: http://www.beckerorthopedic.com/Catalog/StanceControlProductPages/Model9004.html. [Accessed: 01-Aug-2017].

[23] B. Hatton, D. Hatton, and Z. Wallace, “Articulating knee supports,” US Patent 6,635,024 B2, 2003.

[24] G. Nijenbanning and J. A. Goudsmit, “Gravity Operated Locking Hinge,” US 6,979,304 B2, 2005.

[25] J. Naft and W. Newman, “Orthosis knee joint,” US Patent 6,517,503, 2003.

[26] P. E. steven E. Irby, Kenton R. KaufmanBizot, “Electromechanical Joint Control Device with wrap spring clutch,” US 6,500,138 B1, 2002.

[27] W. Y.-W. Tung, “Design And Operation Of Minimally Actuated Medical Exoskeletons For Individual With Paralysis,” University of California, Berkeley, 2013.

[28] J. K. Terris Yakimovich, Edward Lemaire, “Articulating Joint,” US Patent 7,410,472 B2, 2008.

[29] T. Yakimovich, J. Kofman, and E. D. Lemaire, “Design and evaluation of a stance-control knee-ankle-foot orthosis knee joint,” *IEEE Trans. Neural Syst. Rehabil. Eng.*, vol. 14, no. 3, pp. 361–369, 2006.

[30] T. Yakimovich, E. D. Lemaire, and J. Kofman, “Preliminary kinematic evaluation of a new stance-control knee-ankle-foot orthosis,” *Clin. Biomech.*, vol. 21, no. 10, pp. 1081–1089, 2006.

[31] K. Shamaei, P. C. Napolitano, and A. M. Dollar, “Design and Functional Evaluation of a Quasi-Passive Compliant Stance Control Knee #x2013;Ankle #x2013;Foot Orthosis,”

IEEE Trans. Neural Syst. Rehabil. Eng., vol. 22, no. 2, pp. 258–268, 2014.

[32] A. Cullell, J. C. Moreno, E. Rocon, A. Forner-Cordero, and J. L. Pons, “Biologically based design of an actuator system for a knee-ankle-foot orthosis,” *Mech. Mach. Theory*, vol. 44, no. 4, pp. 860–872, 2009.

[33] F. Tian, M. S. Hefzy, and M. Elahinia, “Development of a Dynamic Knee Actuator For a KAFO Using,” 2014.

[34] A. G. McMillan, K. Kendrick, J. W. Michael, J. Aronson, and G. W. Horton, “Preliminary Evidence for Effectiveness of a Stance Control Orthosis,” *JPO J. Prosthetics Orthot.*, vol. 16, no. 1, pp. 6–13, 2004.

[35] K. R. Kaufman, S. E. Irby, J. W. Mathewson, R. W. Wirta, and D. H. Sutherland, “Energy Efficient Knee Ankle Foot Orthosis A Case.3.pdf,” *J. Prosthetics Orthot.*, vol. 8, no. 3, pp. 79–85, 1996.

[36] J. S. Hebert and A. B. Liggins, “Gait evaluation of an automatic stance-control knee orthosis in a patient with postpoliomyelitis,” *Arch. Phys. Med. Rehabil.*, vol. 86, no. 8, pp. 1676–1680, 2005.

[37] S. E. Irby, K. R. Kaufman, J. W. Mathewson, and D. H. Sutherland, “Automatic control design for a dynamic knee-brace system.,” *IEEE Trans. Rehabil. Eng.*, vol. 7, no. 2, pp. 135–9, 1999.

[38] B. Perry, “Approaches to Minimally Actuated Exoskeleton Gait Development,” University of California, Berkeley, 2016.

[39] D. A. Winter, *Biomechanics and Motor Control of Human Movement*, 4th ed. John Wiley & Sons, Inc, 2009.

[40] M. G. Mckinley, “Design of a Novel Orthotic Knee Joint for Use in an Assistive Exoskeleton for Paraplegics,” University of California at Berkeley, 2011.

[41] J. Rose and J. G. Gamble, *Human Walking*, 3rd ed. Lippincott williams & wilkins, 2006.

[42] D. A. Winter, *Biomechanics and Motor Control of Human Movement*, 2nd ed. ohn Wiley & Sons, 1990.

[43] D. A. Winter, “2D Walking Data,” *International Society of Biomechanics*. [Online]. Available: https://isbweb.org/resources/data-resources/140-movement-data.

[44] M. Meinders, A. Gitter, and J. M. Czerniecki, “The role of ankle plantar flexor muscle work during walking.,” *Scand. J. Rehabil. Med.*, vol. 30, no. 1, pp. 39–46, 1998.

[45] H. M. Herr, G. T. Huang, and T. a McMahon, “A model of scale effects in mammalian quadrupedal running.,” *J. Exp. Biol.*, vol. 205, no. Pt 7, pp. 959–967, 2002.

[46] E. Todorov and M. I. Jordan, “Optimal feedback control as a theory of motor coordination,” *Nat. Neurosci.*, vol. 5, no. 11, pp. 1226–1235, 2002.

[47] D. A. Winter, “Human balance and posture control during standing and walking,” *Gait Posture*, vol. 3, no. 4, pp. 193–214, 1995.

[48] D. A. Winter, A. E. Patla, F. Prince, M. Ishac, and K. Gielo-Perczak, “Stiffness control of balance in quiet standing.,” *J. Neurophysiol.*, vol. 80, no. 3, pp. 1211–21, 1998.

[49] D. A. Winter and D. G. E. Robertson, “Joint Torque and Energy patters in Normal Gait,” *Biol. Cybern.*, vol. 29, pp. 137–142, 1978.

[50] A. P. Murray and P. M. Larochelle, “A classification scheme for planar 4R, spherical 4R, and spatial RCCC linkages to facilitate computer animation,” in *Proceeding of DETC’98 ASME Design Engineering Technical Conferences*, 1998.

[51] C. R. Barker, “A Complete Classification of Planar Four-Bar Linkages,” *Mech. Mach. Theory*, vol. 20, no. 6, pp. 535–554, 1985.

[52] H. J. Van Hedel, M. Wirz, and V. Dietz, “Assessing walking ability in subjects with spinal cord injury: Validity and reliability of 3 walking tests,” *Arch. Phys. Med. Rehabil.*, vol. 86, no. 2, pp. 190–196, 2005.

[53] P. Rossier and D. T. Wade, “Validity and reliability comparison of 4 mobility measures in patients presenting with neurologic impairment,” *Arch. Phys. Med. Rehabil.*, vol. 82, no. 1, pp. 9–13, 2001.

[54] D. A. Winter, “Foot trajectory in human gait: a precise and multifactorial motor control task.,” *Phys. Ther.*, vol. 72, no. 1, pp. 45-53–6, 1992.

[55] S.-L. Wu, “Design of a Ground Clearance Assistive Device on Passive Medical Exoskeleton Knee,” University of California, Berkeley, 2015.

[56] D. T. Bartel, Donald L. and Davy, *Orthopaedic Biomechanics: Mechanics and Design in Musculoskeletal Systems*. Prentice Hall, 2006.

7 APPENDIX: COMPUTATIONAL MODEL

The computational model simulates the toe clearance during swing. The model comprises two parts: a pre-swing model and a swing dynamics model. The pre-swing model is used to generate the initial conditions for the swing dynamics model. The outline of the MATLAB model is shown in Figure 7-1.

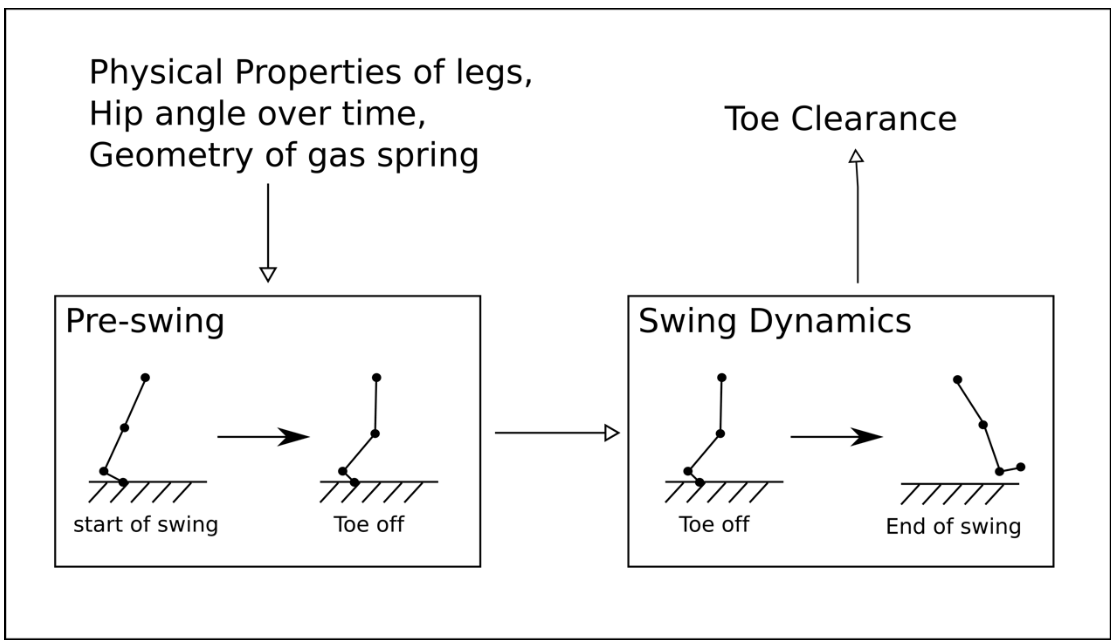

Figure 7-1: Outline of the toe clearance model

7.1 PRE-SWING MODEL

Pre-swing model utilizes kinematics to calculate the initial conditions for the swing dynamic model as shown in Figure 7-2. The inputs of the pre-swing model include an assigned hip trajectory, a profile of knee supportive torque, and the limb lengths. The model is a link segment model that assumes all joints are frictionless rotational joints. It includes three segments: thigh, shank, and foot. The hip position is virtually fixed. The ankle angle is assumed a free joint throughout the pre-swing phase considering the brace has compliancy. The initial knee and ankle angle is 0° and 90°, respectively. Toe off is assumed to take place when thigh is vertical to the ground, and torso is assumed be also vertical to the ground. The toe does not slide and is fixed on the ground in the pre-swing model. Segment lengths are assigned based on anthropology data [56].

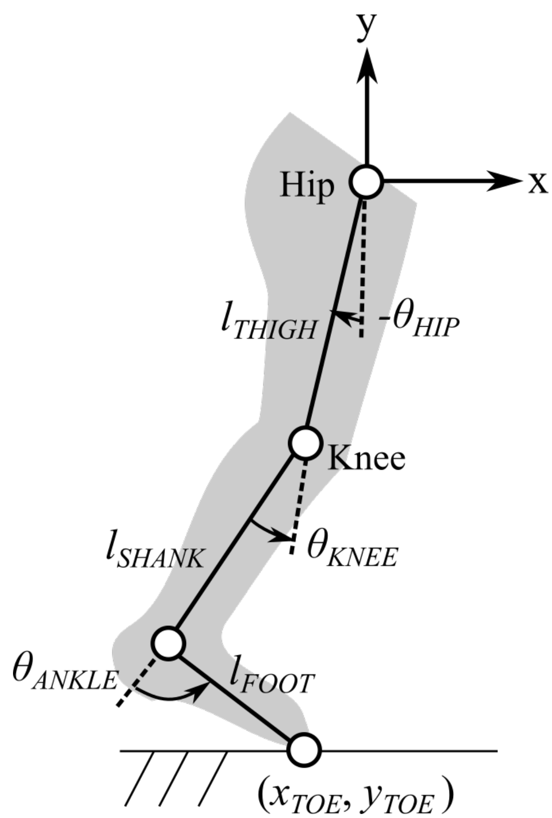

Figure 7-2: Illustration of model defined in pre-swing model.

Where:

θ_{HIP}= Hip angle	l_{THIGH} = Length of thigh
θ_{KNEE}= Knee angle	l_{SHANK} = Length of shank
θ_{ANKLE} = Ankle angle	l_{FOOT} = Length from foot

$$\begin{cases} x_{TOE} = l_{THIGH}\sin(-\theta_{HIP}) + l_{SHANK}\sin(-\theta_{HIP}+\theta_{KNEE}) + l_{FOOT}\sin(-\theta_{HIP}+\theta_{KNEE}-\theta_{ANKLE}) \\ y_{TOE} = -l_{THIGH}\cos(-\theta_{HIP}) - l_{SHANK}\cos(-\theta_{HIP}+\theta_{KNEE}) - l_{FOOT}\cos(-\theta_{HIP}+\theta_{KNEE}-\theta_{ANKLE}) \end{cases} \quad (15)$$

x_{TOE} and y_{TOE} can be calculated with the assumed initial knee and ankle angle. Then θ_{KNEE} and θ_{ANKLE} can be solved simultaneously with the input θ_{HIP} (vpasolve function, MATLAB Inc.).

7.2 SWING DYNAMICS MODEL

The swing model calculates the positions of the toe using Lagrangian dynamics. Similar to the pre-swing model, this model is a link-segment model. It simulates the leg as double pendulum with point masses located at the center of mass of each link segment as shown in Figure 7-3 (data from [56]). The ankle mass is ignored and the ankle angle is assumed remaining at its initial condition. Assume hip motor can drive the thigh following the assigned trajectory. The only forces active on the shank are the gravity force, inertia force and the torque from the knee mechanism. The knee cannot hyperextend.

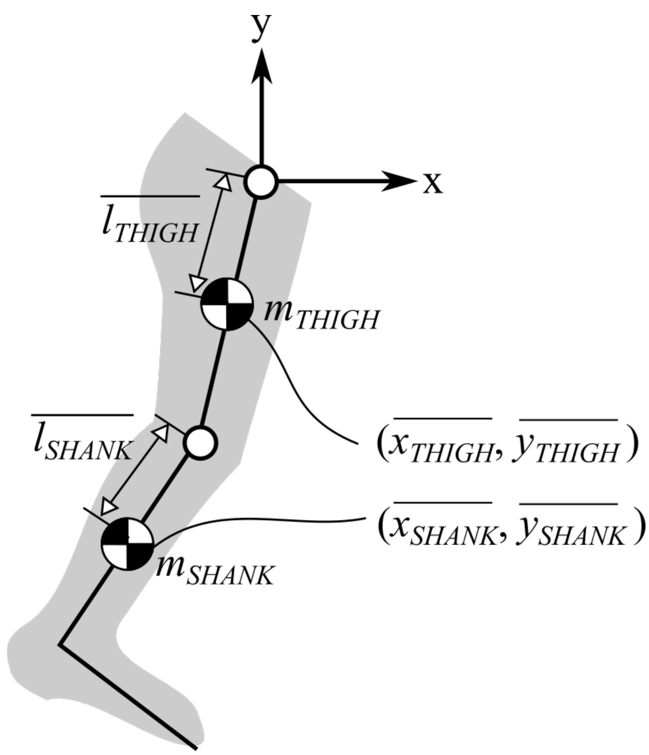

Figure 7-3: The swing dynamic model simulates the leg as double pendulum with point masses on thigh and shank.

Where additional parameters are added:
m_{THIGH} = Mass of upper leg
m_{SHANK} = Mass of lower leg
$\overline{l_{THIGH}}$ = Length from hip to center of mass m_{THIGH}
$\overline{l_{SHANK}}$= Length from knee to center of mass m_{SHANK}

The position of the center of mass of the thigh and shank are:

$$\begin{cases} \overline{x_{THIGH}} = \overline{l_{THIGH}} \times \sin(\theta_{HIP}) \\ \overline{y_{THIGH}} = -\overline{l_{THIGH}} \times \cos(\theta_{HIP}) \end{cases} \tag{16}$$

$$\begin{cases} \overline{x_{SHANK}} = l_{THIGH} \times \sin(\theta_{HIP}) + \overline{l_{SHANK}} \times \sin(\theta_{HIP} - \theta_{KNEE}) \\ \overline{y_{SHANK}} = -l_{THIGH} \times \cos(\theta_{HIP}) - \overline{l_{SHANK}} \times \cos(\theta_{HIP} - \theta_{KNEE}) \end{cases} \tag{17}$$

Taking derivatives with respect to time:

$$\overline{\dot{x}_{THIGH}} = \overline{l_{THIGH}} \times \dot{\theta}_{HIP} \times cos(\theta_{HIP}) \tag{18}$$

$$\overline{\dot{y}_{THIGH}} = \overline{l_{THIGH}} \times \dot{\theta}_{HIP} \times sin(\theta_{HIP}) \tag{19}$$

$$\overline{\dot{x}_{SHANK}} = l_{THIGH} \times \dot{\theta}_{HIP} \times \cos(\theta_{HIP}) + (\dot{\theta}_{HIP} - \dot{\theta}_{KNEE}) \times \overline{l_{SHANK}} \times \cos(\theta_{HIP} - \theta_{KNEE}) \tag{20}$$

$$\overline{\dot{y}_{SHANK}} = l_{THIGH} \times \dot{\theta}_{HIP} \times \sin(\theta_{HIP}) + (\dot{\theta}_{HIP} - \dot{\theta}_{KNEE}) \times \overline{l_{SHANK}} \times \sin(\theta_{HIP} - \theta_{KNEE}) \tag{21}$$

The kinematic energy (KE) and potential energy (PE) can be calculated:

$$\begin{aligned} KE = \frac{1}{2} m_{THIGH} \left(\overline{\dot{x}_{THIGH}}^2 + \overline{\dot{y}_{THIGH}}^2 \right) + \frac{1}{2} m_{SHANK} \left(\overline{\dot{x}_{SHANK}}^2 + \overline{\dot{y}_{SHANK}}^2 \right) \\ = \frac{1}{2} m_{THIGH} \overline{l_{THIGH}}^2 \dot{\theta}_{HIP}^2 \\ + \frac{1}{2} m_{SHANK} \left\{ l_{THIGH}^2 \dot{\theta}_{HIP}^2 + \overline{l_{SHANK}}^2 (\dot{\theta}_{KNEE} - \dot{\theta}_{HIP})^2 \\ - 2 l_{THIGH} \overline{l_{SHANK}} \dot{\theta}_{HIP} (\dot{\theta}_{KNEE} - \dot{\theta}_{HIP}) cos\theta_{KNEE} \right\} \end{aligned} \tag{22}$$

$$\begin{aligned} PE = -m_{THIGH} g \overline{l_{THIGH}} cos\theta_{HIP} - m_{SHANK} g l_{THIGH} cos\theta_{HIP} \\ - m_{SHANK} g \overline{l_{SHANK}} \cos(\theta_{KNEE} - \theta_{HIP}) \end{aligned} \tag{23}$$

Since knee angle is assigned, only the dynamic around the knee joint is needed to be considered. Using the Lagrangian equation on the knee joint:

$$\frac{d}{dt}\left(\frac{d(KE)}{d\dot{\theta}_{KNEE}}\right) - \frac{dKE}{d\theta_{KNEE}} + \frac{PE}{d\theta_{KNEE}} = T \tag{24}$$

In this equation, T is the torque applied on the knee joint. In this case it is the torque provided by knee mechanism discussed in Chapter 3.

Impose Eq. (22) and Eq. (23) into Eq. (24),

$$\begin{aligned} \Rightarrow \frac{d}{dt} \Big(m_{SHANK} \overline{l_{SHANK}}^2 (\dot{\theta}_{KNEE} - \dot{\theta}_{HIP}) \\ - m_{SHANK} l_{THIGH} \overline{l_{SHANK}} \dot{\theta}_{HIP} cos\theta_{KNEE} \Big) \\ - \left[-m_{SHANK} l_1 \overline{l_{SHANK}} \dot{\theta}_1 (\dot{\theta}_{KNEE} - \dot{\theta}_{HIP})(-sin\theta_{KNEE}) \right] \\ + \left[-m_{SHANK} g \overline{l_{SHANK}} (-\sin(\theta_{KNEE} - \theta_{HIP})) \right] = T \end{aligned} \tag{25}$$

$$\begin{aligned} \Rightarrow m_{SHANK} \overline{l_{SHANK}}^2 (\ddot{\theta}_{KNEE} - \ddot{\theta}_{HIP}) - m_{SHANK} l_{THIGH} \overline{l_{SHANK}} \ddot{\theta}_{HIP} cos\theta_{KNEE} \\ - m_{SHANK} l_{THIGH} \overline{l_{SHANK}} \dot{\theta}_{HIP} (-\dot{\theta}_{KNEE} sin\theta_{KNEE}) \\ - m_{SHANK} l_{THIGH} \overline{l_{SHANK}} \dot{\theta}_{HIP} (\dot{\theta}_{KNEE} - \dot{\theta}_{HIP}) sin\theta_{KNEE} \\ + m_{SHANK} g \overline{l_{SHANK}} \sin(\theta_{KNEE} - \theta_{HIP}) = T \end{aligned} \tag{26}$$

$$\begin{aligned} \Rightarrow m_{SHANK} \overline{l_{SHANK}}^2 (\ddot{\theta}_{KNEE} - \ddot{\theta}_{HIP}) - m_{SHANK} l_{THIGH} \overline{l_{SHANK}} \ddot{\theta}_{HIP} cos\theta_{KNEE} \\ + m_{SHANK} l_{THIGH} \overline{l_{SHANK}} \dot{\theta}_{HIP}^{\ 2} sin\theta_{KNEE} \\ + m_{SHANK} g \overline{l_{SHANK}} \sin(\theta_{KNEE} - \theta_{HIP}) = T \end{aligned} \tag{27}$$

And $\ddot{\theta}_{KNEE}$ can be calculated:

$$\ddot{\theta}_{KNEE} = (T + m_{SHANK} l_{THIGH} \overline{l_{SHANK}} \ddot{\theta}_{HIP} cos\theta_2 - m_{SHANK} l_{THIGH} \overline{l_{SHANK}} \dot{\theta}_{HIP}{}^2 sin\theta_{KNEE} - m_{SHANK} g \overline{l_{SHANK}} \sin(\theta_{KNEE} - \theta_{HIP}))/(m_{SHANK} \overline{l_{SHANK}}^2) - \ddot{\theta}_{HIP} \tag{28}$$

The knee angle is

$$\theta_{KNEE} = \iint_0^t \ddot{\theta}_{KNEE} \, dtdt \tag{29}$$

Knowing the knee angle data, the toe position can be calculated by Eq. (15).